UNIVERSITY OF CALIFORNIA SAN DIEGO

# Brain vasculature in health and disease

A dissertation submitted in partial satisfaction
of the requirements for the degree Doctor of Philosophy

in

Neurosciences with a Specialization in Anthropogeny

by

Caterina Pearsall Profaci

Committee in Charge:

Professor Richard Daneman, Chair
Professor Jerold Chun
Professor Stacey M. Glasgow
Professor Eric Nudleman
Professor Gentry N. Patrick
Professor Binhai Zheng

2022

The dissertation of Caterina Pearsall Profaci is approved, and it is acceptable in quality and form for publication on microfilm and electronically.

University of California San Diego

2022

# DEDICATION

This dissertation is dedicated to Richard and Marion Pearsall for their incredibly generous support of my education. Gram, your genuine desire to understand the details of my research means more to me than you could ever know.

EPIGRAPH

"Understand this, I mean to arrive at the truth.

The truth, however ugly in itself,

is always curious and beautiful to seekers after it."

Hercule Poirot
*The Murder of Roger Ackroyd*
by Agatha Christie

TABLE OF CONTENTS

Dissertation Approval Page……iii
Dedication……iv
Epigraph……v
Table of Contents……vi
List of Abbreviations……vii
List of Figures……ix
Acknowledgements……xi
Vita……xiv
Abstract of the Dissertation……xvi
Introduction……1
Part I: The blood-brain barrier……1
Part II: Endothelial cells in neurovascular coupling……18
Acknowledgements……20
References……21

Chapter I. Pdlim1 is a marker of blood-brain barrier dysfunction in neurological disease and injury……42
Abstract……42
Introduction……42
Methods……44
Results……49
Discussion……59
Acknowledgements……61
References……61

Chapter II. Microglia are not required for blood-brain barrier properties in healthy brain vasculature……64
Abstract……64
Introduction……64
Methods……66
Results……69
Discussion……75
Acknowledgements……76
References……76

Chapter III. Dynamic, activity-dependent regulation of vascular cholesterol metabolism in the healthy brain……79
Abstract……79
Introduction……79
Methods……81
Results……86
Discussion……110
Acknowledgements……113
References……113

LIST OF ABBREVIATIONS

| | |
|---|---|
| Aβ | Beta-amyloid |
| AD | Alzheimer's disease |
| BBB | Blood-brain barrier |
| BM | Basement membrane |
| CBF | Cerebral blood flow |
| CCI | Controlled cortical impact |
| CLDN5 | Claudin-5 |
| CNS | Central nervous system |
| CSF | Cerebrospinal fluid |
| CSF1R | Colony-stimulating factor 1 receptor |
| CVO | Circumventricular organ |
| DPBS | Dulbecco's phosphate-buffered saline |
| EAE | Experimental autoimmune encephalomyelitis |
| FACS | Fluorescently activated cell sorting |
| GFP | Green fluorescent protein |
| $G_q$PCR | $G_q$ protein coupled receptor |
| IGF1R | Insulin growth factor 1 receptor |
| $K^+$ | Potassium ions |
| kDa | Kilodaltons |
| KDR | Kinase insert domain receptor |
| $K_{IR}$2.1 | Inward rectifying potassium channel 2.1 |
| LDLR | Low-density lipoprotein receptor |
| LRP1 | Lipoprotein-related receptor 1 |
| MCAO | Middle cerebral artery occlusion |
| MRI | Magnetic resonance imaging |
| MS | Multiple sclerosis |
| NaFl | Sodium fluorescein |
| NVC | Neurovascular coupling |
| NVU | Neurovascular unit |

| | |
|---|---|
| P2RY12 | Purinergic receptor P2Y12 |
| PDLIM1 | PDZ and LIM domain protein 1 |
| PGP | P-glycoprotein |
| $PIP_2$ | Phosphatidylinositol 4,5-biphosphate |
| PLVAP | Plasmalemma vesicle associated protein |
| RET | Rearranged during transfection |
| RTK | Receptor tyrosine kinase |
| SMC | Smooth muscle cell |
| SVD | Small vessel disease |
| TBI | Traumatic brain injury |
| TEM | Transmission electron microscopy |
| TJ | Tight junction |
| TNFα | Tumor necrosis factor alpha |
| TRE | Tetracycline response element |
| tTA | Tetracycline-controlled transactivator |
| VEGFR2 | Vascular endothelial growth factor receptor 2 |

LIST OF FIGURES

Figure 0.1 Cellular and molecular properties of the BBB…….2

Figure 0.2 Dysfunction of the BBB in disease……12

Figure 1.1 Endothelial PDLIM1 expression correlates with vascular permeability in health and disease..54

Figure 1.2 PDLIM1 failed to inhibit Wnt signaling, and inhibited NF-κB signaling in HEK293 cells but not primary endothelial cells..……..…….…55

Figure 1.3 PDLIM1 overexpression increases cell adhesion molecules and alters post-translational modification ……..……...56

Figure 1.4 PDLIM1 overexpression in a model of multiple sclerosis…….58

Figure 2.1 One month of PLX5622 diet significantly depletes microglia…….……...71

Figure 2.2. Microglial depletion does not affect BBB structure or function……...72

Figure 2.3 Microglial depletion does not alter expression of genes associated with BBB properties…….…….…….……...74

Figure 3.1 PLX5622 treatment increases brain endothelial expression of cholesterol-related genes……..94

Figure 3.2 PLX5622 increases the expression of cholesterol-related genes throughout the vascular tree …….…….…….……...…95

Figure 3.3 PLX5622 increases expression of cholesterol-related genes in CNS, but not non-CNS, vasculature…….…….…….96

Figure 3.4 Long-term PLX5622 treatment causes upregulation of endothelial cholesterol cassette……...98

Figure 3.5 PLX5622 treatment does not increase cholesterol-related gene expression in a mixed glial population.…….…….…….……99

Figure 3.6 PLX5622 treatment does not cause global changes in lipid signatures in brain, liver, or serum ……....100

Figure 3.7 Upregulation of endothelial cholesterol machinery is independent of microglial depletion…102

Figure 3.8 Genetic depletion of microglia does not increase expression of cholesterol uptake receptor in endothelial cells..…….…….…….……104

Figure 3.9 High fat diet does not alter brain endothelial cholesterol metabolism.…….…...105

Figure 3.10 Neuronal activity regulates brain endothelial cholesterol metabolism. ……106

Figure 3.11 Increased vascular cholesterol induced by PLX5622 treatment inhibits retrograde hyperpolarization in response to $K^+$……107

Figure 3.12 PLX5622 acts on another receptor tyrosine kinase to increase endothelial cholesterol metabolism……108

Figure 3.13 Model: endothelial cholesterol as a negative feedback mechanism in neurovascular coupling……109

ACKNOWLEDGEMENTS

First and foremost, I want to thank my thesis advisor, Dr. Richard Daneman. I never imagined that I could be so fully supported in the endeavor of a PhD as I have been. Rich, you have taught me an immeasurable amount about how to be a scientist – how to ask big questions, design properly-controlled experiments to attack these questions, always preserve scientific integrity, and engage an audience while presenting work. You have introduced me to countless scientists whom I look up to, and you've nominated me for countless awards and opportunities – a large portion of the accolades on my CV would not have been possible without your advocacy. You've also indulged my desire to get more practice in grant-writing, taking the time and effort to edit and advise me on multiple drafts of my own fellowships as well as grants for the lab. Not only has your guidance made me a better scientist and writer, but you've also taught me that one can be a successful, impactful scientist while also being a warm, empathetic, silly, 100% genuine person, and a devoted mentor. Rich – endless thanks.

I would also like to thank the entire Daneman lab, past and present, for keeping me sane and happy through the ups and (mostly) downs of experiments. A special thank you to Marie who essentially taught me everything I know in lab while always making me laugh as well. Marie, seeing you perform the caliber of work fitting a *Nature* paper while also raising a young child was unbelievably impactful to me as a woman scientist who wants to have a family in the future. Your example means more to me than you know. I also want to specifically thank Rob and Cayce – I am endlessly grateful that Rich's other OG graduate students were two amazing people such as yourselves. And Kaja, your friendship over the years has meant the world to me. Tony, Joseph, and Alex – thank you for your years of help, and I cannot wait to see your successes as doctors! And apologies for bringing you on the frustrating journey of Pdlim1 with me ☺. Sean and Lucija, thank you for your recent help with my projects – it has been fun to work with each of you.

I am also grateful to have been a part of several fruitful collaborations. I want to particularly thank Andy for his invaluable guidance on how to go about studying neurovascular coupling and his continued involvement in the project. I also want to thank Fabrice and Gesine for their enthusiasm in the project and

willingness to contribute to it. And Chris and Tom for their willingness to share resources. I also want to thank the people in these labs – Lena, Vanessa, Jackson, Kelsey, and Gabe – for taking time away from their own projects to work on mine!

A couple of the main techniques performed in this paper would not have been possible without the help of core facilities. I particularly want to thank Tara and Neil for sorting *countless* cells for me – it really means a lot that both of you so clearly always wanted my experiments to go well. I also want to thank Kristen for her incredible advice and help – several times I was convinced that all was lost re my sequencing samples, and somehow you made it all ok. I must also thank Ana for her incredible oversight of the LBR vivarium, without you our experiments would undoubtedly run less smoothly.

I would like to thank my thesis committee – Eric, Gentry, Binhai, Jerold, and Stacey – for their guidance and support over the (many!) years of my graduate experience.

A very, very special thank you to the NGP class of 2014. I truly cannot imagine going through the process of graduate school with a different group of people. I have learned so much from all of you, and you have kept me grounded during the long journey of graduate school. From Oscars parties to post-bar pasta to brunch club to star parties – you all will always hold a very special place in my heart, and I cannot wait for the reunions to come. I also want to thank the entire NGP community – this community has been such an integral part of my grad school experience. Particular thanks to Erin and Linh for their impeccable management of the program during most of my years here – for taking care of all of our minute concerns and genuinely caring for the wellbeing of each of us. And to Tim for his leadership of the program throughout my years in it, particularly for his countless inspiring speeches. Tim, thank you for taking a chance on my dubious-sounding request to transfer. It changed my life.

In the same vein, thank you to Sequoyah. Your bold seat swap on that plane to Phoenix put my life on an entirely different path, and without it I likely would never have ended up at UCSD. I don't know what my life would look like. Part of your influence was also the introduction to Pascal. Pascal, thank you for welcoming me into CARTA and for teaching me so much during my years in the program. Thank you also to all the students in the specialization – I so enjoyed learning from all your diverse perspectives. The

specialization was truly a life-changing experience. And special shout-out to Alex for facilitating the spectacular field course.

Lastly, I want to thank my family and friends who supported me through this experience. It was a long and often very difficult journey, and your love has meant everything.

Part I of the Introduction is a reprint of the material as it appears in Profaci CP, Munji RM, Pulido RS, Daneman R (2020). The blood-brain barrier in health and disease: Important unanswered questions. *Journal of Experimental Medicine* Apr 6;217(4). The dissertation author was the first author of this review article. The figures have been slightly modified here, and the section on traumatic brain injury has been added.

Chapter I, in full, is currently being prepared for submission for publication and will include Kaja Bajc, Lucija Pintarić, Alexander Z. Zhang, Tony Z. Zhang, Joseph P. Miller, and Fabien Sohet as co-authors, and Professor Richard Daneman as the senior author. The dissertation author was the primary investigator and author of this material.

Chapter II, in full, is currently being prepared for submission for publication and will include Tony Z. Zhang as a co-author and Professor Richard Daneman as the senior author. The dissertation author was the primary investigator and author of this material.

Chapter III, in full, is currently being prepared for submission for publication and will include Lena Spieth, Sean S. Harvey, Alexander Z. Zhang, Jackson T. Fontaine, Vanessa Coelho-Santos, Kelsey M. Nemec, Gabriel L. McKinsey, Thomas D. Arnold, Frederick C. Bennett, Andy Y. Shih, Gesine Saher, and Fabrice Dabertrand as co-authors, and Professor Richard Daneman as the senior author. The dissertation author was the primary investigator and author of this material.

VITA

| | |
|---|---|
| 2012 | Bachelor of Science, Neurobiology with a Minor in English<br>Georgetown University, Washington DC, USA |
| 2014 | Master of Arts, Neurobiology and Behavior<br>Columbia University, New York, NY, USA |
| 2022 | Doctor of Philosophy, Neurosciences with a Specialization in Anthropogeny<br>University of California San Diego, La Jolla, CA, USA |

PUBLICATIONS

**Profaci CP**, Spieth L, Harvey SS, Zhang AZ, Fontaine JT, Coelho-Santos V, Nemec KM, McKinsey GL, Arnold TD, Bennett FC, Shih AY, Saher G, Dabertrand F, Daneman R. Dynamic, activity-dependent regulation of vascular cholesterol metabolism in the healthy brain. *In preparation*.

**Profaci CP**, Zhang TZ, Daneman R. Microglia are not required for blood-brain barrier properties in healthy brain vasculature. *In preparation.*

Blanchette M, Bajc K, Gastfriend BD, **Profaci CP**, Ruderisch N, Dorrier CE, Zhong G, Cuevas-Diaz Duran R, Harvey SS, Garcia-pak IH, Wang A, Panti D, Tsai LT, Isoherranen N, Palecek SP, Shusta EV, Wu J, Daneman R. Regional Specializations of the blood-brain barrier regulate local brain function. *Under revision.*

Martin M, Vermeiren S, Bostaille N, Eubelen M, Spitzer D, Vermeersch M, **Profaci CP**, Pozuelo E, Toussay X, Raman-Nair J, Tebabi P, America M, Sandersson LE, Cabochette P, Germano RFV, Torres D, Boutry S, Perez-Morgan D, de Kerckhove d'Exaerde A, Bellefroid E, Phoenix TN, Devraj K, Lacoste B, Daneman R, Liebner S, Vanhollebeke B. Engineered Wnt ligands enable blood-brain-barrier repair in neurological disorders. In Press, *Science*.

Pulido RS, Munji RN, Chan TC, Quirk CR, Weiner GA, Weger BD, Rossi MJ, Elmsaouri S, Malfavon M, Deng A, **Profaci CP**, Blanchette M, Qian T, Foreman KL, Shusta EV, Gorman MR, Gachon F, Leutgeb S, Daneman R. Neuronal Activity Regulates Blood-Brain Barrier Efflux Transport through Endothelial Circadian Genes. *Neuron.* 2020 Dec 9;108(5):937-952.e7.

**Profaci CP**, Munji RN, Pulido RS, Daneman R. The blood-brain barrier in health and disease: Important unanswered questions. *J Exp Med.* 2020 Apr 6;217(4).

Fu H, Hussaini SA, Wegmann S, **Profaci C**, Daniels JD, Herman M, Emrani S, Figueroa HY, Hyman BT, Davies P, Duff KE. 3D Visualization of the Temporal and Spatial Spread of Tau Pathology Reveals Extensive Sites of Tau Accumulation Associated with Neuronal Loss and Recognition Memory Deficit in Aged Tau Transgenic Mice. *PLoS One.* 2016 Jul 28;11(7):e0159463.

Khan UA, Liu L, Provenzano FA, Berman DE, **Profaci CP**, Sloan R, Mayeux R, Duff KE, Small SA. Molecular drivers and cortical spread of lateral entorhinal cortex dysfunction in preclinical Alzheimer's disease. *Nat Neurosc*i. 2014 Feb;17(2):304-11.

Stillman CM, Coane JH, **Profaci CP,** Howard JH Jr, Howard DV. The effects of healthy aging on the mnemonic benefit of survival processing. *Mem Cognit*. 2014 Feb;42(2):175-85.

Olszewski RT, Janczura KJ, Ball SR, Madore JC, Lavin KM, Lee JC, Lee MJ, Der EK, Hark TJ, Farago PR, **Profaci CP,** Bzdega T, Neale JH. NAAG peptidase inhibitors block cognitive deficit induced by MK-801 and motor activation induced by d-amphetamine in animal models of schizophrenia. *Transl Psychiatry*. 2012 Jul 31;2:e145.

Neale JH, Olszewski RT, Zuo D, Janczura KJ, **Profaci CP**, Lavin KM, Madore JC, Bzdega T. Advances in understanding the peptide neurotransmitter NAAG and appearance of new member of the NAAG neuropeptide family. *J Neurochem.* 2011 Aug;118(4): 490-8.

**Profaci CP**, Krolikowski KA, Olszewski RT, Neale JH. Group II mGluR agonist LY354740 and NAAG peptidase inhibitor effects on prepulse inhibition in PCP and D-amphetamine models of schizophrenia. *Psychopharmacology (Berl).* 2011 Jul;216(2):235-43.

ABSTRACT OF THE DISSERTATION

Brain vasculature in health and disease

by

Caterina Pearsall Profaci

Doctor of Philosophy in Neurosciences with a Specialization in Anthropogeny

University of California San Diego, 2022

Professor Richard Daneman, Chair

Throughout the body, the vasculature functions as a delivery system, supplying oxygen and nutrients crucial for cell activity and survival. Central nervous system (CNS) vasculature plays a second critical role as a barrier system, limiting brain entry of bloodborne ions, molecules, and cells. Indeed, CNS blood vessels are endowed with a series of unique properties that allow them to tightly regulate the extracellular environment of the brain, and together these properties are termed the “blood-brain barrier” (BBB). The barrier properties of CNS vasculature are critical for proper brain function; BBB dysfunction during disease or injury can lead to a cascade of consequences resulting in neuronal death. Several questions

remain regarding how BBB properties are maintained in health and the mechanisms underlying their dysfunction in neuropathologies.

The brain uses an extraordinary amount of the body's energy, and without constant blood supply from the vasculature, its functions quickly deteriorate. Indeed, neuronal activity leads to a temporary increase in local blood flow to provide neurons with sufficient energy and oxygen, and this phenomenon is known as neurovascular coupling (NVC). NVC has been shown to involve various cell types and signaling molecules, but it is still unclear to what extent endothelial cells, the cells that form the innermost walls of the vasculature, participate in NVC.

This dissertation explores brain vasculature in health and disease. Chapter I focuses on BBB dysfunction in disease, identifying PDLIM1 as a marker for BBB dysfunction and characterizing its role in CNS endothelial cells. Chapter II focuses on the neurovascular unit, specifically whether microglia play a role in maintaining barrier properties in healthy vasculature. Chapter III demonstrates the dynamic nature of neurovascular cholesterol metabolism and how this metabolic pathway influences NVC.

# INTRODUCTION

## PART I: THE BLOOD-BRAIN BARRIER

Blood vessels provide the vital infrastructure for delivery of oxygen and essential nutrients throughout the body, and the term "blood–brain barrier" (BBB) is used to describe the unique characteristics of the blood vessels that vascularize the central nervous system (CNS)[1-3]. The BBB is not a single physical entity but rather the combined function of a series of physiological properties possessed by endothelial cells that limit vessel permeability. The BBB tightly regulates the movement of ions, molecules, and cells between the blood and the parenchyma, thus regulating the extracellular environment of the neural tissue. It is critical for neuronal function and protection. The interaction of endothelial cells with different neural and immune cells is commonly referred to as the neurovascular unit (NVU) (Fig 0.1A). The complex properties that define the BBB are often altered in disease states, and BBB dysfunction has been identified as a critical component in several neurological conditions.

### The NVU

Multiple cell-types are juxtaposed at the boundary between the blood vessels and the brain, many of which play key roles in the development and maintenance of a functional BBB[4]. The cluster of different cells that comprise the blood-brain interface is commonly referred to as the neurovascular unit (NVU).

#### *Endothelial cells*

Endothelial cells make up the inner-most layer of blood vessels. A cross-section of an artery or vein might contain dozens of endothelial cells, while in the smallest capillaries, a single endothelial cell forms the vessel circumference[5]. In all tissues, adherens junctions, composed of vascular endothelial cadherin and catenins, comprise the basic cellular adhesions between endothelial cells, supporting the

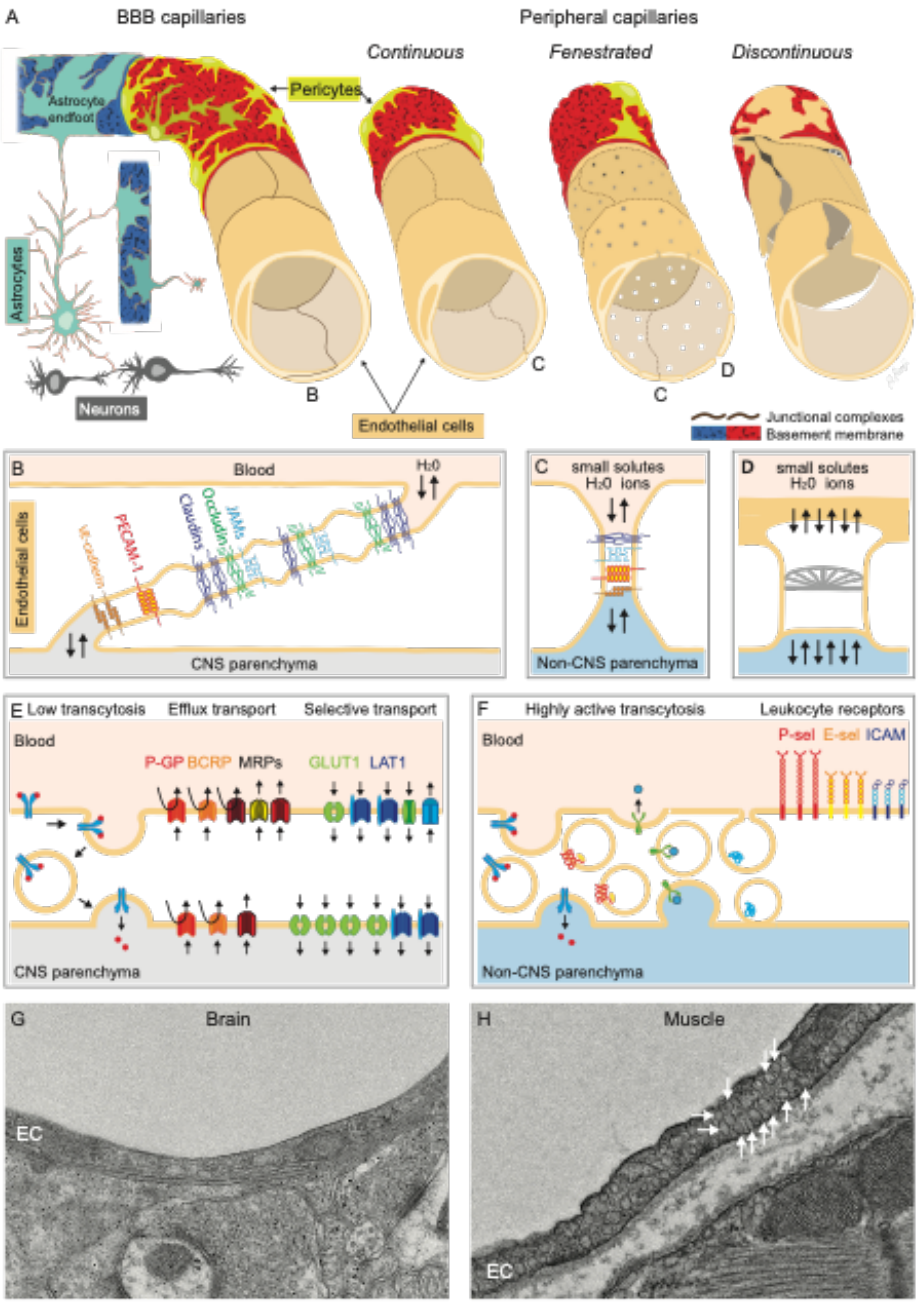


**Figure 0.1 Cellular and molecular properties of the BBB**. **A)** A schematic comparison of the BBB capillaries with the continuous non-fenestrated, continuous fenestrated, and discontinuous capillaries found in peripheral organs. **B-F)** Schematic of the molecular composition of **B)** junctional complexes of BBB endothelial cells, **C)** endothelial cells in peripheral organs, **D)** peripheral endothelial fenestra, **E)** transport mechanisms in CNS endothelial cells, and **F)** transport mechanisms in peripheral endothelial cells. **G)** Electron micrograph of a mouse brain endothelial cell. **H)** Electron micrograph of a mouse muscle endothelial cell, densely packed with vesicles (arrows).

cell adhesion, promoting adherens junction formation[6,7]. CNS endothelial cells are further specialized to restrict paracellular and transcellular movement of solutes.

*Tight junctions (TJs)*

TJs are cell adhesions consisting of multiple transmembrane proteins that directly interact via their extracellular components, linking two cells' membranes together[8] (Fig 0.1B). CNS TJs are specialized in their molecular and structural P-face composition to form a high-resistance electrical barrier, and the specific combination of TJ proteins at the BBB determines its paracellular permeability. The composition of claudins, a family of 27 four-pass transmembrane proteins, within a TJ is thought to determine the size and charge selectivity of paracellular permeability[9-11]. Claudin 5 (CLDN5) is the most abundant claudin at the BBB, and Cldn5 knockout mice exhibit size-selective leakage of the BBB and die at birth[12,13]. Endothelial cells in peripheral vascular beds also express CLDN5, and thus its expression alone is not sufficient for barrier formation. Other key components of TJs include claudin 12, occludin, and junctional adhesion molecules. Cytoplasmic proteins including ZO-1, ZO-2, ZO-3, cingulin, JACOP, MAG1, and MUPP1 aid TJ formation, binding TJs to the cytoskeleton, adherens junctions, and polarity complexes[14-16]. It is still unknown why CLDN5 and ZO-1 expression does not confer the same low paracellular permeability in peripheral vessels as in the CNS. Expression data suggest that the answer might lie in the CNS-specific enrichment of certain cytoplasmic adaptors (e.g., JACOP, MPP7) and tricellular TJ molecules such as LSR and MARVELD2[17,18].

*Transcellular permeability*

Peripheral endothelial cells possess properties that confer transcellular permeability, including high rates of caveolin-mediated transcytosis, diaphragm-containing pores termed fenestrae, or large discontinuities or gaps in the endothelial layer[19] (Fig 0.1). In contrast, CNS endothelial cells form a continuous lining that lacks fenestrations and has low levels of transcytosis, properties that greatly limit

transcellular permeability (Fig 0.1). MFSD2A, enriched in CNS endothelial cells, limits caveolin-dependent transcytosis by regulating endothelial cell lipid composition[20-22]. Plasmalemma vesicle-associated protein (PLVAP) is important both for vesicle formation and fenestrations in peripheral endothelial cells. Its down-regulation in CNS endothelial cells, along with up-regulation of MFSD2A, coincides with BBB formation during embryogenesis, coinciding with a decrease in CNS endothelial transcytosis[23-25].

*Transporters*

Numerous transporters are enriched in brain endothelial cells, which fall into two main categories: efflux and solute transporters[26-28] (Fig 0.1E).

Efflux transporters, concentrated on the luminal side of the membrane, use ATP hydrolysis to transport a wide range of small molecules up their concentration gradients back into the blood[29]. MDR1/P-glycoprotein (PGP) and breast cancer resistance protein are the most abundant BBB efflux proteins and limit entry of many xenobiotics and endogenous molecules, including steroids such as aldosterone[30].

Solute transporters carry specific substrates down their concentration gradients, ensuring barrier passage to specific nutrients, such as glucose, that are vital for energy and homeostasis[31]. Transport of glucose, lactate, amino acids, and fatty acids occurs via GLUT1 (Slc2a1), MCT1 (Slc16a1), LAT1 (Slc7a5), and MFSD2A, respectively[21,32-34]. Other transporters provide receptor-mediated vesicular transport, including the transferrin receptor (TFR1) and low-density lipoprotein receptors[35,36]. Substrate-specific solute transporters can also be important for removing molecules from the CNS; lipoprotein receptor-related protein-1 (LRP1) is a critical transporter for eliminating β-amyloid[37,38].

*Leukocyte adhesion molecules*

Leukocyte adhesion molecules on endothelial cell surfaces initiate binding of leukocytes, the first step of their entrance into tissues[39]. Healthy CNS Endothelial cells exhibit lower leukocyte adhesion molecule expression compared with peripheral endothelial cells[17], and thus there is minimal leukocyte

crossing of the BBB in health (Fig 0.1E-F; Fig. 0.2A). Instead, CNS immune surveillance by lymphocytes in health occurs primarily at the blood–CSF interfaces of the meninges and choroid plexus[40-42]. In the context of disease, CNS endothelial cells upregulate specific leukocyte adhesion molecules such as ICAM1, E-selectin, and P-selectin primarily at post-capillary venules, thus contributing to neuroinflammation.

*Glycocalyx*

The luminal surface of the capillary endothelium is covered by the endothelial cell glycocalyx[43-45]. Brain endothelial cells have a denser glycocalyx than peripheral vasculature; average glycocalyx coverage is 40.1% in brain vessels compared with 15.1% and 3.2% in cardiac and pulmonary vessels, respectively[46]. This dense network of luminal glycoproteins prevents larger molecules from interacting with the endothelial cell. While small dyes such as fluorescein (376 daltons) and Alexa Fluor (643 daltons) permeate the glycocalyx, dextrans (40–150 kD) penetrate <60% of its volume[47]. In disease, glycocalyx degradation is associated with more severe BBB leakage in models of multiple sclerosis (MS) and cardiac arrest[48,49].

*The NVU*

The abluminal surface of the endothelial cell is covered by the basal lamina (Fig 0.1A), a structural matrix of laminins, fibronectin, collagens, tenascin, and proteoglycans. This basement membrane (BM) surrounds endothelial cells and pericytes, acting as an interface for the binding of molecules and migration of cells, while also limiting passage of macromolecules[50]. The BM consists of two layers: the inner vascular BM secreted by endothelial cells and mural cells, and the outer glial BM secreted by astrocytes[51]. These BMs are merged surrounding capillaries but separate at post-capillary venules, creating a CSF-drained perivascular space for immune surveillance[52].

Mural cells—vascular smooth muscle cells (SMCs) and pericytes—are found on the abluminal side of blood vessels in all tissues. SMCs line all larger vessels but are more abundant on arteries and arterioles, forming a complete layer around them[53-55]. SMCs contract or dilate to cause vasoconstriction and vasodilation, thus regulating blood flow[5]. Pericytes are embedded in the BM and form an incomplete layer

on the surface of CNS micro-vessels (Fig 0.1A). Pericytes play a key role in the regulation of angiogenesis, vascular remodeling, vascular tone, and BBB formation[56-59]. Perivascular fibroblasts are found in the walls of large vessels[55]; however, their role in cerebrovascular function remains unexplored.

Astrocytes extend cellular processes terminating in endfeet that ensheath synapses, nodes of Ranvier, and endothelial cells, contacting the BM around parenchymal vessels (Fig. 0.1A). This astrocyte-endothelial interaction is critical in regulating blood flow[60,61]. Additionally, several groups have shown that CSF flows between the BM and astrocyte endfeet, with arteriole pulsations driving bulk fluid flow through the parenchyma, although others have argued about the extent of bulk flow[62,63]. This "glymphatic" system helps to clear interstitial solutes such as amyloid via paravenous drainage pathways[64-66] and has been visualized in human patients via magnetic resonance imaging (MRI)[67,68]. Expression of water channel aquaporin-4 in astrocyte endfeet has been reported to play a critical role in the movement of CSF into the parenchyma[64,66,69].

CNS-associated macrophages include choroid plexus, dural, leptomeningeal, and perivascular macrophages[70,71]. Perivascular macrophages are elongated cells residing between the astrocytic endfeet and parenchymal vessels (primarily arteries and veins). While nonmotile, they extend processes along the perivascular space, providing the first line of defense by collecting debris[72,73]. Microglia, derived from yolk-sac progenitor cells[74-76], reside within the CNS parenchyma. They possess a highly ramified morphology and perform immune surveillance, phagocytosing infectious agents that evade the barrier[77,78]. Microglia have also been shown to regulate BBB resealing following vascular injury and disease[79,80]. However, whether microglia play a role at the healthy BBB is unknown and will be tested as a part of this thesis. In disease states, leukocytes such as neutrophils and T cells can interact with the BBB, increasing permeability via release of cytokines, reactive oxygen species, and other mediators of barrier dysfunction[81-83].

Thus, the BBB is a series of structural, transport, and metabolic barriers that together limit CNS entry of nonspecific molecules while ensuring the delivery of specific nutrients, thereby controlling the extracellular environment. Several important questions remain. What exactly gets through the barrier, how much, and by which route(s)? The barrier is not absolute. Small, nonpolar molecules enter unrestricted

through passive diffusion unless they are substrates of efflux transporters. In contrast, large or polar molecules are greatly restricted in access unless they are substrates of specific nutrient transporters. However, even large molecules enter the CNS parenchyma at 0.1% of their blood concentration through an unsaturable mechanism[84,85], likely via nonspecific transcytosis, which occurs at low rates. Future work fully characterizing the substrate specificity of BBB transporters and their dynamic response to various stimuli may enable manipulation of these transporters for CNS drug delivery.

There is heterogeneity of gene expression among different branches of the vascular tree[55,86,87]. It is thought that this heterogeneity enables capillaries, arterioles, and venules to be specialized for regulation of solute transport, blood flow, and inflammation, respectively. But what is the relevance of this arteriovenous zonation in terms of barrier function? How is this phenotypic continuum programmed during development?

It is also currently unknown whether there is regional heterogeneity of the BBB. Several regions of the CNS termed circumventricular organs (CVOs) – the area postrema, subfornical organ, pineal gland, and median eminence of the hypothalamus – have fenestrated capillaries that lack BBB properties[88]. This vascular permeability allows for the exchange of sensory or secretory signaling molecules between the brain and blood, enabling CVO-mediated regulation of body homeostasis. Much less is known about whether there are region-specific differences among areas with a functional BBB, including the cortex, hippocampus, cerebellum, and white matter tracks, and whether BBB heterogeneity might contribute to the specialized function of a particular brain region or render that region more vulnerable to disease.

**BBB formation and regulation**

How BBB properties are regulated in development and maintained in adulthood remains a fundamental field of study[89]. Transplanted CNS tissue is sufficient to induce BBB-like properties in the gut endothelium in vivo[90], suggesting a role for the neural microenvironment in BBB formation. Transplantation of astrocytes into nonneural tissues of adult rats induces barrier properties in local endothelial cells[91], and several astrocyte-secreted proteins are sufficient to induce endothelial cell barrier

properties in vitro and in vivo, including Sonic hedgehog, angiotensin, and basic fibroblast growth factor[92-94]. However, barrier properties arise during development before astrogliogenesis takes place[18,20,56,95], delaying astrocytic contact with endothelial cells does not affect barrier formation[96], and laser ablation of astrocyte endfeet in adult mice does not induce BBB leakage[97]. These data suggest that astrocytes are not necessary for BBB formation, but perhaps provide dynamic BBB regulation in response to specific stimuli. For instance, reactive astrocytes have been shown to be critical for BBB repair following neurological disease[98].

Neural progenitor-derived Wnt signaling induces BBB properties during the angiogenic program[99-105]. Loss of Wnt signaling disrupts angiogenesis specifically in the CNS, reducing the expression of TJ proteins and solute transporters while increasing PLVAP[99-101]. Interestingly, β-catenin activation in the more permeable CVO vessels is sufficient to induce BBB properties[106,107]. These data suggest that the same signal that drives angiogenic invasion of the CNS also induces initial BBB properties within the endothelium.

Pericytes are also essential in BBB development, and endothelial cell recruitment of pericytes is concomitant with development of particular barrier properties. The BBB fails to completely seal in mice lacking CNS pericytes, as they inhibit nonspecific transcytosis and leukocyte adhesion molecule expression[56,58].

Thus, the BBB is regulated by a series of different cellular interactions: BBB "tight" properties are induced during the angiogenic program by Wnt signaling, "leaky" properties are inhibited by pericytes, and the overall phenotype of the BBB can be influenced by astrocytes, pericytes, and other cell types throughout life.

Important questions still remain. How is the induction of different BBB properties coordinated? Interestingly, Wnt signaling induces endothelial secretion of platelet-derived growth factor B, the key ligand for pericyte recruitment[108], suggesting that induction of different BBB properties is tightly coordinated via Wnt-mediated pericyte recruitment. Are the same signals required for induction also responsible for regulating BBB maintenance in adulthood? Although Wnt signaling decreases in endothelial

cells after angiogenesis, this pathway is critical for BBB maintenance; disruption of Wnt signaling in adulthood leads to cell-autonomous loss of TJ integrity and an increase in PLVAP in the retina and cerebellum[103]. Additionally, pericytes are important for BBB function throughout life[58], suggesting that similar signals are required for BBB formation and maintenance. Do region-specific differences in signaling influence BBB heterogeneity? Different Wnt ligands and receptor complexes have been shown to promote BBB formation in different regions of the CNS[99,103,104,109]; however, it is not clear whether this induces regional heterogeneity or is merely a remnant of dorsal–ventral and rostral–caudal axis specification.

How dynamic is each BBB property in a healthy CNS? Are properties modulated by neural activity or environmental stimuli such as exercise and diet? Single-cell sequencing has revealed vascular changes in response to neural activity[110], and neuronal activity has been shown to modulate BBB insulin-like growth factor 1[111]. Using chemogenetics and a volitional behavior paradigm, Pulido et al. found a set of brain endothelial genes that were reciprocally modulated by activating and silencing neural activity. Interestingly, neural activity regulates a group of BBB efflux transporters[112]; the implications of these results for CNS drug delivery and waste clearance remain unknown. While exercise might help to protect against BBB dysfunction in aging or disease, solid evidence is still forthcoming[113]. A high-fat diet can increase BBB permeability[114-116], but the specific BBB properties affected have not been thoroughly characterized. Not only can diet affect the BBB, but the BBB can in turn dynamically regulate nutrient availability; animals entering hibernation up-regulate ketone transporters at the BBB to modulate energy utilization during inactivity[117]. How dynamic are BBB properties over the course of 24 hours, and how might these fluctuations influence brain microenvironment and waste clearance? PGP expression levels follow a diurnal pattern[112,118,119], and a circadian clock in glial cells of the Drosophila melanogaster BBB regulates xenobiotic efflux [120,121], but the extent and functional implications of circadian oscillations at the BBB remain unclear.

Are there differences in the BBB across individuals? Are there sex differences in BBB properties? There is evidence for variation in male and female patient CSF/serum albumin ratio[122], and BBB sexual

dimorphism has been proposed to underlie differences in response to traumatic brain injury and infection and in proclivity to autoimmune disease[123-125].

How do BBB properties change in age? Several studies have reported age-related decline in BBB function[126-131]. Age-related pericyte dysfunction contributes to BBB permeability[127], and endothelial VCAM1 upregulation leads to age-related cognitive deficits and increased inflammatory tone[130]. Yang and colleagues elegantly demonstrated an age-related decrease in receptor-mediated transport and increase in caveolin-mediated non-specific transcytosis across the BBB, coinciding with loss of pericyte coverage[131]. It is likely that these deficits in BBB function contribute to age-related neurodegeneration.

**BBB dysfunction**

BBB dysfunction occurs in a number of neuropathologies, including MS, epilepsy, stroke, and traumatic brain injury (TBI). In these conditions, BBB dysfunction is a central element of the pathology, whereas in others, such as Alzheimer's disease (AD), the incidence and extent of breakdown are more controversial and an area of burgeoning research. BBB disruption causes ion dysregulation, edema, and neuroinflammation, which can lead to neuronal dysfunction, increased intracranial pressure, and neuronal degeneration (Fig 0.2A-B). However, the mechanisms underlying BBB dysfunction and its role in the onset and progression of disease or recovery are not fully understood.

The phrase "BBB breakdown" conjures images of the destruction of a physical wall, allowing an unabated flow of molecules from the blood into the brain. However, the BBB is not a wall but a series of physiological properties, and a change in just one property (transcytosis, transport) can significantly alter the neural environment (Fig 0.2). For instance, dysfunction of GLUT1 glucose transport, LAT1 amino acid transport, and MCT8 thyroid hormone transport across the BBB leads to seizure, autism spectrum, and psychomotor retardation syndromes, respectively[132-134].

Importantly, leakage of nonspecific molecules is distinct from leukocyte extravasation, which occurs via an active trafficking process. Single-cell sequencing has identified many subsets of immune cells with distinct roles in neuroinflammation that likely interact with the BBB in disease[70,71,135-137]. Parenchymal

endothelial cells upregulate leukocyte adhesion molecules, thus increasing leukocyte trafficking. P-selectin and E-selectin mediate the rolling of leukocytes along the endothelium, ICAM1 and VCAM1 mediate firm adhesion, and proteins like PLVAP—also upregulated in disease—aid in transmigration across endothelial cells[52,138]. Leukocyte extravasation across the BBB can be either transcellular or paracellular[139,140]. Levels of ICAM1 and PECAM1 can influence T cell diapedesis route[141,142], and specific subsets of T cells prefer different routes[143].

Thus, the BBB is not an on–off switch, and it is critical to understand the specificities and consequences underlying each instance of dysfunction.

*Multiple sclerosis*

BBB dysfunction is a central feature of MS, and the time course of leakage has been studied with dynamic contrast-enhanced MRI[144-147] (Fig 0.2 G). While barrier leakage is almost always present in new lesions, it is rarely observed in older lesions[144,145]. Interestingly, MRI evidence suggests that BBB permeability is the initial event in the formation of a subset of lesions, but in others, lesion formation occurs before barrier dysfunction[146].

CNS immune infiltration is a critical step in MS pathophysiology, and the dynamics of this process have been primarily studied in experimental autoimmune encephalomyelitis (EAE), a rodent model of MS (Fig 0.2C-D). The primary sites of CNS immune surveillance in health are the blood–CSF barriers of the choroid plexus and meninges, and both are important sites of initial lymphocyte activation in EAE[137,148-153]. Leukocyte-derived cytokines activate CNS parenchymal blood vessels, inducing expression of leukocyte adhesion molecules[152,154,155], which leads to massive parenchymal infiltration of immune cells. These immune cells first enter the perivascular space surrounding postcapillary venules[156] and gain parenchymal access after breaking down the BM[157,158]. Limiting immune cell trafficking across the BBB has proven effective in treating MS. Natalizumab, which targets the α4 integrin on immune cells, preventing their interaction with endothelial VCAM1, greatly reduces new lesion formation[159].

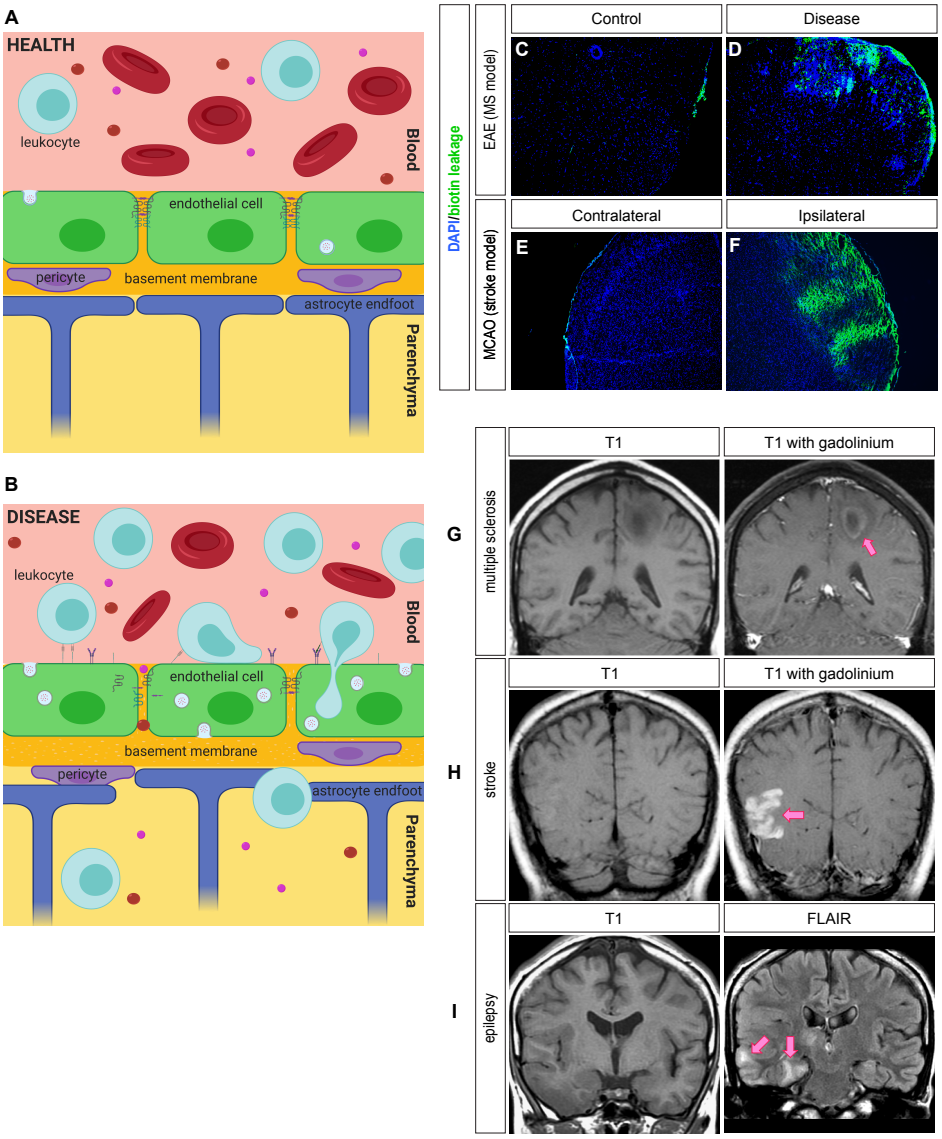


**Figure 0.2 Dysfunction of the BBB in disease. (A-B)** Schematic representation of the neurovascular unit in health and disease. (**A**) In health, CNS ECs exhibit tight junctions, low rates of transcytosis, and low expression of leukocyte adhesion molecules. Pericytes embedded in the BM help to maintain the barrier, and astrocyte endfeet contact the BM. (**B**) In disease, tight junctions are internalized or downregulated, rates of transcytosis increase, increased leukocyte adhesion molecule expression leads to increased leukocyte extravasation, the BM degrades, and pericytes and astrocytes less tightly cover the ECs. *Made with BioRender.* (**C-F**) Blood-brain barrier disruption in models of multiple sclerosis, traumatic brain injury, and stroke. Sections showing blood-brain barrier leakage to a sulfo-NHS biotin tracer (green) in three disease models. (**C-D**) A section of spinal cord from a healthy mouse (C) and from the EAE model of multiple sclerosis (D). **(E-F)** The contralateral (E) and ipsilateral (F) hemispheres in a coronal section of the middle-cerebral artery occlusion model (MCAO) of ischemic stroke. (**G-I**) Blood-brain barrier leakage and edema in human cases of multiple sclerosis, stroke, and epilepsy. T-1 weighted MRI images with gadolinium enhancement to show blood-brain barrier leakage in (**G**) multiple sclerosis lesions and (**H**) stroke infarct. (**I**) T-1 weighted and FLAIR MRI images showing edema in epilepsy. Images courtesy of Dr. John Hesselink, University of California, San Diego.

CNS immune infiltration is a critical step in MS pathophysiology, and the dynamics of this process have been primarily studied in experimental autoimmune encephalomyelitis (EAE), a rodent model of MS (Fig 0.2C-D). The primary sites of CNS immune surveillance in health are the blood–CSF barriers of the choroid plexus and meninges, and both are important sites of initial lymphocyte activation in EAE[137,148-153]. Leukocyte-derived cytokines activate CNS parenchymal blood vessels, inducing expression of leukocyte adhesion molecules[152,154,155], which leads to massive parenchymal infiltration of immune cells. These immune cells first enter the perivascular space surrounding postcapillary venules[156] and gain parenchymal access after breaking down the BM[157,158]. Limiting immune cell trafficking across the BBB has proven effective in treating MS. Natalizumab, which targets the α4 integrin on immune cells, preventing their interaction with endothelial VCAM1, greatly reduces new lesion formation[159].

It is critical to note that while leukocyte invasion is often assumed to be detrimental, leukocyte trafficking is required at low levels in order to limit infections. Of great interest is the identification of leukocyte adhesion molecules that facilitate the extravasation of only certain subsets of immune cells[160]. This could enable targeting pathological inflammation without rendering patients more vulnerable to infection. Indeed, ninjurin1 (NINJ1; monocytes), activated leukocyte cell adhesion molecule (ALCAM; CD4+ T cells, monocytes), junction adhesion molecule–like (JAML; monocytes, CD8+ T cells), and melanoma cell adhesion molecule (MCAM; CD8, T helper cell 17) regulate the entry of specific immune cell populations into the CNS[161-165]. It will be necessary to ensure that targeting these molecules does not produce secondary effects; *Alcam* knockout mice develop more severe EAE as ALCAM also enforces TJ integrity[166].

Many questions remain unanswered. How much of MS pathophysiology directly results from BBB dysfunction? Is there a subset of lesions caused by leakage while others have a different etiology? If these lesion subsets exist, do they vary with respect to severity and repair processes? Does the BBB interact with the lymphatic system to regulate leukocyte efflux during remission?

*Ischemia/stroke*

BBB dysfunction during stroke follows a biphasic time course. Leakage is evident within hours of the primary insult, is subsequently reduced, and then reappears the day after[167,168] (Fig 0.2E-F; 0.2H). An increase in transcytosis of nonspecific molecules is the first stage of dysfunction, followed by structural alteration of TJs[169]. Questions still remain regarding the importance of leukocyte infiltration in pathogenesis. Several reports have shown that leukocyte adhesion molecule knockouts or antibodies directed against leukocyte adhesion molecules minimize infarct volume[170-172], whereas others have not been able to replicate this effect[173].

Much of the cell death that leads to neurological deficits occurs in the days following a stroke; thus, the second phase of BBB leakage may be an important therapeutic target. Major outstanding questions in stroke research surround the relevance of this biphasic BBB dysfunction. It is unknown whether the first and second openings are mechanistically different; perhaps the first opening is due to dynamic signaling while the second results from changes in BBB gene expression.

*Epilepsy*

There is a clear association between epilepsy and BBB dysfunction. BBB leakage in epilepsy patients is visible with contrast-enhanced MRI[174-176] (Fig 0.2I), and analysis of brain tissue from epileptic patients shows increased parenchymal albumin[177,178], implicating blood-to-brain extravasation of large molecules. Furthermore, patient samples exhibit regional reduction in GLUT1[179], and positron emission tomography scans demonstrate decreased glucose uptake and metabolism in seizure foci[177,180].

BBB dysfunction itself may be epileptogenic or may help propagate seizures. Experimental disruption of the BBB with osmotic shock leads to seizures in patients[181], and diseases in which the BBB is compromised such as infection, inflammation, stroke, and traumatic brain injury can lead to seizures and epilepsy[182,183]. Furthermore, neuroinflammation has been hypothesized to be involved in seizure etiology; blockage of leukocyte-vascular interactions either pharmacologically or by genetic knockout inhibits both induction and recurrence of seizures[184]. Interestingly, patients with a BBB-GLUT1 deficiency develop epilepsy[185,186], demonstrating a critical role for BBB transport in normal brain function.

*Traumatic brain injury*

As in stroke, BBB dysfunction in TBI is biphasic, with leakage in rodent models starting and peaking in the hours following insult, improving by 24 hours, but then worsening again in the first days after injury[187,188]. Some have suggested that BBB permeability persists into a chronic stage in human patients; there is evidence of increased fibrinogen and immunoglobulin G years after injury[189]. As with stroke, a key outstanding question in TBI research is the importance of the biphasic BBB opening. It is still unclear how long the second opening lasts and to what extent it contributes to inflammation and chronic symptoms.

Another major outstanding question is whether mild head trauma, such as concussion, also leads to BBB dysfunction and how this may play a role in the progression of neurological symptoms. Several studies suggest that there is indeed leakage following activity-related concussions. BBB abnormalities were identified in 40% of football players analyzed with contrast-enhanced MRI[190], and single photon emission computed tomography showed BBB leakage in 75% of patients with post-concussion syndrome[191]. Elevated serum S100B levels have been used to identify BBB dysfunction and have been shown to correlate with MRI abnormalities and cognitive changes in football players who have sustained head injuries during games[192]. While BBB dysfunction is generally associated with harmful molecules penetrating the parenchyma, the leakage of CNS proteins into the blood might also be a cause for concern. It has been proposed that after TBI, S100B in the blood spurs the creation of auto-antibodies that increase inflammation[193]. Ultimately, it will be essential to identify novel serum markers of BBB dysfunction and/or noninvasive imaging techniques that allow for rapid determination of whether a head injury has damaged the neurovasculature, and how this affects the prognosis for downstream sequelae.

*Looking forward*

Several important questions remain regarding the BBB in the context of disease. How is each BBB property altered in neurological diseases, and how do these changes affect the extracellular environment of

the CNS? One problem is that different studies in humans or mouse models often use a single modality to detect BBB breakdown, whether sampling postmortem tissue, measuring markers in the CSF or blood, quantifying leakage of an exogenous tracer, or performing live imaging with a contrast agent. The BBB is not a single entity that is "open" or "shut," and moving forward, it is imperative to understand exactly how the complex physiology of the BBB changes in each disease. It is especially important to consider whether alterations are induced by the same or different signals across neurological conditions. If mechanistic similarities exist, it might be possible to design a therapeutic strategy applicable to a wide range of disorders[194]. Indeed, several molecular factors regulate BBB dysfunction in multiple diseases, including vascular endothelial growth factor[195,196], inflammatory cytokines (tumor necrosis factor α[197], interleukins 1 and 6[198-200]), reactive oxygen species[201-203], and matrix metalloproteinases[204,205]. However, there is also evidence that barrier dysfunction is due not only to "breakdown signals" but also to disrupted maintenance signals. Disruption of Wnt signaling can lead to vascular permeability and worse disease outcomes[103,206]; thus, increasing CNS endothelial cell Wnt signaling might have therapeutic potential.

Can subtle changes in different BBB properties cause specific neurological symptoms? Dysfunction in several BBB transporters causes specific developmental disorders[132-134], and there may be more undiscovered instances of this pattern. It is possible that regional heterogeneity at the BBB renders particular brain regions vulnerable to certain disease pathologies. For instance, if the BBB is indeed specialized to cater to the distinct nutrient and signaling needs of individual brain regions, loss of one of those BBB specializations might lead to deficits in local circuit function.

It is also important to also think beyond endothelial cells. Disruption of pericyte coverage leads to an increase in endothelial cell nonspecific transcytosis and leukocyte adhesion molecules expression, and it is unclear to what extent this drives neurological disease. Furthermore, disruption of astrocyte endfeet at the NVU would decrease glymphatic clearance, potentially contributing to pathological accumulation of proteins including Aβ. Future work analyzing how each cell type of the NVU, and the glycocalyx and BMs, is altered will be critical to understand the pathophysiology of different neurological diseases.

Another fundamental question is how the BBB is repaired. While the BBB becomes less permeable to molecular tracers at chronic phases of disease models, it is unclear whether there are functional or structural compromises made in the process of reversing leakiness. More work is needed to fully characterize the repaired BBB at the levels of physical integrity and transcriptomics. It is also unknown what endogenous signals induce BBB repair, and whether repair occurs cell-autonomously within endothelial cells or with mediation from other cell types. Interestingly, both microglia and reactive astrocytes regulate repair of the BBB in response to injury, highlighting the importance of the interactions of cells within the NVU[79,80,98].

**Concluding remarks**

The BBB is not a single entity, but rather a complex series of physiological properties allowing CNS endothelial cells to tightly regulate the extracellular environment of the parenchyma. These properties are vital for proper neural function, and dysfunction of the BBB can lead to critical pathology in many neurological diseases. However, more work is needed to understand exactly what crosses the healthy BBB, the degree to which the BBB dynamically responds to environmental stimuli, the extent of its regional heterogeneity, and the signaling mechanisms underlying its maintenance, disruption, and repair. As future research answers these questions and further reveals the cellular and molecular intricacies underlying the BBB, the clinical advantages will be twofold: a deeper knowledge of the BBB will provide therapeutic targets for BBB repair in a range of neurological conditions and will also enable more effective strategies for delivering drugs to the CNS.

## PART II: ENDOTHELIAL CELLS IN NEUROVASCULAR COUPLING

Proper brain function is dependent on a continuous supply of bloodborne oxygen and nutrients, such that a brief lapse in cerebral blood supply can have catastrophic consequences for brain health. While specific transporters are important for delivery of nutrients across the BBB, blood flow dynamics regulate how much of these nutrients are available for transport by altering the volume of blood traveling through the brain. Because neurons require a greater supply of oxygen and nutrients when active, there is increased local blood flow immediately following neuronal activity. This phenomenon is termed "neurovascular coupling" (NVC). The first indication that brain activity modulates blood flow came in the late 1800s[207-209]. In 1882, studying humans with skull defects, Mosso described an increase in brain volume upon certain mental and emotional stimuli, and he attributed this volume increase to blood flow dynamics[208,209]. In 1890, Roy and Sherrington observed cerebral expansion in dogs, cats, and rabbits in response to the stimulation of different nerves and application of various drugs. They surmised, "These facts seem to us to indicate the existence of an automatic mechanism by which the blood-supply of any part of the cerebral tissue is varied in accordance with the activity of the chemical changes which underlie the functional action of that part. Bearing in mind that strong evidence exists of localisation of function in the brain, we are of opinion that an automatic mechanism, of the kind just referred to, is well fitted to provide for a local variation of the blood-supply in accordance with local variations of the functional activity."[207] More than a century later, there is much known – and still much unknown – about the cellular and molecular mechanisms underlying NVC[210-212]. Studies have implicated several vasoactive ions and molecules in NVC, including potassium ions ($K^+$), nitric oxide, prostaglandin, neuropeptide Y, and vasoactive intestinal peptide, and both neurons and astrocytes are involved in initiating NVC signaling[209,211]. Smooth muscle cells (SMCs) are generally considered the primary target of these factors. SMCs line arteries and arterioles, forming a complete layer around them, and constriction or dilation of SMCs causes vasoconstriction or vasodilation in the underlying vessel. More recently, it has been suggested that pericytes on capillaries also help to regulate blood flow[61,213].

Endothelial cells were long considered passive players in the processes driving NVC, yet evidence now points to their having an active and important role in driving blood flow changes[214-217]. Our understanding of endothelial contributions to functional hyperemia is likely still in its infant stages. It appears as if different parts of the vascular tree possess distinct mechanisms for sensing and responding to neural activity, yet it remains unclear exactly how these various mechanisms work in concert in the context of functional hyperemia. In resistance arteries, activation of endothelial TRPV4 channels causes local $Ca^{2+}$ "sparklets" which activate intermediate-conductance (IK) and small-conductance (SK) $Ca^{2+}$-dependent $K^+$ channels[218]. The resulting $K^+$ influx hyperpolarizes endothelial cells and ultimately leads to vasodilation, likely via endothelial-SMC signaling and SMC relaxation.

While penetrating arterioles control blood flow to an expansive web of downstream capillary beds[219], these larger, sparser vessels are not necessarily in the best position to quickly sense local neural activity. Capillaries, on the other hand, form a dense network throughout the brain such that an active neuron is never far from the nearest capillary. Thus, it makes sense that capillaries would somehow signal to upstream vessels and their associated SMCs to increase local blood flow. While there is some controversy in the field regarding at what branching point an "arteriole" becomes a "capillary", it is clear that smaller vessels dilate before penetrating arterioles[220] and that neural activity causes hyperpolarization in capillaries, an electric signal that travels upstream to cause arteriolar dilation[216,221]. In an elegant study, Longden and Dabertrand et al. showed that extracellular $K^+$ applied directly to capillaries causes hyperpolarization via activation of the endothelial inward-rectifying $K^+$ channel $K_{IR}2.1$. This hyperpolarization propagates upstream via endothelial gap junctions and causes dilation of upstream arterioles, likely through the relaxation of associated SMCs[216,222]. Prostaglandin $E_2$ ($PGE_2$) or TRPA1 agonist application to capillaries also causes upstream arteriole dilation, albeit with a slower onset and time-to-peak dilation compared to $K^+$ stimulation[221,223].

Not only is the field still uncovering the extent of an active role for endothelial cells in NVC, but the mechanisms regulating this endothelial signaling are largely unknown. Interestingly, high concentrations (>25 mM) of $K^+$ applied to capillaries do not cause arteriole dilation[216], suggesting a

regulatory mechanism is in place to prevent excessive arteriole dilation in case of pathologically high levels of neural activity, for instance during seizures. Indeed, activation of $G_q$ protein-coupled receptor ($G_q$PCR) channels by several ligands leads to the decay of $K^+$-mediated currents in endothelial cells through the depletion of phosphatidylinositol 4,5-biphosphate ($PIP_2$)[224], shedding light on one such internal regulatory mechanism.

NVC is compromised in age[225-228] and in people with small vessel disease (SVD)[229-231] and Alzheimer's disease (AD)[232,233], such that neural activity elicits a weaker blood flow response. NVC deficits have also been observed in mouse models of SVD[234,235] and AD[236-240]. As NVC is critically important for supporting neuronal activity, NVC deficits can contribute to cognitive impairment[241]. Thus, gaining a more thorough understanding of NVC will help inform therapeutic strategies for rescuing cognitive dysfunction in AD and other neurodegenerative diseases.

_____

This thesis explores the cellular and molecular characteristics of brain endothelial function and dysfunction. The first chapter identifies a marker for BBB dysfunction during disease, characterizes its expression pattern throughout several disease models, and explores its function. The second chapter assesses BBB structure, function, and transcriptome in the absence of microglia, the brain's resident immune cell. The third chapter describes a novel function for cholesterol in regulating neurovascular coupling in endothelial cells.

**Acknowledgements**

Part I of the Introduction is a reprint of the material as it appears in Profaci CP, Munji RM, Pulido RS, Daneman R (2020). The blood-brain barrier in health and disease: Important unanswered questions. *Journal of Experimental Medicine* Apr 6;217(4). The dissertation author was the first author of this review article. The figures have been slightly modified here, and the section on traumatic brain injury has been added.

**References**


1 Saunders, N. R., Ek, C. J., Habgood, M. D. & Dziegielewska, K. M. Barriers in the brain: a renaissance? *Trends Neurosci* **31**, 279-286, doi:10.1016/j.tins.2008.03.003 (2008).

2 Zlokovic, B. V. The blood-brain barrier in health and chronic neurodegenerative disorders. *Neuron* **57**, 178-201, doi:10.1016/j.neuron.2008.01.003 (2008).

3 Obermeier, B., Daneman, R. & Ransohoff, R. M. Development, maintenance and disruption of the blood-brain barrier. *Nat Med* **19**, 1584-1596, doi:10.1038/nm.3407 (2013).

4 Hawkins, B. T. & Davis, T. P. The blood-brain barrier/neurovascular unit in health and disease. *Pharmacol Rev* **57**, 173-185, doi:10.1124/pr.57.2.4 (2005).

5 Aird, W. C. Phenotypic heterogeneity of the endothelium: I. Structure, function, and mechanisms. *Circ Res* **100**, 158-173, doi:10.1161/01.RES.0000255691.76142.4a (2007).

6 Biswas, P., Canosa, S., Schoenfeld, D., Schoenfeld, J., Li, P., Cheas, L. C., Zhang, J., Cordova, A., Sumpio, B. & Madri, J. A. PECAM-1 affects GSK-3beta-mediated beta-catenin phosphorylation and degradation. *Am J Pathol* **169**, 314-324, doi:10.2353/ajpath.2006.051112 (2006).

7 Privratsky, J. R. & Newman, P. J. PECAM-1: regulator of endothelial junctional integrity. *Cell Tissue Res* **355**, 607-619, doi:10.1007/s00441-013-1779-3 (2014).

8 Furuse, M. Molecular basis of the core structure of tight junctions. *Cold Spring Harb Perspect Biol* **2**, a002907, doi:10.1101/cshperspect.a002907 (2010).

9 Furuse, M., Sasaki, H. & Tsukita, S. Manner of interaction of heterogeneous claudin species within and between tight junction strands. *J Cell Biol* **147**, 891-903, doi:10.1083/jcb.147.4.891 (1999).

10 Amasheh, S., Schmidt, T., Mahn, M., Florian, P., Mankertz, J., Tavalali, S., Gitter, A. H., Schulzke, J. D. & Fromm, M. Contribution of claudin-5 to barrier properties in tight junctions of epithelial cells. *Cell Tissue Res* **321**, 89-96 (2005).

11 Hou, J., Gomes, A. S., Paul, D. L. & Goodenough, D. A. Study of claudin function by RNA interference. *J Biol Chem* **281**, 36117-36123, doi:10.1074/jbc.M608853200 (2006).

12 Morita, K., Sasaki, H., Furuse, M. & Tsukita, S. Endothelial claudin: claudin-5/TMVCF constitutes tight junction strands in endothelial cells. *J Cell Biol* **147**, 185-194, doi:10.1083/jcb.147.1.185 (1999).

13 Nitta, T., Hata, M., Gotoh, S., Seo, Y., Sasaki, H., Hashimoto, N., Furuse, M. & Tsukita, S. Size-selective loosening of the blood-brain barrier in claudin-5-deficient mice. *J Cell Biol* **161**, 653-660, doi:10.1083/jcb.200302070 (2003).

14 Umeda, K., Matsui, T., Nakayama, M., Furuse, K., Sasaki, H., Furuse, M. & Tsukita, S. Establishment and characterization of cultured epithelial cells lacking expression of ZO-1. *J Biol Chem* **279**, 44785-44794, doi:10.1074/jbc.M406563200 (2004).

15 Sawada, N. Tight junction-related human diseases. *Pathol Int* **63**, 1-12, doi:10.1111/pin.12021 (2013).

16 Tietz, S. & Engelhardt, B. Brain barriers: Crosstalk between complex tight junctions and adherens junctions. *J Cell Biol* **209**, 493-506, doi:10.1083/jcb.201412147 (2015).

17 Daneman, R., Zhou, L., Agalliu, D., Cahoy, J. D., Kaushal, A. & Barres, B. A. The mouse blood-brain barrier transcriptome: a new resource for understanding the development and function of brain endothelial cells. *PLoS One* **5**, e13741, doi:10.1371/journal.pone.0013741 (2010).

18 Sohet, F., Lin, C., Munji, R. N., Lee, S. Y., Ruderisch, N., Soung, A., Arnold, T. D., Derugin, N., Vexler, Z. S., Yen, F. T. & Daneman, R. LSR/angulin-1 is a tricellular tight junction protein involved in blood-brain barrier formation. *J Cell Biol* **208**, 703-711, doi:10.1083/jcb.201410131 (2015).

19 Aird, W. C. Phenotypic heterogeneity of the endothelium: II. Representative vascular beds. *Circ Res* **100**, 174-190, doi:10.1161/01.RES.0000255690.03436.ae (2007).

20 Ben-Zvi, A., Lacoste, B., Kur, E., Andreone, B. J., Mayshar, Y., Yan, H. & Gu, C. Mfsd2a is critical for the formation and function of the blood-brain barrier. *Nature* **509**, 507-511, doi:10.1038/nature13324 (2014).

21 Nguyen, L. N., Ma, D., Shui, G., Wong, P., Cazenave-Gassiot, A., Zhang, X., Wenk, M. R., Goh, E. L. & Silver, D. L. Mfsd2a is a transporter for the essential omega-3 fatty acid docosahexaenoic acid. *Nature* **509**, 503-506, doi:10.1038/nature13241 (2014).

22 Andreone, B. J., Chow, B. W., Tata, A., Lacoste, B., Ben-Zvi, A., Bullock, K., Deik, A. A., Ginty, D. D., Clish, C. B. & Gu, C. Blood-Brain Barrier Permeability Is Regulated by Lipid Transport-Dependent Suppression of Caveolae-Mediated Transcytosis. *Neuron* **94**, 581-594 e585, doi:10.1016/j.neuron.2017.03.043 (2017).

23 Hallmann, R., Mayer, D. N., Berg, E. L., Broermann, R. & Butcher, E. C. Novel mouse endothelial cell surface marker is suppressed during differentiation of the blood brain barrier. *Dev Dyn* **202**, 325-332, doi:10.1002/aja.1002020402 (1995).

24 Hnasko, R., McFarland, M. & Ben-Jonathan, N. Distribution and characterization of plasmalemma vesicle protein-1 in rat endocrine glands. *J Endocrinol* **175**, 649-661 (2002).

25 Chow, B. W. & Gu, C. Gradual Suppression of Transcytosis Governs Functional Blood-Retinal Barrier Formation. *Neuron* **93**, 1325-1333 e1323, doi:10.1016/j.neuron.2017.02.043 (2017).

26 Miller, D. S. Regulation of ABC transporters at the blood-brain barrier. *Clin Pharmacol Ther* **97**, 395-403, doi:10.1002/cpt.64 (2015).

27 Strazielle, N. & Ghersi-Egea, J. F. Efflux transporters in blood-brain interfaces of the developing brain. *Front Neurosci* **9**, 21, doi:10.3389/fnins.2015.00021 (2015).

28 Nalecz, K. A. Solute Carriers in the Blood-Brain Barier: Safety in Abundance. *Neurochem Res* **42**, 795-809, doi:10.1007/s11064-016-2030-x (2017).

29 Shen, S. & Zhang, W. ABC transporters and drug efflux at the blood-brain barrier. *Rev Neurosci* **21**, 29-53, doi:10.1515/revneuro.2010.21.1.29 (2010).

30 Hindle, S. J., Munji, R. N., Dolghih, E., Gaskins, G., Orng, S., Ishimoto, H., Soung, A., DeSalvo, M., Kitamoto, T., Keiser, M. J., Jacobson, M. P., Daneman, R. & Bainton, R. J. Evolutionarily Conserved Roles for Blood-Brain Barrier Xenobiotic Transporters in Endogenous Steroid Partitioning and Behavior. *Cell Rep* **21**, 1304-1316, doi:10.1016/j.celrep.2017.10.026 (2017).

31 Simpson, I. A., Carruthers, A. & Vannucci, S. J. Supply and demand in cerebral energy metabolism: the role of nutrient transporters. *J Cereb Blood Flow Metab* **27**, 1766-1791, doi:10.1038/sj.jcbfm.9600521 (2007).

32 Cornford, E. M., Hyman, S. & Swartz, B. E. The human brain GLUT1 glucose transporter: ultrastructural localization to the blood-brain barrier endothelia. *J Cereb Blood Flow Metab* **14**, 106-112, doi:10.1038/jcbfm.1994.15 (1994).

33 Boado, R. J., Li, J. Y., Nagaya, M., Zhang, C. & Pardridge, W. M. Selective expression of the large neutral amino acid transporter at the blood-brain barrier. *Proc Natl Acad Sci U S A* **96**, 12079-12084, doi:10.1073/pnas.96.21.12079 (1999).

34 Kido, Y., Tamai, I., Okamoto, M., Suzuki, F. & Tsuji, A. Functional clarification of MCT1-mediated transport of monocarboxylic acids at the blood-brain barrier using in vitro cultured cells and in vivo BUI studies. *Pharm Res* **17**, 55-62 (2000).

35 Jefferies, W. A., Brandon, M. R., Hunt, S. V., Williams, A. F., Gatter, K. C. & Mason, D. Y. Transferrin receptor on endothelium of brain capillaries. *Nature* **312**, 162-163 (1984).

36 Meresse, S., Delbart, C., Fruchart, J. C. & Cecchelli, R. Low-density lipoprotein receptor on endothelium of brain capillaries. *J Neurochem* **53**, 340-345 (1989).

37 Shibata, M., Yamada, S., Kumar, S. R., Calero, M., Bading, J., Frangione, B., Holtzman, D. M., Miller, C. A., Strickland, D. K., Ghiso, J. & Zlokovic, B. V. Clearance of Alzheimer's amyloid-ss(1-40) peptide from brain by LDL receptor-related protein-1 at the blood-brain barrier. *J Clin Invest* **106**, 1489-1499, doi:10.1172/JCI10498 (2000).

38 Storck, S. E., Meister, S., Nahrath, J., Meissner, J. N., Schubert, N., Di Spiezio, A., Baches, S., Vandenbroucke, R. E., Bouter, Y., Prikulis, I., Korth, C., Weggen, S., Heimann, A., Schwaninger, M., Bayer, T. A. & Pietrzik, C. U. Endothelial LRP1 transports amyloid-beta(1-42) across the blood-brain barrier. *J Clin Invest* **126**, 123-136, doi:10.1172/JCI81108 (2016).

39 Bevilacqua, M. P. Endothelial-leukocyte adhesion molecules. *Annu Rev Immunol* **11**, 767-804, doi:10.1146/annurev.iy.11.040193.004003 (1993).

40 Ransohoff, R. M. & Engelhardt, B. The anatomical and cellular basis of immune surveillance in the central nervous system. *Nat Rev Immunol* **12**, 623-635, doi:10.1038/nri3265 (2012).

41 Kipnis, J., Gadani, S. & Derecki, N. C. Pro-cognitive properties of T cells. *Nat Rev Immunol* **12**, 663-669, doi:10.1038/nri3280 (2012).

42 Shechter, R., London, A. & Schwartz, M. Orchestrated leukocyte recruitment to immune-privileged sites: absolute barriers versus educational gates. *Nat Rev Immunol* **13**, 206-218, doi:10.1038/nri3391 (2013).

43 Ausprunk, D. H., Boudreau, C. L. & Nelson, D. A. Proteoglycans in the microvasculature. I. Histochemical localization in microvessels of the rabbit eye. *Am J Pathol* **103**, 353-366 (1981).

44 Ausprunk, D. H., Boudreau, C. L. & Nelson, D. A. Proteoglycans in the microvascular. II. Histochemical localization in proliferating capillaries of the rabbit cornea. *Am J Pathol* **103**, 367-375 (1981).

45 Pillinger, N. L. & Kam, P. Endothelial glycocalyx: basic science and clinical implications. *Anaesth Intensive Care* **45**, 295-307, doi:10.1177/0310057X1704500305 (2017).

46 Ando, Y., Okada, H., Takemura, G., Suzuki, K., Takada, C., Tomita, H., Zaikokuji, R., Hotta, Y., Miyazaki, N., Yano, H., Muraki, I., Kuroda, A., Fukuda, H., Kawasaki, Y., Okamoto, H., Kawaguchi, T., Watanabe, T., Doi, T., Yoshida, T., Ushikoshi, H., Yoshida, S. & Ogura, S. Brain-Specific Ultrastructure of Capillary Endothelial Glycocalyx and Its Possible Contribution for Blood Brain Barrier. *Sci Rep* **8**, 17523, doi:10.1038/s41598-018-35976-2 (2018).

47 Kutuzov, N., Flyvbjerg, H. & Lauritzen, M. Contributions of the glycocalyx, endothelium, and extravascular compartment to the blood-brain barrier. *Proc Natl Acad Sci U S A* **115**, E9429-E9438, doi:10.1073/pnas.1802155115 (2018).

48 DellaValle, B., Hasseldam, H., Johansen, F. F., Iversen, H. K., Rungby, J. & Hempel, C. Multiple Soluble Components of the Glycocalyx Are Increased in Patient Plasma After Ischemic Stroke. *Stroke* **50**, 2948-2951, doi:10.1161/STROKEAHA.119.025953 (2019).

49 Zhu, J., Li, X., Yin, J., Hu, Y., Gu, Y. & Pan, S. Glycocalyx degradation leads to blood-brain barrier dysfunction and brain edema after asphyxia cardiac arrest in rats. *J Cereb Blood Flow Metab* **38**, 1979-1992, doi:10.1177/0271678X17726062 (2018).

50 Del Zoppo, G. J., Milner, R., Mabuchi, T., Hung, S., Wang, X. & Koziol, J. A. Vascular matrix adhesion and the blood-brain barrier. *Biochem Soc Trans* **34**, 1261-1266, doi:10.1042/BST0341261 (2006).

51 Sorokin, L. The impact of the extracellular matrix on inflammation. *Nat Rev Immunol* **10**, 712-723, doi:10.1038/nri2852 (2010).

52 Engelhardt, B. & Ransohoff, R. M. Capture, crawl, cross: the T cell code to breach the blood-brain barriers. *Trends Immunol* **33**, 579-589, doi:10.1016/j.it.2012.07.004 (2012).

53 Smyth, L. C. D., Rustenhoven, J., Scotter, E. L., Schweder, P., Faull, R. L. M., Park, T. I. H. & Dragunow, M. Markers for human brain pericytes and smooth muscle cells. *J Chem Neuroanat* **92**, 48-60, doi:10.1016/j.jchemneu.2018.06.001 (2018).

54 Armulik, A., Genove, G. & Betsholtz, C. Pericytes: developmental, physiological, and pathological perspectives, problems, and promises. *Dev Cell* **21**, 193-215, doi:10.1016/j.devcel.2011.07.001 (2011).

55 Vanlandewijck, M., He, L., Mae, M. A., Andrae, J., Ando, K., Del Gaudio, F., Nahar, K., Lebouvier, T., Lavina, B., Gouveia, L., Sun, Y., Raschperger, E., Rasanen, M., Zarb, Y., Mochizuki, N., Keller, A., Lendahl, U. & Betsholtz, C. A molecular atlas of cell types and zonation in the brain vasculature. *Nature* **554**, 475-480, doi:10.1038/nature25739 (2018).

56 Daneman, R., Zhou, L., Kebede, A. A. & Barres, B. A. Pericytes are required for blood-brain barrier integrity during embryogenesis. *Nature* **468**, 562-566, doi:10.1038/nature09513 (2010).

57 Armulik, A., Abramsson, A. & Betsholtz, C. Endothelial/pericyte interactions. *Circ Res* **97**, 512-523, doi:10.1161/01.RES.0000182903.16652.d7 (2005).

58 Armulik, A., Genove, G., Mae, M., Nisancioglu, M. H., Wallgard, E., Niaudet, C., He, L., Norlin, J., Lindblom, P., Strittmatter, K., Johansson, B. R. & Betsholtz, C. Pericytes regulate the blood-brain barrier. *Nature* **468**, 557-561, doi:10.1038/nature09522 (2010).

59 Winkler, E. A., Bell, R. D. & Zlokovic, B. V. Central nervous system pericytes in health and disease. *Nat Neurosci* **14**, 1398-1405, doi:10.1038/nn.2946 (2011).

60 Takano, T., Tian, G. F., Peng, W., Lou, N., Libionka, W., Han, X. & Nedergaard, M. Astrocyte-mediated control of cerebral blood flow. *Nat Neurosci* **9**, 260-267, doi:10.1038/nn1623 (2006).

61 Mishra, A., Reynolds, J. P., Chen, Y., Gourine, A. V., Rusakov, D. A. & Attwell, D. Astrocytes mediate neurovascular signaling to capillary pericytes but not to arterioles. *Nat Neurosci* **19**, 1619-1627, doi:10.1038/nn.4428 (2016).

62 Abbott, N. J., Pizzo, M. E., Preston, J. E., Janigro, D. & Thorne, R. G. The role of brain barriers in fluid movement in the CNS: is there a 'glymphatic' system? *Acta Neuropathol* **135**, 387-407, doi:10.1007/s00401-018-1812-4 (2018).

63 Hladky, S. B. & Barrand, M. A. Is solute movement within the extracellular spaces of brain gray matter brought about primarily by diffusion or flow? A commentary on "Analysis of convective and diffusive transport in the brain interstitium" Fluids and Barriers of the CNS (2019) 16:6 by L. Ray, J.J. Iliff and J.J. Heys. *Fluids Barriers CNS* **16**, 24, doi:10.1186/s12987-019-0141-x (2019).

64 Iliff, J. J., Wang, M., Liao, Y., Plogg, B. A., Peng, W., Gundersen, G. A., Benveniste, H., Vates, G. E., Deane, R., Goldman, S. A., Nagelhus, E. A. & Nedergaard, M. A paravascular pathway facilitates CSF flow through the brain parenchyma and the clearance of interstitial solutes, including amyloid beta. *Sci Transl Med* **4**, 147ra111, doi:10.1126/scitranslmed.3003748 (2012).

65 Xie, L., Kang, H., Xu, Q., Chen, M. J., Liao, Y., Thiyagarajan, M., O'Donnell, J., Christensen, D. J., Nicholson, C., Iliff, J. J., Takano, T., Deane, R. & Nedergaard, M. Sleep drives metabolite clearance from the adult brain. *Science* **342**, 373-377, doi:10.1126/science.1241224 (2013).

66 Mestre, H., Hablitz, L. M., Xavier, A. L., Feng, W., Zou, W., Pu, T., Monai, H., Murlidharan, G., Castellanos Rivera, R. M., Simon, M. J., Pike, M. M., Pla, V., Du, T., Kress, B. T., Wang, X., Plog, B. A., Thrane, A. S., Lundgaard, I., Abe, Y., Yasui, M., Thomas, J. H., Xiao, M., Hirase, H., Asokan, A., Iliff, J. J. & Nedergaard, M. Aquaporin-4-dependent glymphatic solute transport in the rodent brain. *Elife* **7**, doi:10.7554/eLife.40070 (2018).

67 Meng, Y., Abrahao, A., Heyn, C. C., Bethune, A. J., Huang, Y., Pople, C., Aubert, I., Hamani, C., Zinman, L., Hynynen, K., Black, S. E. & Lipsman, N. Glymphatics visualization after focused ultrasound induced blood-brain barrier opening in humans. *Ann Neurol*, doi:10.1002/ana.25604 (2019).

68 Fultz, N. E., Bonmassar, G., Setsompop, K., Stickgold, R. A., Rosen, B. R., Polimeni, J. R. & Lewis, L. D. Coupled electrophysiological, hemodynamic, and cerebrospinal fluid oscillations in human sleep. *Science* **366**, 628-631, doi:10.1126/science.aax5440 (2019).

69 Haj-Yasein, N. N., Vindedal, G. F., Eilert-Olsen, M., Gundersen, G. A., Skare, O., Laake, P., Klungland, A., Thoren, A. E., Burkhardt, J. M., Ottersen, O. P. & Nagelhus, E. A. Glial-conditional deletion of aquaporin-4 (Aqp4) reduces blood-brain water uptake and confers barrier function on perivascular astrocyte endfeet. *Proc Natl Acad Sci U S A* **108**, 17815-17820, doi:10.1073/pnas.1110655108 (2011).

70 Kierdorf, K., Masuda, T., Jordao, M. J. C. & Prinz, M. Macrophages at CNS interfaces: ontogeny and function in health and disease. *Nat Rev Neurosci*, doi:10.1038/s41583-019-0201-x (2019).

71 Jordao, M. J. C., Sankowski, R., Brendecke, S. M., Sagar, Locatelli, G., Tai, Y. H., Tay, T. L., Schramm, E., Armbruster, S., Hagemeyer, N., Gross, O., Mai, D., Cicek, O., Falk, T., Kerschensteiner, M., Grun, D. & Prinz, M. Single-cell profiling identifies myeloid cell subsets with distinct fates during neuroinflammation. *Science* **363**, doi:10.1126/science.aat7554 (2019).

72 Hickey, W. F. & Kimura, H. Perivascular microglial cells of the CNS are bone marrow-derived and present antigen in vivo. *Science* **239**, 290-292 (1988).

73 Prinz, M., Erny, D. & Hagemeyer, N. Ontogeny and homeostasis of CNS myeloid cells. *Nat Immunol* **18**, 385-392, doi:10.1038/ni.3703 (2017).

74 Takahashi, K., Yamamura, F. & Naito, M. Differentiation, maturation, and proliferation of macrophages in the mouse yolk sac: a light-microscopic, enzyme-cytochemical, immunohistochemical, and ultrastructural study. *J Leukoc Biol* **45**, 87-96, doi:10.1002/jlb.45.2.87 (1989).

75 Alliot, F., Godin, I. & Pessac, B. Microglia derive from progenitors, originating from the yolk sac, and which proliferate in the brain. *Brain Res Dev Brain Res* **117**, 145-152, doi:10.1016/s0165-3806(99)00113-3 (1999).

76 Ginhoux, F., Greter, M., Leboeuf, M., Nandi, S., See, P., Gokhan, S., Mehler, M. F., Conway, S. J., Ng, L. G., Stanley, E. R., Samokhvalov, I. M. & Merad, M. Fate mapping analysis reveals that adult microglia derive from primitive macrophages. *Science* **330**, 841-845, doi:10.1126/science.1194637 (2010).

77 Streit, W. J., Conde, J. R., Fendrick, S. E., Flanary, B. E. & Mariani, C. L. Role of microglia in the central nervous system's immune response. *Neurol Res* **27**, 685-691, doi:10.1179/016164105X49463 (2005).

78 Prinz, M., Priller, J., Sisodia, S. S. & Ransohoff, R. M. Heterogeneity of CNS myeloid cells and their roles in neurodegeneration. *Nat Neurosci* **14**, 1227-1235, doi:10.1038/nn.2923 (2011).

79 Fernandez-Lopez, D., Faustino, J., Klibanov, A. L., Derugin, N., Blanchard, E., Simon, F., Leib, S. L. & Vexler, Z. S. Microglial Cells Prevent Hemorrhage in Neonatal Focal Arterial Stroke. *J Neurosci* **36**, 2881-2893, doi:10.1523/JNEUROSCI.0140-15.2016 (2016).

80 Lou, N., Takano, T., Pei, Y., Xavier, A. L., Goldman, S. A. & Nedergaard, M. Purinergic receptor P2RY12-dependent microglial closure of the injured blood-brain barrier. *Proc Natl Acad Sci U S A* **113**, 1074-1079, doi:10.1073/pnas.1520398113 (2016).

81 Hudson, L. C., Bragg, D. C., Tompkins, M. B. & Meeker, R. B. Astrocytes and microglia differentially regulate trafficking of lymphocyte subsets across brain endothelial cells. *Brain Res* **1058**, 148-160, doi:10.1016/j.brainres.2005.07.071 (2005).

82 Persidsky, Y., Ghorpade, A., Rasmussen, J., Limoges, J., Liu, X. J., Stins, M., Fiala, M., Way, D., Kim, K. S., Witte, M. H., Weinand, M., Carhart, L. & Gendelman, H. E. Microglial and astrocyte chemokines regulate monocyte migration through the blood-brain barrier in human immunodeficiency virus-1 encephalitis. *Am J Pathol* **155**, 1599-1611, doi:10.1016/S0002-9440(10)65476-4 (1999).

83 Aydin, S., Pareja, J., Schallenberg, V. M., Klopstein, A., Gruber, T., Page, N., Kaba, E., Deutsch, U., Johnson, A. J., Schenk, M., Merkler, D. & Engelhardt, B. Brain endothelial antigen presentation detains $CD8^+$ T cells at the blood-brain barrier leading to its breakdown. *bioRxiv*, 2021.2010.2012.464035, doi:10.1101/2021.10.12.464035 (2021).

84 Yu, Y. J. & Watts, R. J. Developing therapeutic antibodies for neurodegenerative disease. *Neurotherapeutics* **10**, 459-472, doi:10.1007/s13311-013-0187-4 (2013).

85 Poduslo, J. F., Curran, G. L. & Berg, C. T. Macromolecular permeability across the blood-nerve and blood-brain barriers. *Proc Natl Acad Sci U S A* **91**, 5705-5709, doi:10.1073/pnas.91.12.5705 (1994).

86 Macdonald, J. A., Murugesan, N. & Pachter, J. S. Endothelial cell heterogeneity of blood-brain barrier gene expression along the cerebral microvasculature. *J Neurosci Res* **88**, 1457-1474, doi:10.1002/jnr.22316 (2010).

87 Murugesan, N., Macdonald, J. A., Lu, Q., Wu, S. L., Hancock, W. S. & Pachter, J. S. Analysis of mouse brain microvascular endothelium using laser capture microdissection coupled with proteomics. *Methods Mol Biol* **686**, 297-311, doi:10.1007/978-1-60761-938-3_14 (2011).

88 Gross, P. M. Circumventricular organ capillaries. *Prog Brain Res* **91**, 219-233 (1992).

89 Blanchette, M. & Daneman, R. Formation and maintenance of the BBB. *Mech Dev* **138 Pt 1**, 8-16, doi:10.1016/j.mod.2015.07.007 (2015).

90 Stewart, P. A. & Wiley, M. J. Developing nervous tissue induces formation of blood-brain barrier characteristics in invading endothelial cells: a study using quail--chick transplantation chimeras. *Dev Biol* **84**, 183-192 (1981).

91 Janzer, R. C. & Raff, M. C. Astrocytes induce blood-brain barrier properties in endothelial cells. *Nature* **325**, 253-257, doi:10.1038/325253a0 (1987).

92 Alvarez, J. I., Dodelet-Devillers, A., Kebir, H., Ifergan, I., Fabre, P. J., Terouz, S., Sabbagh, M., Wosik, K., Bourbonniere, L., Bernard, M., van Horssen, J., de Vries, H. E., Charron, F. & Prat, A. The Hedgehog pathway promotes blood-brain barrier integrity and CNS immune quiescence. *Science* **334**, 1727-1731, doi:10.1126/science.1206936 (2011).

93 Sobue, K., Yamamoto, N., Yoneda, K., Hodgson, M. E., Yamashiro, K., Tsuruoka, N., Tsuda, T., Katsuya, H., Miura, Y., Asai, K. & Kato, T. Induction of blood-brain barrier properties in immortalized bovine brain endothelial cells by astrocytic factors. *Neurosci Res* **35**, 155-164 (1999).

94 Wosik, K., Cayrol, R., Dodelet-Devillers, A., Berthelet, F., Bernard, M., Moumdjian, R., Bouthillier, A., Reudelhuber, T. L. & Prat, A. Angiotensin II controls occludin function and is required for blood brain barrier maintenance: relevance to multiple sclerosis. *J Neurosci* **27**, 9032-9042, doi:10.1523/JNEUROSCI.2088-07.2007 (2007).

95 Sauvageot, C. M. & Stiles, C. D. Molecular mechanisms controlling cortical gliogenesis. *Curr Opin Neurobiol* **12**, 244-249, doi:10.1016/s0959-4388(02)00322-7 (2002).

96 Saunders, N. R., Dziegielewska, K. M., Unsicker, K. & Ek, C. J. Delayed astrocytic contact with cerebral blood vessels in FGF-2 deficient mice does not compromise permeability properties at the developing blood-brain barrier. *Dev Neurobiol* **76**, 1201-1212, doi:10.1002/dneu.22383 (2016).

97 Kubotera, H., Ikeshima-Kataoka, H., Hatashita, Y., Allegra Mascaro, A. L., Pavone, F. S. & Inoue, T. Astrocytic endfeet re-cover blood vessels after removal by laser ablation. *Sci Rep* **9**, 1263, doi:10.1038/s41598-018-37419-4 (2019).

98 Bush, T. G., Puvanachandra, N., Horner, C. H., Polito, A., Ostenfeld, T., Svendsen, C. N., Mucke, L., Johnson, M. H. & Sofroniew, M. V. Leukocyte infiltration, neuronal degeneration, and neurite outgrowth after ablation of scar-forming, reactive astrocytes in adult transgenic mice. *Neuron* **23**, 297-308 (1999).

99 Daneman, R., Agalliu, D., Zhou, L., Kuhnert, F., Kuo, C. J. & Barres, B. A. Wnt/beta-catenin signaling is required for CNS, but not non-CNS, angiogenesis. *Proc Natl Acad Sci U S A* **106**, 641-646, doi:10.1073/pnas.0805165106 (2009).

100 Liebner, S., Corada, M., Bangsow, T., Babbage, J., Taddei, A., Czupalla, C. J., Reis, M., Felici, A., Wolburg, H., Fruttiger, M., Taketo, M. M., von Melchner, H., Plate, K. H., Gerhardt, H. & Dejana, E. Wnt/beta-catenin signaling controls development of the blood-brain barrier. *J Cell Biol* **183**, 409-417, doi:10.1083/jcb.200806024 (2008).

101 Stenman, J. M., Rajagopal, J., Carroll, T. J., Ishibashi, M., McMahon, J. & McMahon, A. P. Canonical Wnt signaling regulates organ-specific assembly and differentiation of CNS vasculature. *Science* **322**, 1247-1250, doi:10.1126/science.1164594 (2008).

102 Ye, X., Wang, Y., Cahill, H., Yu, M., Badea, T. C., Smallwood, P. M., Peachey, N. S. & Nathans, J. Norrin, frizzled-4, and Lrp5 signaling in endothelial cells controls a genetic program for retinal vascularization. *Cell* **139**, 285-298, doi:10.1016/j.cell.2009.07.047 (2009).

103 Wang, Y., Rattner, A., Zhou, Y., Williams, J., Smallwood, P. M. & Nathans, J. Norrin/Frizzled4 signaling in retinal vascular development and blood brain barrier plasticity. *Cell* **151**, 1332-1344, doi:10.1016/j.cell.2012.10.042 (2012).

104 Zhou, Y. & Nathans, J. Gpr124 controls CNS angiogenesis and blood-brain barrier integrity by promoting ligand-specific canonical wnt signaling. *Dev Cell* **31**, 248-256, doi:10.1016/j.devcel.2014.08.018 (2014).

105 Cho, C., Smallwood, P. M. & Nathans, J. Reck and Gpr124 Are Essential Receptor Cofactors for Wnt7a/Wnt7b-Specific Signaling in Mammalian CNS Angiogenesis and Blood-Brain Barrier Regulation. *Neuron* **95**, 1056-1073 e1055, doi:10.1016/j.neuron.2017.07.031 (2017).

106 Benz, F., Wichitnaowarat, V., Lehmann, M., Germano, R. F., Mihova, D., Macas, J., Adams, R. H., Taketo, M. M., Plate, K. H., Guerit, S., Vanhollebeke, B. & Liebner, S. Low wnt/beta-catenin signaling determines leaky vessels in the subfornical organ and affects water homeostasis in mice. *Elife* **8**, doi:10.7554/eLife.43818 (2019).

107 Wang, Y., Sabbagh, M. F., Gu, X., Rattner, A., Williams, J. & Nathans, J. Beta-catenin signaling regulates barrier-specific gene expression in circumventricular organ and ocular vasculatures. *Elife* **8**, doi:10.7554/eLife.43257 (2019).

108 Reis, M., Czupalla, C. J., Ziegler, N., Devraj, K., Zinke, J., Seidel, S., Heck, R., Thom, S., Macas, J., Bockamp, E., Fruttiger, M., Taketo, M. M., Dimmeler, S., Plate, K. H. & Liebner, S. Endothelial Wnt/beta-catenin signaling inhibits glioma angiogenesis and normalizes tumor blood vessels by inducing PDGF-B expression. *J Exp Med* **209**, 1611-1627, doi:10.1084/jem.20111580 (2012).

109 Wang, Y., Cho, C., Williams, J., Smallwood, P. M., Zhang, C., Junge, H. J. & Nathans, J. Interplay of the Norrin and Wnt7a/Wnt7b signaling systems in blood-brain barrier and blood-retina barrier development and maintenance. *Proc Natl Acad Sci U S A* **115**, E11827-E11836, doi:10.1073/pnas.1813217115 (2018).

110 Hrvatin, S., Hochbaum, D. R., Nagy, M. A., Cicconet, M., Robertson, K., Cheadle, L., Zilionis, R., Ratner, A., Borges-Monroy, R., Klein, A. M., Sabatini, B. L. & Greenberg, M. E. Single-cell analysis of experience-dependent transcriptomic states in the mouse visual cortex. *Nat Neurosci* **21**, 120-129, doi:10.1038/s41593-017-0029-5 (2018).

111 Nishijima, T., Piriz, J., Duflot, S., Fernandez, A. M., Gaitan, G., Gomez-Pinedo, U., Verdugo, J. M., Leroy, F., Soya, H., Nunez, A. & Torres-Aleman, I. Neuronal activity drives localized blood-brain-barrier transport of serum insulin-like growth factor-I into the CNS. *Neuron* **67**, 834-846, doi:10.1016/j.neuron.2010.08.007 (2010).

112 Pulido, R. S., Munji, R. N., Chan, T. C., Quirk, C. R., Weiner, G. A., Weger, B. D., Rossi, M. J., Elmsaouri, S., Malfavon, M., Deng, A., Profaci, C. P., Blanchette, M., Qian, T., Foreman, K. L., Shusta, E. V., Gorman, M. R., Gachon, F., Leutgeb, S. & Daneman, R. Neuronal Activity Regulates Blood-Brain Barrier Efflux Transport through Endothelial Circadian Genes. *Neuron* **108**, 937-952 e937, doi:10.1016/j.neuron.2020.09.002 (2020).

113 Malkiewicz, M. A., Szarmach, A., Sabisz, A., Cubala, W. J., Szurowska, E. & Winklewski, P. J. Blood-brain barrier permeability and physical exercise. *J Neuroinflammation* **16**, 15, doi:10.1186/s12974-019-1403-x (2019).

114 de Aquino, C. C., Leitao, R. A., Oliveira Alves, L. A., Coelho-Santos, V., Guerrant, R. L., Ribeiro, C. F., Malva, J. O., Silva, A. P. & Oria, R. B. Effect of Hypoproteic and High-Fat Diets on Hippocampal Blood-Brain Barrier Permeability and Oxidative Stress. *Front Nutr* **5**, 131, doi:10.3389/fnut.2018.00131 (2018).

115 Salameh, T. S., Mortell, W. G., Logsdon, A. F., Butterfield, D. A. & Banks, W. A. Disruption of the hippocampal and hypothalamic blood-brain barrier in a diet-induced obese model of type II

diabetes: prevention and treatment by the mitochondrial carbonic anhydrase inhibitor, topiramate. *Fluids Barriers CNS* **16**, 1, doi:10.1186/s12987-018-0121-6 (2019).

116 Yamamoto, M., Guo, D. H., Hernandez, C. M. & Stranahan, A. M. Endothelial Adora2a Activation Promotes Blood-Brain Barrier Breakdown and Cognitive Impairment in Mice with Diet-Induced Insulin Resistance. *J Neurosci* **39**, 4179-4192, doi:10.1523/JNEUROSCI.2506-18.2019 (2019).

117 Andrews, M. T., Russeth, K. P., Drewes, L. R. & Henry, P. G. Adaptive mechanisms regulate preferred utilization of ketones in the heart and brain of a hibernating mammal during arousal from torpor. *Am J Physiol Regul Integr Comp Physiol* **296**, R383-393, doi:10.1152/ajpregu.90795.2008 (2009).

118 Savolainen, H., Meerlo, P., Elsinga, P. H., Windhorst, A. D., Dierckx, R. A., Colabufo, N. A., van Waarde, A. & Luurtsema, G. P-glycoprotein Function in the Rodent Brain Displays a Daily Rhythm, a Quantitative In Vivo PET Study. *AAPS J* **18**, 1524-1531, doi:10.1208/s12248-016-9973-3 (2016).

119 Kervezee, L., Hartman, R., van den Berg, D. J., Shimizu, S., Emoto-Yamamoto, Y., Meijer, J. H. & de Lange, E. C. Diurnal variation in P-glycoprotein-mediated transport and cerebrospinal fluid turnover in the brain. *AAPS J* **16**, 1029-1037, doi:10.1208/s12248-014-9625-4 (2014).

120 Cuddapah, V. A., Zhang, S. L. & Sehgal, A. Regulation of the Blood-Brain Barrier by Circadian Rhythms and Sleep. *Trends Neurosci* **42**, 500-510, doi:10.1016/j.tins.2019.05.001 (2019).

121 Zhang, S. L., Yue, Z., Arnold, D. M., Artiushin, G. & Sehgal, A. A Circadian Clock in the Blood-Brain Barrier Regulates Xenobiotic Efflux. *Cell* **173**, 130-139 e110, doi:10.1016/j.cell.2018.02.017 (2018).

122 Parrado-Fernandez, C., Blennow, K., Hansson, M., Leoni, V., Cedazo-Minguez, A. & Bjorkhem, I. Evidence for sex difference in the CSF/plasma albumin ratio in ~20 000 patients and 335 healthy volunteers. *J Cell Mol Med* **22**, 5151-5154, doi:10.1111/jcmm.13767 (2018).

123 Cruz-Orengo, L., Daniels, B. P., Dorsey, D., Basak, S. A., Grajales-Reyes, J. G., McCandless, E. E., Piccio, L., Schmidt, R. E., Cross, A. H., Crosby, S. D. & Klein, R. S. Enhanced sphingosine-1-phosphate receptor 2 expression underlies female CNS autoimmunity susceptibility. *J Clin Invest* **124**, 2571-2584, doi:10.1172/JCI73408 (2014).

124 Jullienne, A., Salehi, A., Affeldt, B., Baghchechi, M., Haddad, E., Avitua, A., Walsworth, M., Enjalric, I., Hamer, M., Bhakta, S., Tang, J., Zhang, J. H., Pearce, W. J. & Obenaus, A. Male and Female Mice Exhibit Divergent Responses of the Cortical Vasculature to Traumatic Brain Injury. *J Neurotrauma* **35**, 1646-1658, doi:10.1089/neu.2017.5547 (2018).

125 Maggioli, E., McArthur, S., Mauro, C., Kieswich, J., Kusters, D. H., Reutelingsperger, C. P., Yaqoob, M. & Solito, E. Estrogen protects the blood-brain barrier from inflammation-induced disruption and increased lymphocyte trafficking. *Brain Behav Immun* **51**, 212-222, doi:10.1016/j.bbi.2015.08.020 (2016).

126 Mooradian, A. D. Effect of aging on the blood-brain barrier. *Neurobiol Aging* **9**, 31-39 (1988).

127 Bell, R. D., Winkler, E. A., Sagare, A. P., Singh, I., LaRue, B., Deane, R. & Zlokovic, B. V. Pericytes control key neurovascular functions and neuronal phenotype in the adult brain and during brain aging. *Neuron* **68**, 409-427, doi:10.1016/j.neuron.2010.09.043 (2010).

128 Montagne, A., Barnes, S. R., Sweeney, M. D., Halliday, M. R., Sagare, A. P., Zhao, Z., Toga, A. W., Jacobs, R. E., Liu, C. Y., Amezcua, L., Harrington, M. G., Chui, H. C., Law, M. & Zlokovic, B. V. Blood-brain barrier breakdown in the aging human hippocampus. *Neuron* **85**, 296-302, doi:10.1016/j.neuron.2014.12.032 (2015).

129 Erdo, F., Denes, L. & de Lange, E. Age-associated physiological and pathological changes at the blood-brain barrier: A review. *J Cereb Blood Flow Metab* **37**, 4-24, doi:10.1177/0271678X16679420 (2017).

130 Yousef, H., Czupalla, C. J., Lee, D., Chen, M. B., Burke, A. N., Zera, K. A., Zandstra, J., Berber, E., Lehallier, B., Mathur, V., Nair, R. V., Bonanno, L. N., Yang, A. C., Peterson, T., Hadeiba, H., Merkel, T., Korbelin, J., Schwaninger, M., Buckwalter, M. S., Quake, S. R., Butcher, E. C. & Wyss-Coray, T. Aged blood impairs hippocampal neural precursor activity and activates microglia via brain endothelial cell VCAM1. *Nat Med* **25**, 988-1000, doi:10.1038/s41591-019-0440-4 (2019).

131 Yang, A. C., Stevens, M. Y., Chen, M. B., Lee, D. P., Stahli, D., Gate, D., Contrepois, K., Chen, W., Iram, T., Zhang, L., Vest, R. T., Chaney, A., Lehallier, B., Olsson, N., du Bois, H., Hsieh, R., Cropper, H. C., Berdnik, D., Li, L., Wang, E. Y., Traber, G. M., Bertozzi, C. R., Luo, J., Snyder, M. P., Elias, J. E., Quake, S. R., James, M. L. & Wyss-Coray, T. Physiological blood-brain transport is impaired with age by a shift in transcytosis. *Nature* **583**, 425-430, doi:10.1038/s41586-020-2453-z (2020).

132 Seidner, G., Alvarez, M. G., Yeh, J. I., O'Driscoll, K. R., Klepper, J., Stump, T. S., Wang, D., Spinner, N. B., Birnbaum, M. J. & De Vivo, D. C. GLUT-1 deficiency syndrome caused by haploinsufficiency of the blood-brain barrier hexose carrier. *Nat Genet* **18**, 188-191, doi:10.1038/ng0298-188 (1998).

133 Tarlungeanu, D. C., Deliu, E., Dotter, C. P., Kara, M., Janiesch, P. C., Scalise, M., Galluccio, M., Tesulov, M., Morelli, E., Sonmez, F. M., Bilguvar, K., Ohgaki, R., Kanai, Y., Johansen, A., Esharif, S., Ben-Omran, T., Topcu, M., Schlessinger, A., Indiveri, C., Duncan, K. E., Caglayan, A. O., Gunel, M., Gleeson, J. G. & Novarino, G. Impaired Amino Acid Transport at the Blood Brain Barrier Is a Cause of Autism Spectrum Disorder. *Cell* **167**, 1481-1494 e1418, doi:10.1016/j.cell.2016.11.013 (2016).

134 Vatine, G. D., Al-Ahmad, A., Barriga, B. K., Svendsen, S., Salim, A., Garcia, L., Garcia, V. J., Ho, R., Yucer, N., Qian, T., Lim, R. G., Wu, J., Thompson, L. M., Spivia, W. R., Chen, Z., Van Eyk, J., Palecek, S. P., Refetoff, S., Shusta, E. V. & Svendsen, C. N. Modeling Psychomotor Retardation using iPSCs from MCT8-Deficient Patients Indicates a Prominent Role for the Blood-Brain Barrier. *Cell Stem Cell* **20**, 831-843 e835, doi:10.1016/j.stem.2017.04.002 (2017).

135 Mrdjen, D., Pavlovic, A., Hartmann, F. J., Schreiner, B., Utz, S. G., Leung, B. P., Lelios, I., Heppner, F. L., Kipnis, J., Merkler, D., Greter, M. & Becher, B. High-Dimensional Single-Cell Mapping of Central Nervous System Immune Cells Reveals Distinct Myeloid Subsets in Health, Aging, and Disease. *Immunity* **48**, 599, doi:10.1016/j.immuni.2018.02.014 (2018).

136 Masuda, T., Sankowski, R., Staszewski, O., Bottcher, C., Amann, L., Sagar, Scheiwe, C., Nessler, S., Kunz, P., van Loo, G., Coenen, V. A., Reinacher, P. C., Michel, A., Sure, U., Gold, R., Grun,

D., Priller, J., Stadelmann, C. & Prinz, M. Spatial and temporal heterogeneity of mouse and human microglia at single-cell resolution. *Nature* **566**, 388-392, doi:10.1038/s41586-019-0924-x (2019).

137 Mundt, S., Mrdjen, D., Utz, S. G., Greter, M., Schreiner, B. & Becher, B. Conventional DCs sample and present myelin antigens in the healthy CNS and allow parenchymal T cell entry to initiate neuroinflammation. *Sci Immunol* **4**, doi:10.1126/sciimmunol.aau8380 (2019).

138 Ioannidou, S., Deinhardt, K., Miotla, J., Bradley, J., Cheung, E., Samuelsson, S., Ng, Y. S. & Shima, D. T. An in vitro assay reveals a role for the diaphragm protein PV-1 in endothelial fenestra morphogenesis. *Proc Natl Acad Sci U S A* **103**, 16770-16775, doi:10.1073/pnas.0603501103 (2006).

139 Carman, C. V., Sage, P. T., Sciuto, T. E., de la Fuente, M. A., Geha, R. S., Ochs, H. D., Dvorak, H. F., Dvorak, A. M. & Springer, T. A. Transcellular diapedesis is initiated by invasive podosomes. *Immunity* **26**, 784-797, doi:10.1016/j.immuni.2007.04.015 (2007).

140 Winger, R. C., Koblinski, J. E., Kanda, T., Ransohoff, R. M. & Muller, W. A. Rapid remodeling of tight junctions during paracellular diapedesis in a human model of the blood-brain barrier. *J Immunol* **193**, 2427-2437, doi:10.4049/jimmunol.1400700 (2014).

141 Abadier, M., Haghayegh Jahromi, N., Cardoso Alves, L., Boscacci, R., Vestweber, D., Barnum, S., Deutsch, U., Engelhardt, B. & Lyck, R. Cell surface levels of endothelial ICAM-1 influence the transcellular or paracellular T-cell diapedesis across the blood-brain barrier. *Eur J Immunol* **45**, 1043-1058, doi:10.1002/eji.201445125 (2015).

142 Wimmer, I., Tietz, S., Nishihara, H., Deutsch, U., Sallusto, F., Gosselet, F., Lyck, R., Muller, W. A., Lassmann, H. & Engelhardt, B. PECAM-1 Stabilizes Blood-Brain Barrier Integrity and Favors Paracellular T-Cell Diapedesis Across the Blood-Brain Barrier During Neuroinflammation. *Front Immunol* **10**, 711, doi:10.3389/fimmu.2019.00711 (2019).

143 Lutz, S. E., Smith, J. R., Kim, D. H., Olson, C. V. L., Ellefsen, K., Bates, J. M., Gandhi, S. P. & Agalliu, D. Caveolin1 Is Required for Th1 Cell Infiltration, but Not Tight Junction Remodeling, at the Blood-Brain Barrier in Autoimmune Neuroinflammation. *Cell Rep* **21**, 2104-2117, doi:10.1016/j.celrep.2017.10.094 (2017).

144 Bastianello, S., Pozzilli, C., Bernardi, S., Bozzao, L., Fantozzi, L. M., Buttinelli, C. & Fieschi, C. Serial study of gadolinium-DTPA MRI enhancement in multiple sclerosis. *Neurology* **40**, 591-595, doi:10.1212/wnl.40.4.591 (1990).

145 Harris, J. O., Frank, J. A., Patronas, N., McFarlin, D. E. & McFarland, H. F. Serial gadolinium-enhanced magnetic resonance imaging scans in patients with early, relapsing-remitting multiple sclerosis: implications for clinical trials and natural history. *Ann Neurol* **29**, 548-555, doi:10.1002/ana.410290515 (1991).

146 Guttmann, C. R., Rousset, M., Roch, J. A., Hannoun, S., Durand-Dubief, F., Belaroussi, B., Cavallari, M., Rabilloud, M., Sappey-Marinier, D., Vukusic, S. & Cotton, F. Multiple sclerosis lesion formation and early evolution revisited: A weekly high-resolution magnetic resonance imaging study. *Mult Scler* **22**, 761-769, doi:10.1177/1352458515600247 (2016).

147 Gaitan, M. I., Shea, C. D., Evangelou, I. E., Stone, R. D., Fenton, K. M., Bielekova, B., Massacesi, L. & Reich, D. S. Evolution of the blood-brain barrier in newly forming multiple sclerosis lesions. *Ann Neurol* **70**, 22-29, doi:10.1002/ana.22472 (2011).

148 Bartholomaus, I., Kawakami, N., Odoardi, F., Schlager, C., Miljkovic, D., Ellwart, J. W., Klinkert, W. E., Flugel-Koch, C., Issekutz, T. B., Wekerle, H. & Flugel, A. Effector T cell interactions with meningeal vascular structures in nascent autoimmune CNS lesions. *Nature* **462**, 94-98, doi:10.1038/nature08478 (2009).

149 Schlager, C., Korner, H., Krueger, M., Vidoli, S., Haberl, M., Mielke, D., Brylla, E., Issekutz, T., Cabanas, C., Nelson, P. J., Ziemssen, T., Rohde, V., Bechmann, I., Lodygin, D., Odoardi, F. & Flugel, A. Effector T-cell trafficking between the leptomeninges and the cerebrospinal fluid. *Nature* **530**, 349-353, doi:10.1038/nature16939 (2016).

150 Engelhardt, B., Wolburg-Buchholz, K. & Wolburg, H. Involvement of the choroid plexus in central nervous system inflammation. *Microsc Res Tech* **52**, 112-129, doi:10.1002/1097-0029(20010101)52:1<112::AID-JEMT13>3.0.CO;2-5 (2001).

151 Engelhardt, B., Vajkoczy, P. & Weller, R. O. The movers and shapers in immune privilege of the CNS. *Nat Immunol* **18**, 123-131, doi:10.1038/ni.3666 (2017).

152 Carrithers, M. D., Visintin, I., Kang, S. J. & Janeway, C. A., Jr. Differential adhesion molecule requirements for immune surveillance and inflammatory recruitment. *Brain* **123 ( Pt 6)**, 1092-1101, doi:10.1093/brain/123.6.1092 (2000).

153 Reboldi, A., Coisne, C., Baumjohann, D., Benvenuto, F., Bottinelli, D., Lira, S., Uccelli, A., Lanzavecchia, A., Engelhardt, B. & Sallusto, F. C-C chemokine receptor 6-regulated entry of TH-17 cells into the CNS through the choroid plexus is required for the initiation of EAE. *Nat Immunol* **10**, 514-523, doi:10.1038/ni.1716 (2009).

154 Barkalow, F. J., Goodman, M. J., Gerritsen, M. E. & Mayadas, T. N. Brain endothelium lack one of two pathways of P-selectin-mediated neutrophil adhesion. *Blood* **88**, 4585-4593 (1996).

155 Lou, J., Dayer, J. M., Grau, G. E. & Burger, D. Direct cell/cell contact with stimulated T lymphocytes induces the expression of cell adhesion molecules and cytokines by human brain microvascular endothelial cells. *Eur J Immunol* **26**, 3107-3113, doi:10.1002/eji.1830261242 (1996).

156 Greter, M., Heppner, F. L., Lemos, M. P., Odermatt, B. M., Goebels, N., Laufer, T., Noelle, R. J. & Becher, B. Dendritic cells permit immune invasion of the CNS in an animal model of multiple sclerosis. *Nat Med* **11**, 328-334, doi:10.1038/nm1197 (2005).

157 Song, J., Zhang, X., Buscher, K., Wang, Y., Wang, H., Di Russo, J., Li, L., Lutke-Enking, S., Zarbock, A., Stadtmann, A., Striewski, P., Wirth, B., Kuzmanov, I., Wiendl, H., Schulte, D., Vestweber, D. & Sorokin, L. Endothelial Basement Membrane Laminin 511 Contributes to Endothelial Junctional Tightness and Thereby Inhibits Leukocyte Transmigration. *Cell Rep* **18**, 1256-1269, doi:10.1016/j.celrep.2016.12.092 (2017).

158 Wu, C., Ivars, F., Anderson, P., Hallmann, R., Vestweber, D., Nilsson, P., Robenek, H., Tryggvason, K., Song, J., Korpos, E., Loser, K., Beissert, S., Georges-Labouesse, E. & Sorokin, L.

M. Endothelial basement membrane laminin alpha5 selectively inhibits T lymphocyte extravasation into the brain. *Nat Med* **15**, 519-527, doi:10.1038/nm.1957 (2009).

159 Miller, D. H., Khan, O. A., Sheremata, W. A., Blumhardt, L. D., Rice, G. P., Libonati, M. A., Willmer-Hulme, A. J., Dalton, C. M., Miszkiel, K. A., O'Connor, P. W. & International Natalizumab Multiple Sclerosis Trial, G. A controlled trial of natalizumab for relapsing multiple sclerosis. *N Engl J Med* **348**, 15-23, doi:10.1056/NEJMoa020696 (2003).

160 Steinman, L. The re-emergence of antigen-specific tolerance as a potential therapy for MS. *Mult Scler* **21**, 1223-1238, doi:10.1177/1352458515581441 (2015).

161 Alvarez, J. I., Kebir, H., Cheslow, L., Chabarati, M., Larochelle, C. & Prat, A. JAML mediates monocyte and CD8 T cell migration across the brain endothelium. *Ann Clin Transl Neurol* **2**, 1032-1037, doi:10.1002/acn3.255 (2015).

162 Cayrol, R., Wosik, K., Berard, J. L., Dodelet-Devillers, A., Ifergan, I., Kebir, H., Haqqani, A. S., Kreymborg, K., Krug, S., Moumdjian, R., Bouthillier, A., Becher, B., Arbour, N., David, S., Stanimirovic, D. & Prat, A. Activated leukocyte cell adhesion molecule promotes leukocyte trafficking into the central nervous system. *Nat Immunol* **9**, 137-145, doi:10.1038/ni1551 (2008).

163 Flanagan, K., Fitzgerald, K., Baker, J., Regnstrom, K., Gardai, S., Bard, F., Mocci, S., Seto, P., You, M., Larochelle, C., Prat, A., Chow, S., Li, L., Vandevert, C., Zago, W., Lorenzana, C., Nishioka, C., Hoffman, J., Botelho, R., Willits, C., Tanaka, K., Johnston, J. & Yednock, T. Laminin-411 is a vascular ligand for MCAM and facilitates TH17 cell entry into the CNS. *PLoS One* **7**, e40443, doi:10.1371/journal.pone.0040443 (2012).

164 Ifergan, I., Kebir, H., Terouz, S., Alvarez, J. I., Lecuyer, M. A., Gendron, S., Bourbonniere, L., Dunay, I. R., Bouthillier, A., Moumdjian, R., Fontana, A., Haqqani, A., Klopstein, A., Prinz, M., Lopez-Vales, R., Birchler, T. & Prat, A. Role of Ninjurin-1 in the migration of myeloid cells to central nervous system inflammatory lesions. *Ann Neurol* **70**, 751-763, doi:10.1002/ana.22519 (2011).

165 Larochelle, C., Lecuyer, M. A., Alvarez, J. I., Charabati, M., Saint-Laurent, O., Ghannam, S., Kebir, H., Flanagan, K., Yednock, T., Duquette, P., Arbour, N. & Prat, A. Melanoma cell adhesion molecule-positive CD8 T lymphocytes mediate central nervous system inflammation. *Ann Neurol* **78**, 39-53, doi:10.1002/ana.24415 (2015).

166 Lecuyer, M. A., Saint-Laurent, O., Bourbonniere, L., Larouche, S., Larochelle, C., Michel, L., Charabati, M., Abadier, M., Zandee, S., Haghayegh Jahromi, N., Gowing, E., Pittet, C., Lyck, R., Engelhardt, B. & Prat, A. Dual role of ALCAM in neuroinflammation and blood-brain barrier homeostasis. *Proc Natl Acad Sci U S A* **114**, E524-E533, doi:10.1073/pnas.1614336114 (2017).

167 Huang, Z. G., Xue, D., Preston, E., Karbalai, H. & Buchan, A. M. Biphasic opening of the blood-brain barrier following transient focal ischemia: effects of hypothermia. *Can J Neurol Sci* **26**, 298-304 (1999).

168 Kuroiwa, T., Ting, P., Martinez, H. & Klatzo, I. The biphasic opening of the blood-brain barrier to proteins following temporary middle cerebral artery occlusion. *Acta Neuropathol* **68**, 122-129 (1985).

169 Knowland, D., Arac, A., Sekiguchi, K. J., Hsu, M., Lutz, S. E., Perrino, J., Steinberg, G. K., Barres, B. A., Nimmerjahn, A. & Agalliu, D. Stepwise recruitment of transcellular and paracellular pathways underlies blood-brain barrier breakdown in stroke. *Neuron* **82**, 603-617, doi:10.1016/j.neuron.2014.03.003 (2014).

170 Bowes, M. P., Zivin, J. A. & Rothlein, R. Monoclonal antibody to the ICAM-1 adhesion site reduces neurological damage in a rabbit cerebral embolism stroke model. *Exp Neurol* **119**, 215-219, doi:10.1006/exnr.1993.1023 (1993).

171 Connolly, E. S., Jr., Winfree, C. J., Springer, T. A., Naka, Y., Liao, H., Yan, S. D., Stern, D. M., Solomon, R. A., Gutierrez-Ramos, J. C. & Pinsky, D. J. Cerebral protection in homozygous null ICAM-1 mice after middle cerebral artery occlusion. Role of neutrophil adhesion in the pathogenesis of stroke. *J Clin Invest* **97**, 209-216, doi:10.1172/JCI118392 (1996).

172 Mayadas, T. N., Johnson, R. C., Rayburn, H., Hynes, R. O. & Wagner, D. D. Leukocyte rolling and extravasation are severely compromised in P selectin-deficient mice. *Cell* **74**, 541-554 (1993).

173 Enzmann, G. U., Pavlidou, S., Vaas, M., Klohs, J. & Engelhardt, B. ICAM-1(null) C57BL/6 Mice Are Not Protected from Experimental Ischemic Stroke. *Transl Stroke Res* **9**, 608-621, doi:10.1007/s12975-018-0612-4 (2018).

174 Horowitz, S. W., Merchut, M., Fine, M. & Azar-Kia, B. Complex partial seizure-induced transient MR enhancement. *J Comput Assist Tomogr* **16**, 814-816, doi:10.1097/00004728-199209000-00025 (1992).

175 Alvarez, V., Maeder, P. & Rossetti, A. O. Postictal blood-brain barrier breakdown on contrast-enhanced MRI. *Epilepsy Behav* **17**, 302-303, doi:10.1016/j.yebeh.2009.12.025 (2010).

176 Ruber, T., David, B., Luchters, G., Nass, R. D., Friedman, A., Surges, R., Stocker, T., Weber, B., Deichmann, R., Schlaug, G., Hattingen, E. & Elger, C. E. Evidence for peri-ictal blood-brain barrier dysfunction in patients with epilepsy. *Brain* **141**, 2952-2965, doi:10.1093/brain/awy242 (2018).

177 Cornford, E. M., Gee, M. N., Swartz, B. E., Mandelkern, M. A., Blahd, W. H., Landaw, E. M. & Delgado-Escueta, A. V. Dynamic [18F]fluorodeoxyglucose positron emission tomography and hypometabolic zones in seizures: reduced capillary influx. *Ann Neurol* **43**, 801-808, doi:10.1002/ana.410430615 (1998).

178 Mihaly, A. & Bozoky, B. Immunohistochemical localization of extravasated serum albumin in the hippocampus of human subjects with partial and generalized epilepsies and epileptiform convulsions. *Acta Neuropathol* **65**, 25-34 (1984).

179 Cornford, E. M., Hyman, S., Cornford, M. E., Landaw, E. M. & Delgado-Escueta, A. V. Interictal seizure resections show two configurations of endothelial Glut1 glucose transporter in the human blood-brain barrier. *J Cereb Blood Flow Metab* **18**, 26-42, doi:10.1097/00004647-199801000-00003 (1998).

180 Janigro, D. Blood-brain barrier, ion homeostatis and epilepsy: possible implications towards the understanding of ketogenic diet mechanisms. *Epilepsy Res* **37**, 223-232 (1999).

181 Marchi, N., Angelov, L., Masaryk, T., Fazio, V., Granata, T., Hernandez, N., Hallene, K., Diglaw, T., Franic, L., Najm, I. & Janigro, D. Seizure-promoting effect of blood-brain barrier disruption. *Epilepsia* **48**, 732-742, doi:10.1111/j.1528-1167.2007.00988.x (2007).

182 Oby, E. & Janigro, D. The blood-brain barrier and epilepsy. *Epilepsia* **47**, 1761-1774, doi:10.1111/j.1528-1167.2006.00817.x (2006).

183 van Vliet, E. A., da Costa Araujo, S., Redeker, S., van Schaik, R., Aronica, E. & Gorter, J. A. Blood-brain barrier leakage may lead to progression of temporal lobe epilepsy. *Brain* **130**, 521-534, doi:10.1093/brain/awl318 (2007).

184 Fabene, P. F., Navarro Mora, G., Martinello, M., Rossi, B., Merigo, F., Ottoboni, L., Bach, S., Angiari, S., Benati, D., Chakir, A., Zanetti, L., Schio, F., Osculati, A., Marzola, P., Nicolato, E., Homeister, J. W., Xia, L., Lowe, J. B., McEver, R. P., Osculati, F., Sbarbati, A., Butcher, E. C. & Constantin, G. A role for leukocyte-endothelial adhesion mechanisms in epilepsy. *Nat Med* **14**, 1377-1383, doi:10.1038/nm.1878 (2008).

185 De Vivo, D. C., Leary, L. & Wang, D. Glucose transporter 1 deficiency syndrome and other glycolytic defects. *J Child Neurol* **17 Suppl 3**, 3S15-23; discussion 13S24-15 (2002).

186 De Vivo, D. C., Trifiletti, R. R., Jacobson, R. I., Ronen, G. M., Behmand, R. A. & Harik, S. I. Defective glucose transport across the blood-brain barrier as a cause of persistent hypoglycorrhachia, seizures, and developmental delay. *N Engl J Med* **325**, 703-709, doi:10.1056/NEJM199109053251006 (1991).

187 Baldwin, S. A., Fugaccia, I., Brown, D. R., Brown, L. V. & Scheff, S. W. Blood-brain barrier breach following cortical contusion in the rat. *J Neurosurg* **85**, 476-481, doi:10.3171/jns.1996.85.3.0476 (1996).

188 Baskaya, M. K., Rao, A. M., Dogan, A., Donaldson, D. & Dempsey, R. J. The biphasic opening of the blood-brain barrier in the cortex and hippocampus after traumatic brain injury in rats. *Neurosci Lett* **226**, 33-36 (1997).

189 Hay, J. R., Johnson, V. E., Young, A. M., Smith, D. H. & Stewart, W. Blood-Brain Barrier Disruption Is an Early Event That May Persist for Many Years After Traumatic Brain Injury in Humans. *J Neuropathol Exp Neurol* **74**, 1147-1157, doi:10.1097/NEN.0000000000000261 (2015).

190 Weissberg, I., Veksler, R., Kamintsky, L., Saar-Ashkenazy, R., Milikovsky, D. Z., Shelef, I. & Friedman, A. Imaging blood-brain barrier dysfunction in football players. *JAMA Neurol* **71**, 1453-1455, doi:10.1001/jamaneurol.2014.2682 (2014).

191 Korn, A., Golan, H., Melamed, I., Pascual-Marqui, R. & Friedman, A. Focal cortical dysfunction and blood-brain barrier disruption in patients with Postconcussion syndrome. *J Clin Neurophysiol* **22**, 1-9 (2005).

192 Marchi, N., Bazarian, J. J., Puvenna, V., Janigro, M., Ghosh, C., Zhong, J., Zhu, T., Blackman, E., Stewart, D., Ellis, J., Butler, R. & Janigro, D. Consequences of repeated blood-brain barrier disruption in football players. *PLoS One* **8**, e56805, doi:10.1371/journal.pone.0056805 (2013).

193 Bargerstock, E., Puvenna, V., Iffland, P., Falcone, T., Hossain, M., Vetter, S., Man, S., Dickstein, L., Marchi, N., Ghosh, C., Carvalho-Tavares, J. & Janigro, D. Is peripheral immunity regulated by

blood-brain barrier permeability changes? *PLoS One* **9**, e101477, doi:10.1371/journal.pone.0101477 (2014).

194 Munji, R. N., Soung, A. L., Weiner, G. A., Sohet, F., Semple, B. D., Trivedi, A., Gimlin, K., Kotoda, M., Korai, M., Aydin, S., Batugal, A., Cabangcala, A. C., Schupp, P. G., Oldham, M. C., Hashimoto, T., Noble-Haeusslein, L. J. & Daneman, R. Profiling the mouse brain endothelial transcriptome in health and disease models reveals a core blood-brain barrier dysfunction module. *Nat Neurosci*, doi:10.1038/s41593-019-0497-x (2019).

195 Argaw, A. T., Asp, L., Zhang, J., Navrazhina, K., Pham, T., Mariani, J. N., Mahase, S., Dutta, D. J., Seto, J., Kramer, E. G., Ferrara, N., Sofroniew, M. V. & John, G. R. Astrocyte-derived VEGF-A drives blood-brain barrier disruption in CNS inflammatory disease. *J Clin Invest* **122**, 2454-2468, doi:10.1172/JCI60842 (2012).

196 Argaw, A. T., Gurfein, B. T., Zhang, Y., Zameer, A. & John, G. R. VEGF-mediated disruption of endothelial CLN-5 promotes blood-brain barrier breakdown. *Proc Natl Acad Sci U S A* **106**, 1977-1982, doi:10.1073/pnas.0808698106 (2009).

197 Nishioku, T., Matsumoto, J., Dohgu, S., Sumi, N., Miyao, K., Takata, F., Shuto, H., Yamauchi, A. & Kataoka, Y. Tumor necrosis factor-alpha mediates the blood-brain barrier dysfunction induced by activated microglia in mouse brain microvascular endothelial cells. *J Pharmacol Sci* **112**, 251-254 (2010).

198 Chiaretti, A., Genovese, O., Aloe, L., Antonelli, A., Piastra, M., Polidori, G. & Di Rocco, C. Interleukin 1beta and interleukin 6 relationship with paediatric head trauma severity and outcome. *Childs Nerv Syst* **21**, 185-193; discussion 194, doi:10.1007/s00381-004-1032-1 (2005).

199 Pare, A., Mailhot, B., Levesque, S. A., Juzwik, C., Ignatius Arokia Doss, P. M., Lecuyer, M. A., Prat, A., Rangachari, M., Fournier, A. & Lacroix, S. IL-1beta enables CNS access to CCR2(hi) monocytes and the generation of pathogenic cells through GM-CSF released by CNS endothelial cells. *Proc Natl Acad Sci U S A* **115**, E1194-E1203, doi:10.1073/pnas.1714948115 (2018).

200 Wang, Y., Jin, S., Sonobe, Y., Cheng, Y., Horiuchi, H., Parajuli, B., Kawanokuchi, J., Mizuno, T., Takeuchi, H. & Suzumura, A. Interleukin-1beta induces blood-brain barrier disruption by downregulating Sonic hedgehog in astrocytes. *PLoS One* **9**, e110024, doi:10.1371/journal.pone.0110024 (2014).

201 Maier, C. M., Hsieh, L., Crandall, T., Narasimhan, P. & Chan, P. H. Evaluating therapeutic targets for reperfusion-related brain hemorrhage. *Ann Neurol* **59**, 929-938, doi:10.1002/ana.20850 (2006).

202 Pun, P. B., Lu, J. & Moochhala, S. Involvement of ROS in BBB dysfunction. *Free Radic Res* **43**, 348-364, doi:10.1080/10715760902751902 (2009).

203 Relton, J. K., Beckey, V. E., Hanson, W. L. & Whalley, E. T. CP-0597, a selective bradykinin B2 receptor antagonist, inhibits brain injury in a rat model of reversible middle cerebral artery occlusion. *Stroke* **28**, 1430-1436 (1997).

204 Gidday, J. M., Gasche, Y. G., Copin, J. C., Shah, A. R., Perez, R. S., Shapiro, S. D., Chan, P. H. & Park, T. S. Leukocyte-derived matrix metalloproteinase-9 mediates blood-brain barrier breakdown and is proinflammatory after transient focal cerebral ischemia. *Am J Physiol Heart Circ Physiol* **289**, H558-568, doi:10.1152/ajpheart.01275.2004 (2005).

205 Ugarte-Berzal, E., Berghmans, N., Boon, L., Martens, E., Vandooren, J., Cauwe, B., Thijs, G., Proost, P., Van Damme, J. & Opdenakker, G. Gelatinase B/matrix metalloproteinase-9 is a phase-specific effector molecule, independent from Fas, in experimental autoimmune encephalomyelitis. *PLoS One* **13**, e0197944, doi:10.1371/journal.pone.0197944 (2018).

206 Chang, J., Mancuso, M. R., Maier, C., Liang, X., Yuki, K., Yang, L., Kwong, J. W., Wang, J., Rao, V., Vallon, M., Kosinski, C., Zhang, J. J., Mah, A. T., Xu, L., Li, L., Gholamin, S., Reyes, T. F., Li, R., Kuhnert, F., Han, X., Yuan, J., Chiou, S. H., Brettman, A. D., Daly, L., Corney, D. C., Cheshier, S. H., Shortliffe, L. D., Wu, X., Snyder, M., Chan, P., Giffard, R. G., Chang, H. Y., Andreasson, K. & Kuo, C. J. Gpr124 is essential for blood-brain barrier integrity in central nervous system disease. *Nat Med* **23**, 450-460, doi:10.1038/nm.4309 (2017).

207 Roy, C. S. & Sherrington, C. S. On the Regulation of the Blood-supply of the Brain. *J Physiol* **11**, 85-158 117, doi:10.1113/jphysiol.1890.sp000321 (1890).

208 Mosso, A. Sulla circolazione del sangue nel cervello dell'uomo. *Revue Philosophique de la France Et de l* (1882).

209 Iadecola, C. The Neurovascular Unit Coming of Age: A Journey through Neurovascular Coupling in Health and Disease. *Neuron* **96**, 17-42, doi:10.1016/j.neuron.2017.07.030 (2017).

210 Girouard, H. & Iadecola, C. Neurovascular coupling in the normal brain and in hypertension, stroke, and Alzheimer disease. *J Appl Physiol (1985)* **100**, 328-335, doi:10.1152/japplphysiol.00966.2005 (2006).

211 Attwell, D., Buchan, A. M., Charpak, S., Lauritzen, M., Macvicar, B. A. & Newman, E. A. Glial and neuronal control of brain blood flow. *Nature* **468**, 232-243, doi:10.1038/nature09613 (2010).

212 Kaplan, L., Chow, B. W. & Gu, C. Neuronal regulation of the blood-brain barrier and neurovascular coupling. *Nat Rev Neurosci* **21**, 416-432, doi:10.1038/s41583-020-0322-2 (2020).

213 Puro, D. G. Physiology and pathobiology of the pericyte-containing retinal microvasculature: new developments. *Microcirculation* **14**, 1-10, doi:10.1080/10739680601072099 (2007).

214 Hannah, R. M., Dunn, K. M., Bonev, A. D. & Nelson, M. T. Endothelial SK(Ca) and IK(Ca) channels regulate brain parenchymal arteriolar diameter and cortical cerebral blood flow. *J Cereb Blood Flow Metab* **31**, 1175-1186, doi:10.1038/jcbfm.2010.214 (2011).

215 Chen, B. R., Kozberg, M. G., Bouchard, M. B., Shaik, M. A. & Hillman, E. M. A critical role for the vascular endothelium in functional neurovascular coupling in the brain. *J Am Heart Assoc* **3**, e000787, doi:10.1161/JAHA.114.000787 (2014).

216 Longden, T. A., Dabertrand, F., Koide, M., Gonzales, A. L., Tykocki, N. R., Brayden, J. E., Hill-Eubanks, D. & Nelson, M. T. Capillary K(+)-sensing initiates retrograde hyperpolarization to increase local cerebral blood flow. *Nat Neurosci* **20**, 717-726, doi:10.1038/nn.4533 (2017).

217 Chow, B. W., Nunez, V., Kaplan, L., Granger, A. J., Bistrong, K., Zucker, H. L., Kumar, P., Sabatini, B. L. & Gu, C. Caveolae in CNS arterioles mediate neurovascular coupling. *Nature* **579**, 106-110, doi:10.1038/s41586-020-2026-1 (2020).

218 Sonkusare, S. K., Bonev, A. D., Ledoux, J., Liedtke, W., Kotlikoff, M. I., Heppner, T. J., Hill-Eubanks, D. C. & Nelson, M. T. Elementary Ca2+ signals through endothelial TRPV4 channels regulate vascular function. *Science* **336**, 597-601, doi:10.1126/science.1216283 (2012).

219 Nishimura, N., Schaffer, C. B., Friedman, B., Lyden, P. D. & Kleinfeld, D. Penetrating arterioles are a bottleneck in the perfusion of neocortex. *Proc Natl Acad Sci U S A* **104**, 365-370, doi:10.1073/pnas.0609551104 (2007).

220 Hall, C. N., Reynell, C., Gesslein, B., Hamilton, N. B., Mishra, A., Sutherland, B. A., O'Farrell, F. M., Buchan, A. M., Lauritzen, M. & Attwell, D. Capillary pericytes regulate cerebral blood flow in health and disease. *Nature* **508**, 55-60, doi:10.1038/nature13165 (2014).

221 Rosehart, A. C., Longden, T. A., Weir, N., Fontaine, J. T., Joutel, A. & Dabertrand, F. Prostaglandin E2 Dilates Intracerebral Arterioles When Applied to Capillaries: Implications for Small Vessel Diseases. *Front Aging Neurosci* **13**, 695965, doi:10.3389/fnagi.2021.695965 (2021).

222 Beach, J. M., McGahren, E. D. & Duling, B. R. Capillaries and arterioles are electrically coupled in hamster cheek pouch. *Am J Physiol* **275**, H1489-1496, doi:10.1152/ajpheart.1998.275.4.H1489 (1998).

223 Thakore, P., Alvarado, M. G., Ali, S., Mughal, A., Pires, P. W., Yamasaki, E., Pritchard, H. A., Isakson, B. E., Tran, C. H. T. & Earley, S. Brain endothelial cell TRPA1 channels initiate neurovascular coupling. *Elife* **10**, doi:10.7554/eLife.63040 (2021).

224 Harraz, O. F., Longden, T. A., Hill-Eubanks, D. & Nelson, M. T. PIP2 depletion promotes TRPV4 channel activity in mouse brain capillary endothelial cells. *Elife* **7**, doi:10.7554/eLife.38689 (2018).

225 Panczel, G., Daffertshofer, M., Ries, S., Spiegel, D. & Hennerici, M. Age and stimulus dependency of visually evoked cerebral blood flow responses. *Stroke* **30**, 619-623, doi:10.1161/01.str.30.3.619 (1999).

226 Zaletel, M., Strucl, M., Pretnar-Oblak, J. & Zvan, B. Age-related changes in the relationship between visual evoked potentials and visually evoked cerebral blood flow velocity response. *Funct Neurol* **20**, 115-120 (2005).

227 Balbi, M., Ghosh, M., Longden, T. A., Jativa Vega, M., Gesierich, B., Hellal, F., Lourbopoulos, A., Nelson, M. T. & Plesnila, N. Dysfunction of mouse cerebral arteries during early aging. *J Cereb Blood Flow Metab* **35**, 1445-1453, doi:10.1038/jcbfm.2015.107 (2015).

228 Lipecz, A., Csipo, T., Tarantini, S., Hand, R. A., Ngo, B. N., Conley, S., Nemeth, G., Tsorbatzoglou, A., Courtney, D. L., Yabluchanska, V., Csiszar, A., Ungvari, Z. I. & Yabluchanskiy, A. Age-related impairment of neurovascular coupling responses: a dynamic vessel analysis (DVA)-based approach to measure decreased flicker light stimulus-induced retinal arteriolar dilation in healthy older adults. *Geroscience* **41**, 341-349, doi:10.1007/s11357-019-00078-y (2019).

229 Chabriat, H., Pappata, S., Ostergaard, L., Clark, C. A., Pachot-Clouard, M., Vahedi, K., Jobert, A., Le Bihan, D. & Bousser, M. G. Cerebral hemodynamics in CADASIL before and after acetazolamide challenge assessed with MRI bolus tracking. *Stroke* **31**, 1904-1912, doi:10.1161/01.str.31.8.1904 (2000).

230 Pfefferkorn, T., von Stuckrad-Barre, S., Herzog, J., Gasser, T., Hamann, G. F. & Dichgans, M. Reduced cerebrovascular CO(2) reactivity in CADASIL: A transcranial Doppler sonography study. *Stroke* **32**, 17-21, doi:10.1161/01.str.32.1.17 (2001).

231 Liem, M. K., Lesnik Oberstein, S. A., Haan, J., Boom, R., Ferrari, M. D., Buchem, M. A. & Grond, J. Cerebrovascular reactivity is a main determinant of white matter hyperintensity progression in CADASIL. *AJNR Am J Neuroradiol* **30**, 1244-1247, doi:10.3174/ajnr.A1533 (2009).

232 Hock, C., Villringer, K., Muller-Spahn, F., Wenzel, R., Heekeren, H., Schuh-Hofer, S., Hofmann, M., Minoshima, S., Schwaiger, M., Dirnagl, U. & Villringer, A. Decrease in parietal cerebral hemoglobin oxygenation during performance of a verbal fluency task in patients with Alzheimer's disease monitored by means of near-infrared spectroscopy (NIRS)--correlation with simultaneous rCBF-PET measurements. *Brain Res* **755**, 293-303, doi:10.1016/s0006-8993(97)00122-4 (1997).

233 Rombouts, S. A., Barkhof, F., Veltman, D. J., Machielsen, W. C., Witter, M. P., Bierlaagh, M. A., Lazeron, R. H., Valk, J. & Scheltens, P. Functional MR imaging in Alzheimer's disease during memory encoding. *AJNR Am J Neuroradiol* **21**, 1869-1875 (2000).

234 Dubroca, C., Lacombe, P., Domenga, V., Maciazek, J., Levy, B., Tournier-Lasserve, E., Joutel, A. & Henrion, D. Impaired vascular mechanotransduction in a transgenic mouse model of CADASIL arteriopathy. *Stroke* **36**, 113-117, doi:10.1161/01.STR.0000149949.92854.45 (2005).

235 Capone, C., Dabertrand, F., Baron-Menguy, C., Chalaris, A., Ghezali, L., Domenga-Denier, V., Schmidt, S., Huneau, C., Rose-John, S., Nelson, M. T. & Joutel, A. Mechanistic insights into a TIMP3-sensitive pathway constitutively engaged in the regulation of cerebral hemodynamics. *Elife* **5**, doi:10.7554/eLife.17536 (2016).

236 Iadecola, C., Zhang, F., Niwa, K., Eckman, C., Turner, S. K., Fischer, E., Younkin, S., Borchelt, D. R., Hsiao, K. K. & Carlson, G. A. SOD1 rescues cerebral endothelial dysfunction in mice overexpressing amyloid precursor protein. *Nat Neurosci* **2**, 157-161, doi:10.1038/5715 (1999).

237 Niwa, K., Kazama, K., Younkin, L., Younkin, S. G., Carlson, G. A. & Iadecola, C. Cerebrovascular autoregulation is profoundly impaired in mice overexpressing amyloid precursor protein. *Am J Physiol Heart Circ Physiol* **283**, H315-323, doi:10.1152/ajpheart.00022.2002 (2002).

238 Mueggler, T., Sturchler-Pierrat, C., Baumann, D., Rausch, M., Staufenbiel, M. & Rudin, M. Compromised hemodynamic response in amyloid precursor protein transgenic mice. *J Neurosci* **22**, 7218-7224, doi:20026680 (2002).

239 Shin, H. K., Jones, P. B., Garcia-Alloza, M., Borrelli, L., Greenberg, S. M., Bacskai, B. J., Frosch, M. P., Hyman, B. T., Moskowitz, M. A. & Ayata, C. Age-dependent cerebrovascular dysfunction in a transgenic mouse model of cerebral amyloid angiopathy. *Brain* **130**, 2310-2319, doi:10.1093/brain/awm156 (2007).

240 Rancillac, A., Geoffroy, H. & Rossier, J. Impaired neurovascular coupling in the APPxPS1 mouse model of Alzheimer's disease. *Curr Alzheimer Res* **9**, 1221-1230, doi:10.2174/156720512804142859 (2012).

241 Tarantini, S., Hertelendy, P., Tucsek, Z., Valcarcel-Ares, M. N., Smith, N., Menyhart, A., Farkas, E., Hodges, E. L., Towner, R., Deak, F., Sonntag, W. E., Csiszar, A., Ungvari, Z. & Toth, P.

Pharmacologically-induced neurovascular uncoupling is associated with cognitive impairment in mice. *J Cereb Blood Flow Metab* **35**, 1871-1881, doi:10.1038/jcbfm.2015.162 (2015).

# CHAPTER I

## Pdlim1 is a marker of blood-brain barrier dysfunction in neurological disease and injury


### Abstract

The blood-brain barrier (BBB), a series of unique properties possessed by central nervous system (CNS) endothelial cells, is crucial for tightly regulating the extracellular environment of the parenchyma. A series of neuropathologies, including traumatic brain injury, seizures, stroke, and multiple sclerosis, involve disruption of the BBB. BBB dysfunction can lead to ionic dysregulation, edema, and immune cell extravasation, which in turn can cause neuronal injury and death. As BBB dysfunction occurs early in disease and injury progression, it is possible that treating BBB dysfunction could help reduce clinical symptoms in a number of neurological conditions. However, many of the molecular mechanisms of BBB disruption and repair remain unknown. Here we identify a novel marker of BBB dysfunction: PDLIM1. PDLIM1 is upregulated in CNS endothelial cells specifically in areas of BBB leakage during disease and injury. Overexpressing PDLIM1 in endothelial cells increases expression of several junctional adhesion molecules, suggesting that PDLIM1 is upregulated as a protective mechanism in disease. In a mouse model of multiple sclerosis, mice overexpressing PDLIM1 in endothelial cells trended towards having delayed and less severe paralysis, supporting the idea that PDLIM1 is protective at the BBB in disease.


### Introduction

The endothelial cells that make up blood vessel walls in the central nervous system (CNS) exhibit unique physiological properties that greatly limit vessel permeability to the vast majority of blood-borne entities. These properties are referred to as the “blood-brain barrier” (BBB). While peripheral vessels allow high levels of trans- and paracellular movement of molecules and ions between the blood and tissue, CNS vessels exert tighter regulation over what enters the parenchyma. This stringent control is essential for ensuring a toxin-free neural environment and for maintaining precise extracellular ion concentrations for proper neuronal function. Physiological properties that contribute to low BBB permeability include tight

junctions (TJs), low levels of transcytosis, efflux transporters, selective nutrient transporters, and fewer leukocyte adhesion molecules. Together, this set of properties allows CNS endothelial cells to tightly regulate the movement of ions, molecules, and cells between the blood and the CNS, thus controlling the extracellular environment of the neural tissue (reviewed in [1]). These properties are sometimes compromised in disease, and the term "BBB dysfunction" can refer to any changes in these molecular components leading to increased vascular permeability or altered transport.

While many of the cellular and molecular mechanisms underlying initiation and maintenance of the barrier have been identified, less is understood about what drives BBB dysfunction, particularly whether dysfunction is caused by molecular cues that induce disruption, a loss of maintenance cues, or both. Disruption of the BBB is a critical event in many neurological conditions including multiple sclerosis (MS), stroke, epilepsy, and traumatic brain injury (TBI). While in most cases BBB damage is not the trigger of disease, the resulting influx of bloodborne molecules, disruption of ionic homeostasis, and increase in immune cell extravasation contribute to the dysfunction, damage, and even degeneration of neurons, ultimately potentiating clinical symptoms. Furthermore, increased immune cell presence after BBB disruption is particularly detrimental in MS and other autoimmune diseases in which leukocytes are driving pathology. While there is much still unknown about the mechanisms driving BBB disruption, perhaps even less is known about the mechanisms underlying BBB repair. Identifying molecular drivers of BBB dysfunction and repair could point towards a therapeutic target for decreasing vascular permeability, tissue damage, and clinical progression in a wide range of neurological diseases.

To identify the molecular mechanisms of BBB dysfunction and repair, our group performed RNA sequencing on CNS endothelial cells at four different timepoints in four different disease models with known BBB leakage[2]. We identified that PDZ and LIM domain protein 1 (PDLIM1) is upregulated in endothelial cells in all four disease models. The gene encodes a ~36 kDA cytoplasmic protein thought to associate with the cytoskeleton and important for actin stress fiber formation[3,4]. Since its identification, PDLIM1 has been implicated in several different cancer subtypes and is thought to play tissue-specific roles[5]. PDLIM1 has been shown to limit metastasis in colorectal cancer and hepatocellular carcinoma by

stabilizing the E-cadherin/β-catenin complex and by activating Hippo signaling, respectively[6,7]. In contrast, PDLIM1 has been reported to promote cell migration and invasion in breast cancer, glioma, and chronic myelogenous leukemia through its interactions with α-actinin, the p75 neurotrophin receptor, and Wnt/β-catenin signaling, respectively[8-10]. Furthermore, PDLIM1 has been shown to limit pro-inflammatory response in immune cells, in some cases via inhibition of NF-κB signaling[11-13]. PDLIM1's ability to inhibit Wnt or NF-κB signaling could be particularly relevant to BBB dysfunction during disease. Wnt induces TJ formation, increases expression of solute transporters, and reduces vesicle transport as part of the unique CNS angiogenic program[14-16], and Wnt signaling is also important for maintenance of the BBB throughout life[17-21]. Thus, inhibition of Wnt signaling by PDLIM1 could drive BBB disruption. On the other hand, NF-κB is a major pro-inflammatory pathway, so PDLIM1-mediated inhibition of NF-κB could limit inflammatory endothelial activation and help mitigate disease severity. Because of PDLIM1's associations with these two important signaling pathways, we chose to further investigate its role in CNS endothelial cells.

Here, using a previously published dataset[2], we characterize PDLIM1 expression in various endothelial beds in healthy adult mice, finding that PDLIM1 is highly expressed in heart, lung, and liver endothelial cells but not in brain or spinal cord endothelial cells. We further find that PDLIM1 is upregulated in endothelial cells in four disease and injury models and is expressed specifically in areas of BBB leakage. Thus, we identify PDLIM1 as a new histological marker for BBB dysfunction. PDLIM1 overexpression leads to an upregulation of several cell adhesion molecules, suggesting a role for PDLIM1 in mitigating BBB damage during neuropathological conditions. Mice overexpressing PDLIM1 trended towards exhibiting less severe clinical symptoms in a mouse model of multiple sclerosis, further supporting the idea of PDLIM1 as protective against BBB dysfunction.

## Methods

*Animals*

All original disease model experiments were performed on *Rosa-tdTomato*; *VE-Cadherin*-Cre$^{ERT2}$ mice as described in Munji and Soung et al.[2]. *Tie2-tTA; TRE-Pdlim1-IRES-GFP* ("EC-PDLIM1") transgenic mice were generated via pronuclear injection by the UCSD Transgenic Core and back-crossed at least six generations into the C57BL6 background. *Pdlim1*$^{-/-}$ mice were purchased from the Texas A&M Institute for Genomic Medicine. All experiments were performed under Institutional Animal Care and Use committee approval at the University of California, San Diego.

*Endothelial cell enrichment*

Animals were anesthetized with a ketamine/xylazine mix. Mice were decapitated, brains were dissected, and cerebellum and olfactory bulbs were removed and discarded. Brains were rolled on filter paper to remove meninges. Remaining meninges and choroid plexus were removed with fine forceps. Brain tissue was diced using a #10 scalpel blade. Tissue was enzymatically digested with the Papain Dissociation System kit (Worthington, LK003176), using 1 vial (>100 units) per 10 mL EBSS (Sigma, E7510) solution also containing 0.36% D(+)-Glucose, 26 mM NaHCO3, 0.5 mM EDTA, and 62.5 units/mL DNase (Worthington, LS002007) at 35°C for 90 minutes with 95% $O_2$, 5% $CO_2$ continuously passed over the solution. Tissue chunks were washed with a "low-ovomucoid" EBSS solution containing 225 μg/mL ovomucoid (Worthington, LS003089), 225 μg/mL BSA (Sigma A8806), 0.36% D(+)-Glucose, 26 mM NaHCO3, and 55.5 units/mL DNase. Samples were triturated 4 x 10x with 10 mL, 5 mL, and P1000 pipette tips. Cells were spun into "high-ovomucoid" solution containing 450 μg/mL ovomucoid, 450 μg/mL BSA, 0.36% D(+)-Glucose, 26 mM NaHCO3, and 62.5 units/mL DNase. Cells were resuspended in a collagenase/dispase solution of 1 mg/mL collagenase type II (Worthington, LS004176) and 0.4 mg/mL neutral protease (Worthington LS02104) in an EBSS solution containing 0.36% D(+)-Glucose, 26 mM NaHCO3, 0.5 mM EDTA, and 62.5 units/mL DNase. Cells were incubated for 30 min at 35°C with 95% $O_2$, 5% $CO_2$ continuously passed over the solution. After incubation, cells were spun into high-ovomucoid solution and resuspended in a 0.5% BSA (Sigma, A4161) solution with myelin removal beads (Miltenyi

Biotec, 130-096-433). After a 15 min bead incubation, 30 micron pre-separation columns (Miltenyi Biotec, 130-041-407) and LS columns (Miltenyi Biotec, 130-042-401) were used for myelin removal. Cells were blocked with rat IgG in 0.5% BSA solution on ice for 20 min. Cells were stained with AF647-conjugated anti-CD31 (Molecular Probes A14716), Pacific Blue-conjugated lineage cocktail (BioLegend 76724), BV421-conjugated anti-CD13 (BD Biosciences 564354), and DAPI. Cells positive for AF647 and negative for Pacific Blue/BV421/DAPI were sorted into trizol at the UCSD Flow Cytometry Research Core Facility. RNA isolation was performed with the RNeasy Micro kit (Qiagen 74004).

*RNA Sequencing*

V2 non-stranded mRNA library prep and bulk sequencing were carried out by the UCSD Institute of Genomic Medicine Core. EC-PDLIM1 samples were sequenced using single-read, 75 bp reads. HISAT2 was used for alignment to the GRCm38 genome, htseq-count was used to generate count tables, and differential expression was analyzed using DeSeq2. All analysis programs were run through the Galaxy open-source platform. The NIH's DAVID Functional Annotation Tool was used to identify biological processes associated with differentially expressed genes.

*Immunostaining*

Mice were transcardially perfused with DPBS followed by 4% paraformaldehyde in PBS. Tissue was cryopreserved in 30% sucrose, frozen in 2:1 30% sucrose:OCT and sectioned at 10 μm thickness. Sections were blocked with 10% normal goat serum and 0.2% triton-x-100 in PBS. Primary antibodies against PDLIM1 (Abcam ab64971; ab199626) and CD31 (BD Biosciences 553370) were used at 1:1000 and incubated overnight at 4°C. Fluorescent conjugated secondary antibodies (Life Technologies) were used at 1:1000 and incubated for 2 hours at room temperature. Slides were coverslipped using DAPI-Fluoromount-G (SouthernBiothech, 0100-20) and imaged with a Zeiss Axio Imager.D2.

*Quantification of PDLIM1+ vascular length*

PDLIM1 and CD31 were visualized via immunostaining. The ImageJ line tool was used to trace vasculature, excluding meninges. To determine the percent of PDLIM1+ vasculature, the total length of PDLIM1+ vessels was divided by the total length of CD31+ vessels and multiplied by 100.

*Luminescence assays*

HEK293 cells were plated in 96-well plates in growth medium containing 2mM L-glutamine (Life Technologies 25030081), 1 mM sodium pyruvate (Life Technologies 11360070), MEM non-essential amino acids (Life Technologoes 11140050), Pen Strep (Life Technologies, 15070063), and 10% fetal bovine serum in DMEM. For Wnt assays, cells were transfected with Firefly luciferase under TCF/LEF control and *Renilla* luciferase (BPS Bioscience 60500), Wnt7a, Fzd4, Reck, GPR124, and either Pdlim1 or a control vector in Opti-MEM (Life Technologies 31985062) using the Lipofectamine 3000 Transfection Kit (Invitrogen L3000-015). For NF-κB assays, cells were transfected with Firefly luciferase under NF-κB control and *Renilla* luciferase (BPS Bioscience 60614), and Pdlim1 or a control vector. After 24 hours, cells were treated with TNFα (20 ng/mL) or vehicle (0.1% BSA). 24 hours after Wnt pathway transfection or Tnfα treatment, the Pierce *Renilla*-Firefly Luciferase Dual Assay Kit (Life Technologies 16186) was used to produce luminescent signal. Firefly and *Renilla* luminescence were quantified using a Tecan Infinite 200 plate reader. Wells without cells were used as a background control. The average background luminescence was subtracted from that of all experimental wells, and the Firefly signal was divided by the *Renilla* signal. This ratio was used as a proxy for Wnt or NF-κB signaling.

*NFκB assay in primary cultured endothelial cells*

Animals were euthanized with $CO_2$. Brains were dissected and rolled on filter paper to remove meninges. Cerebellum and olfactory bulbs were removed and discarded, and remaining meninges and choroid plexus were removed using fine forceps. Brains were chopped using a #10 scalpel blade and

triturated 25 times with a 5 mL pipette. Tissue was then enzymatically digested in a solution of 1 mg/mL collagenase, type II (Worthington, LS004176), 0.1 mg/mL BSA, and DNase in high glucose DMEM for 1 hour at 37°C shaking at 350 rpm. To remove myelin, cells were triturated 40x with a 5 mL pipette in 20% w/v BSA (Sigma A7906) in high glucose DMEM and spun for 20 minutes at 4°C, and myelin was vacuumed off the top. Cells were resuspended in 1 mg/mL collagenase/dispase (Roche 10269638001) and DNase in high-glucose DMEM. After enzymatic digestion, cells were spun into a Percoll (GE Healthcare 17-0891-01) gradient and the fraction containing endothelial cells was washed with high-glucose DMEM. Cells were plated on coverslips coated with collagen type IV (Sigma C5533) and fibronectin (Sigma F1141). Culture media was Neurobasal medium (Life Technologies 21103049) with 2 mM L-glutamine (Life Technologies 25030081), B-27 (Life Technologies 17504044), Pen Strep (Life Technologies 15070063), bFGF (Invitrogen 13256-029) and puromycin (Sigma P7255). After three days, media was removed and replaced with media without puromycin and containing either TNFα (20 ng/mL, eBioscience) or vehicle (0.1% BSA in PBS). After 24 hours treatment, cells were fixed with 4% PFA, blocked with 10% goat serum and 0.2% Triton-X-100 in PBS, and incubated with primary antibody against p65 (Cell Signaling D14E12) 1:1000 in PBS at 4°C overnight. Cells were incubated with secondary antibody 1:1000 in PBS at room temperature for 1 hour. Coverslips were mounted with DAPI-Fluoromount-G (SouthernBiothech 0100-20) and images were taken with a Zeiss Axio Imager.D2. Nuclear and cytoplasmic ROIs were created using ImageJ, and nuclear mean fluorescence was divided by cytoplasmic mean fluorescence to obtain the nuclear:cytoplasmic fluorescence ratio. This ratio was used to represent p65 nuclear translocation.

*Experimental autoimmune encephalomyelitis (EAE)*

EAE Induction kits from Hooke Laboratories (EK-2110) were used for disease induction. At 10-15 weeks of age, male and female EC-PDLIM1 mice and littermate controls were given an s.c. injection of myelin oligodendrocyte glycoprotein 33-55 ($MOG_{33-35}$) emulsion under the skin on the upper back. They

were also given an i.p. injection of pertussis toxin in glycerol buffer. Approximately 22-26 hours later, a second injection of pertussis toxin was given. For 4 weeks after disease induction, mice were scored daily according to the following scale: 0=asymptomatic; 0.5=partially limp tail; 1=fully limp tail; 1.5=loss of digit reflexes; 2=slow to recover from prone position; 2.5=altered gate; 3=inability to lift abdomen 3.5=partial hindlimb paralysis; 4=full hindlimb paralysis; 4.5=moribund; 5=death.

**Results**

*PDLIM1 expression is correlated to vascular permeability in health and disease*

We recently found that *Pdlim1* is among a cassette of genes whose mRNA is upregulated in endothelial cells during different instances of BBB dysfunction[2]. Specifically, *Pdlim1* mRNA expression was significantly increased at "acute" and "subacute" timepoints in mouse models of MS, stroke, seizures, and TBI – timepoints associated with BBB leakage[2] (Fig 1.1A). These timepoints varied by disease model and were chosen to represent the onset and peak of BBB leakage. For stroke and TBI models, the acute and subacute timepoints were 24 and 72 hours after induction of the hypoxia/injury, respectively. In the seizure model, the acute and subacute timepoints were 3 and 48 hours after kainic acid administration, respectively. In the MS model, the acute and subacute timepoints were at the onset and peak of symptoms, respectively. In all cases, the chronic timepoint was 30 days after induction of the model. The strongest upregulation of *Pdlim1* occurred at the peak of EAE when mRNA expression was more than 9x upregulated in spinal cord endothelial cells (Fig 1.1A). Furthermore, we found that *Pdlim1* mRNA is robustly expressed in heart, lung, and liver endothelial cells, but not in brain or spinal cord endothelial cells (Fig 1.1B). We validated these data by quantifying the percentage of PDLIM1+ vascular length in control CNS tissue and in areas of BBB leakage to a biotin tracer. We found that PDLIM1+ vasculature was 2-9% and 18% of total vascular length in healthy brain and spinal cord, respectively. In areas of BBB leakage, however, the percentage of PDLIM1+ vascular length dramatically increased to 88-99% (Fig 1.1C-D). Thus, in both health and disease, endothelial PDLIM1 expression seems to be correlated to BBB permeability.

*PDLIM1 failed to inhibit Wnt signaling, and inhibited NF-κB signaling in HEK293 cells but not primary endothelial cells*

Based on our expression data, our first hypothesis was that PDLIM1 drives BBB permeability in disease. PDLIM1 has been shown to inhibit nuclear translocation of β-catenin in colorectal cancer cells[6]. This was of particular interest to us because nuclear translocation of β-catenin is an important step in the Wnt signaling pathway, which is known to initiate and maintain BBB integrity[14-17]. To test whether PDLIM1 inhibits Wnt signaling, we performed a luciferase assay using HEK293 cells (Fig 1.2A). Briefly, cells were transfected with a construct containing Firefly luciferase under control of the TCF/LEF promoter, which is known to be turned on by Wnt signaling. A *Renilla* luciferase construct was included as a transfection control. In addition to luciferase constructs, cells were also transfected with Wnt pathway proteins and *Pdlim1* or a control vector. PDLIM1 had no inhibitory effect on luminescence, indicating that it does not inhibit Wnt signaling (Fig 1.2A).

It is also possible that PDLIM1 could be upregulated in disease as a protective mechanism. PDLIM1 has been shown to inhibit nuclear translocation of p65, an essential component of the NF-κB pathway[12]. NF-κB is a major inflammatory signaling pathway, thus we hypothesized that PDLIM1 might inhibit inflammatory activation of endothelial cells, thereby protecting endothelial cells in the context of disease. To confirm that PDLIM1 inhibits NF-kB signaling, we transfected HEK293 cells with Firefly luciferase under the control of NF-κB, again using a *Renilla* luciferase construct as a transfection control. Cells were also transfected with *Pdlim1* or a control vector. Cells were then treated with TNFα to induce inflammatory signaling. We found that PDLIM1 indeed inhibited NF-κB signaling, both under control conditions ($p=0.0235$) and with inflammatory stimulation by TNFα ($p<0.0001$) (Fig 1.2B).

PDLIM1 is known to have varying effects on different cell types, thus results from HEK cells may not translate to endothelial cells. To determine whether PDLIM1 is also able to inhibit NF-κB signaling in endothelial cells, we cultured primary endothelial cells from EC-PDLIM1 mice and littermate controls. Cultured cells were treated with TNFα to induce inflammatory signaling, fixed, and stained for p65. The

ratio of nuclear to cytoplasmic p65 fluorescence was used as a measurement of p65 nuclear translocation (Fig 1.2C). Nuclear translocation of p65 is the final step in the NF-κB pathway, and PDLIM1 had been shown to inhibit this step by sequestering p65 in the cytoplasm[12]. We therefore hypothesized that endothelial cells from EC-PDLIM1 mice would exhibit reduced nuclear p65 concentration in response to TNFα. However, we found no significant inhibitory effect of PDLIM1 overexpression on p65 nuclear translocation (Fig 1.2C), suggesting that PDLIM1 may have an alternative role in endothelial cells.

*Endothelial PDLIM1 overexpression affects cell adhesion and protein phosphorylation*

We next took an unbiased approach to understanding the role of PDLIM1 at the BBB. We created a mouse line that overexpresses PDLIM1 in endothelial cells. Specifically, we created a transgene with the tetracycline-controlled transactivator (tTA) under the *Tie2* promoter to express tTA in endothelial cells. We also created a transgene with *Pdlim1* and GFP under the tetracycline response element (TRE). Thus, double transgenic mice (*Tie2-tTA; TRE-Pdlim1-IRES-GFP*, or "EC-PDLIM1") overexpress PDLIM1 in endothelial cells, the transgene-expressing cells can be visualized with GFP, and overexpression can be turned off with the administration of doxycycline (Fig 1.3A). To understand how CNS endothelial cells are altered by overexpression of PDLIM1, we acutely isolated brain endothelial cells from adult double transgenic EC-PDLIM1 mice and single transgenic or wildtype littermate controls. We used a series of enzymatic digestions and triturations to break up the tissue and then used immunofluorescent staining and fluorescently activated cell sorting (FACS) to purify endothelial cells. Endothelial cells isolated from EC-PDLIM1 mice were further sorted into GFP+ and GFP- pools. We performed bulk RNA sequencing on three cell populations: endothelial cells from littermate control mice, GFP+ endothelial cells from EC-PDLIM1 mice, and GFP- endothelial cells from EC-PDLIM1 mice. We found that, as expected, *Pdlim1* mRNA was highly upregulated in the GFP+ population from EC-PDLIM1 mice compared to the control and EC-PDLIM1 GFP- populations (Fig 1.3B).

We used DAVID bioinformatics to analyze specific biological processes that were up- or downregulated in the EC-PDLIM1 GFP+ population compared to the control population (Fig 1.3C-D). Interestingly, one of the most significantly upregulated processes was cell adhesion (Fig 1.3C), suggesting that endothelial cells might upregulate PDLIM1 as a protective mechanism in disease and injury. These cell adhesion-related genes upregulated by PDLIM1 overexpression included *Frem2*, *Flrt2*, *Itga4*, *Npnt*, *Nid1*, and *Pcdh12* (Fig 1.3E). Protein phosphorylation was among the processes both up- and downregulated (Fig 1.3C-D), suggesting PDLIM1 expression also causes overall shifts in post-translational processing. One of the most significantly downregulated genes was *Reck* (Fig 1.3F). RECK is an important co-factor in the Wnt7a/7b signaling pathway in the CNS[18]. However, *Axin2* mRNA expression – commonly used as a readout of Wnt signaling – was not affected by PDLIM1 overexpression (Fig 1.3F). Other endothelial effectors of Wnt signaling such as *Tcf7*, *Lef1*, *Tcf7l1*, and *Tcf7l2* also did not exhibit significantly altered mRNA expression (data not shown).

*Endothelial PDLIM1 overexpression in a model of multiple sclerosis*

PDLIM1 was upregulated in mouse models of TBI, seizures, stroke, and MS, and it was most strongly upregulated in the EAE model of MS (Fig 1.1A). We therefore used the EAE model to test the effects of modulating PDLIM1 during disease. To characterize whether PDLIM1 drives BBB dysfunction or is protective, we induced EAE in EC-PDLIM1 mice and littermate controls. If PDLIM1 protects BBB integrity by increasing endothelial cell adhesion, we would expect to see that EC-PDLIM1 mice have delayed and/or less severe clinical manifestations in EAE. Conversely, if PDLIM1 drives BBB dysfunction, we would expect mice to exhibit more rapid and/or severe paralysis. Although there was no significant difference in clinical score between EC-PDLIM1 mice and littermate controls, EC-PDLIM1 mice trended towards having a slower and less severe disease course (Fig 1.4). Importantly, these data demonstrate that constitutively upregulating PDLIM1 expression in endothelial cells prior to and during disease does not increase disease severity, suggesting that PDLIM1 is not a primary driver of BBB permeability. Although the effect did not reach statistical significance, the EC-PDLIM1 group had a consistently lower average

clinical score from 8-21 days post immunization, suggesting that PDLIM1 may indeed protect the BBB in contexts of neurological disease.

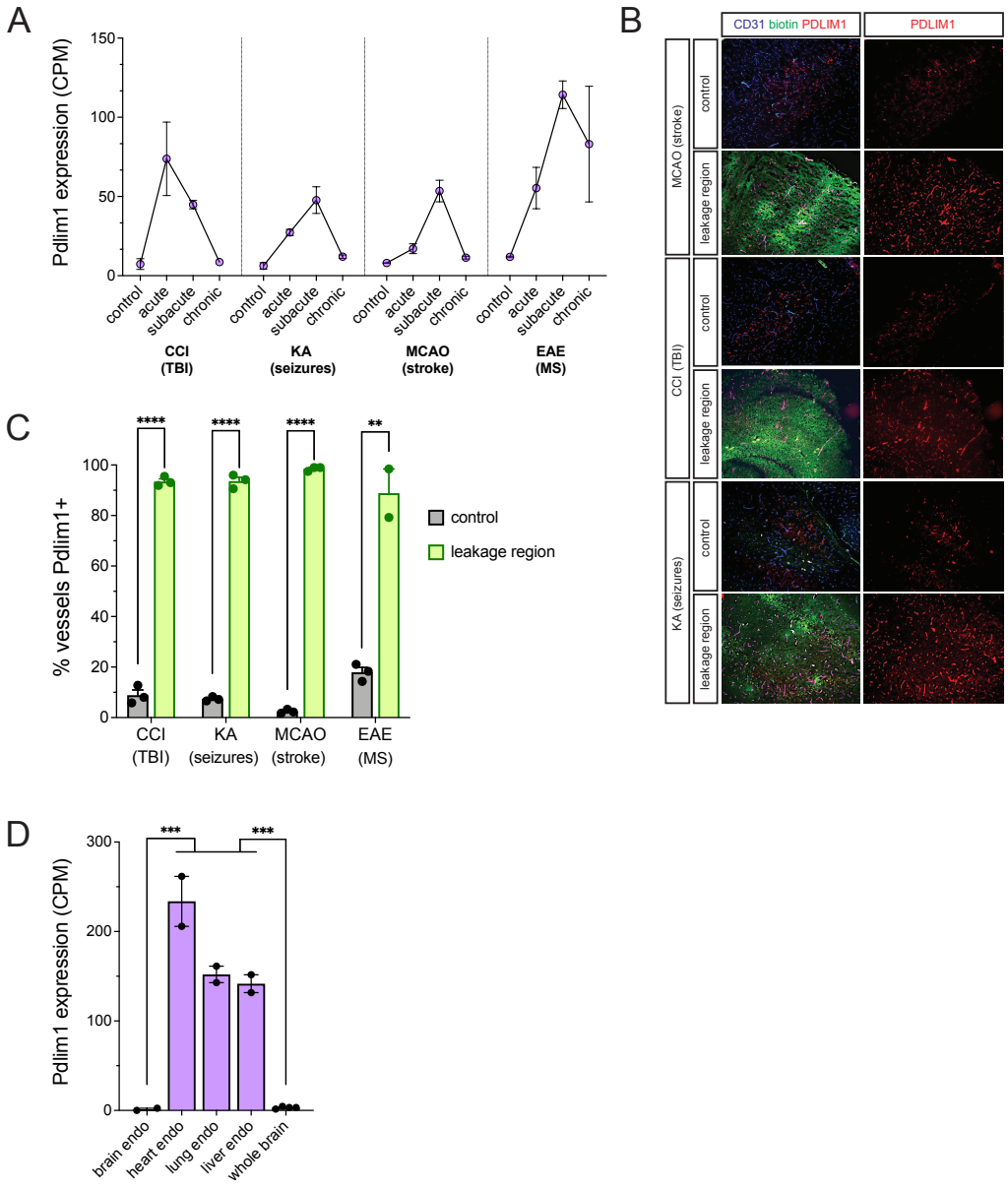


**Figure 1.1 Endothelial PDLIM1 expression correlates with vascular permeability in health and disease. A-C)** Pediatric controlled cortical impact (CCI), kainic acid (KA), permanent middle cerebral artery occlusion (MCAO), and experimental autoimmune myoencephalitis (EAE) were used to model traumatic brain injury (TBI), seizures, stroke, and multiple sclerosis (MS), respectively. **A)** RNA sequencing was performed on isolated endothelial cells from the affected region at four different timepoints for each disease. *Pdlim1* expression was upregulated in each disease at both the acute and subacute timepoints. **B)** Mice were perfused with NHS-sulfo-biotin to visualize BBB leakage (green). Sections were also stained for CD31 (blue) and PDLIM1 (red). **C)** Vascular length positive for PDLIM1 was quantified within leakage and control regions in each disease model. PDLIM1+ vascular length was dramatically increased in regions of BBB leakage. **D)** RNA sequencing was performed on endothelial cells isolated from brain, heart, lung and liver, as well as on whole brain homogenate. *Pdlim1* is expressed in peripheral, but not CNS, endothelial cells.

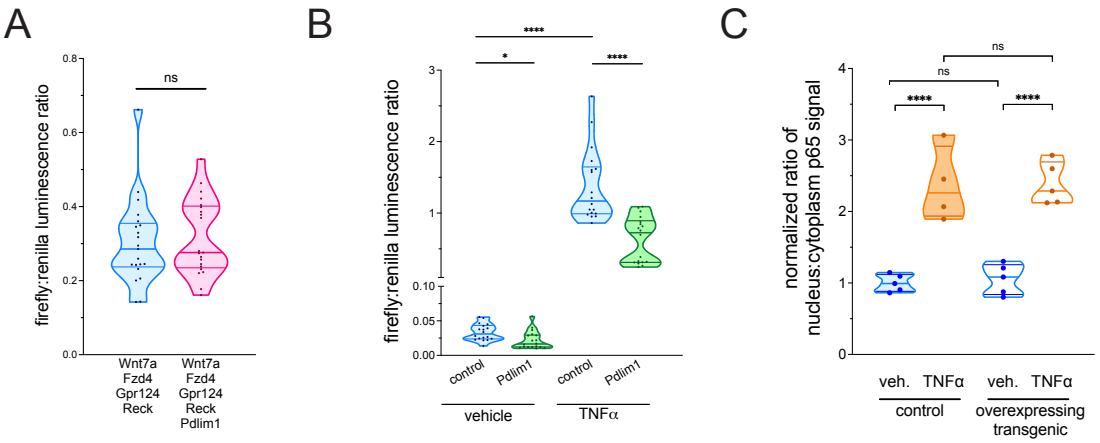


**Figure 1.2 PDLIM1 failed to inhibit Wnt signaling, and inhibited NF-κB signaling in HEK293 cells but not primary endothelial cells. A)** HEK293 cells were transfected with firefly and *Renilla* luciferase, as well as *Wnt7a*, *Fzd4*, *Gpr124*, *Reck*, and *Pdlim1* or a control vector. Firefly luciferase was under the TCF/LEF promoter such that firefly luminescence was a proxy for Wnt signaling, and *Renilla* luciferase acted as a transfection control. *Pdlim1* transfection did not significantly alter the firefly:*Renilla* luminescence ratio. **B)** HEK293 cells were transfected with firefly and *Renilla* luciferases as well as *Pdlim1* or a control vector. Firefly luciferase was expressed under control of NF-κB such that luminescence was a proxy for NF-κB signaling, and *Renilla* was used as a transfection control. Cells were then treated with vehicle or TNFα. *Pdlim1* transfection significantly inhibited firefly:renilla luminescence ratio in both vehicle and TNFα conditions ($p=0.0235$; $p<0.0001$). **C)** Primary endothelial cells were isolated from control or EC-PDLIM1 mice and cultured. They were treated with vehicle or TNFα (20 ng/mL) for 24 hours, then fixed and stained for p65. p65 fluorescence was quantified in endothelial nuclei and cytoplasms, with the average ratio per cell signifying nuclear translocation of p65. TNFα treatment increased p65 nuclear translocation ($p<0.0001$), but PDLIM1 overexpression did not inhibit this increase.

**Figure 1.3 PDLIM1 overexpression increases cell adhesion molecules and alters post-translational modification. A)** *Tie2-tTA* mice were mated to *TRE-Pdlim1-IRES-GFP* mice to create "EC-PDLIM1" mice which overexpress PDLIM1 in endothelial cells. **B-F)** Brains from EC-PDLIM double transgenic and littermate control mice were dissected and dissociated, and endothelial cells were isolated by FACS for RNA sequencing. Three populations were taken from each pair of mice: endothelial cells from the control mice, GFP+ endothelial cells from EC-PDLIM1 mice, and GFP- endothelial cells from the same EC-PDLIM1 mice. **B)** PDLIM1 expression was highly upregulated from control levels in GFP+ but not GFP- endothelial cells from EC-PDLIM1 mice. **C-D)** DAVID was used for biological processes analysis comparing control and EC-PDLIM1 GFP+ endothelial cells. Enriched pathways in GFP+ endothelial cells included cell adhesion. Genes associated with protein phosphorylation were both up- and downregulated. **E)** Expression levels of six cell-adhesion related genes significantly upregulated in EC-PDLIM1 GFP+ endothelial cells. **F)** *Reck* expression was downregulated in EC-PDLIM1 GFP+ endothelial cells, but *Axin2* levels did not change.

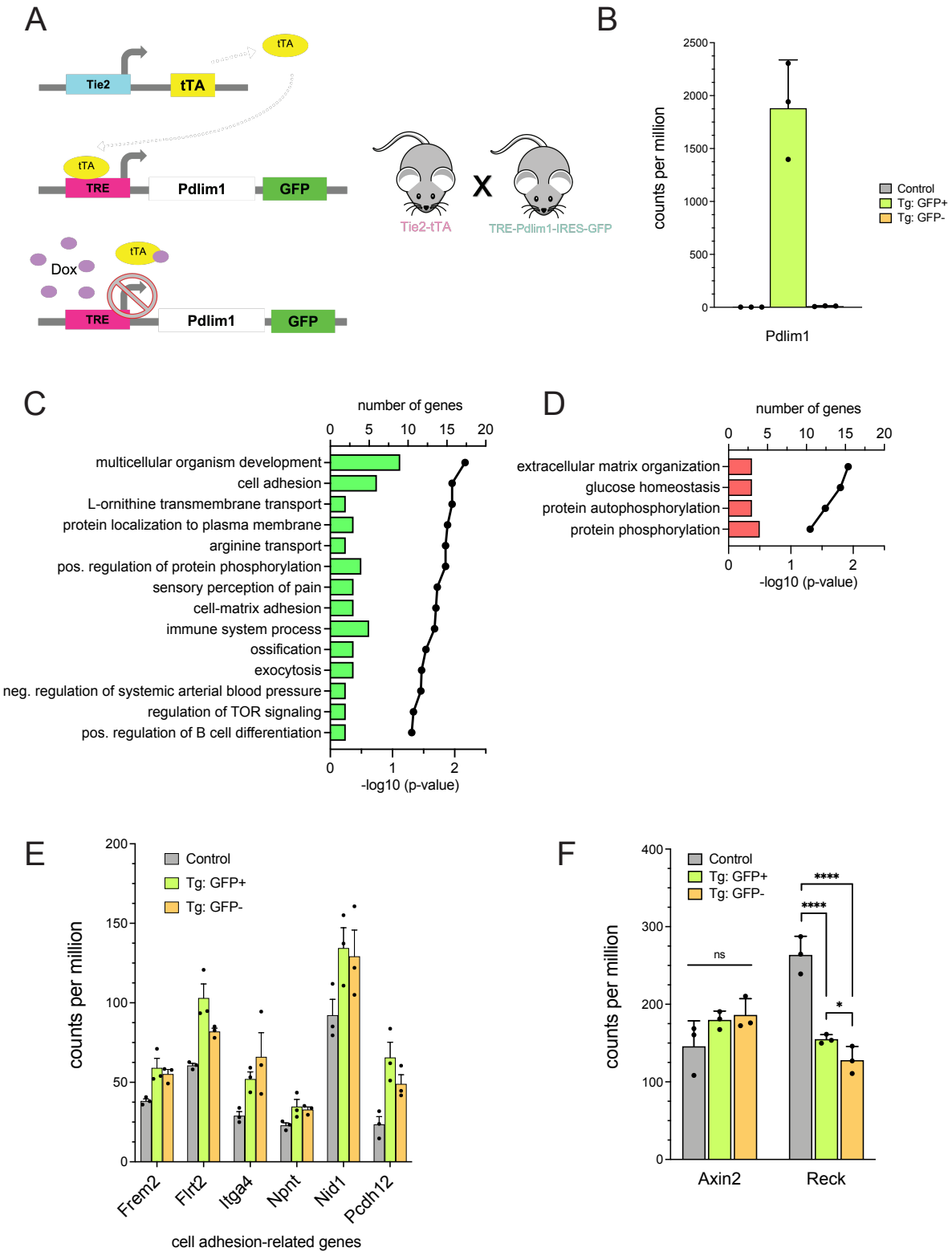
A
Tie2
tTA
tTA
TRE
Pdlim1
GFP
Dox
tTA
TRE
Pdlim1
GFP
Tie2-tTA
X
TRE-Pdlim1-IRES-GFP
B
counts per million
2500
2000
1500
1000
500
0
Pdlim1
Control
Tg: GFP+
Tg: GFP-
C
number of genes
0 5 10 15 20
multicellular organism development
cell adhesion
L-ornithine transmembrane transport
protein localization to plasma membrane
arginine transport
pos. regulation of protein phosphorylation
sensory perception of pain
cell-matrix adhesion
immune system process
ossification
exocytosis
neg. regulation of systemic arterial blood pressure
regulation of TOR signaling
pos. regulation of B cell differentiation
0 1 2
-log10 (p-value)
D
number of genes
0 5 10 15 20
extracellular matrix organization
glucose homeostasis
protein autophosphorylation
protein phosphorylation
0 1 2
-log10 (p-value)
E
counts per million
200
150
100
50
0
Control
Tg: GFP+
Tg: GFP-
Frem2
Flrt2
Itga4
Npnt
Nid1
Pcdh12
cell adhesion-related genes
F
counts per million
400
300
200
100
0
Control
Tg: GFP+
Tg: GFP-
ns
****
****
*
Axin2
Reck

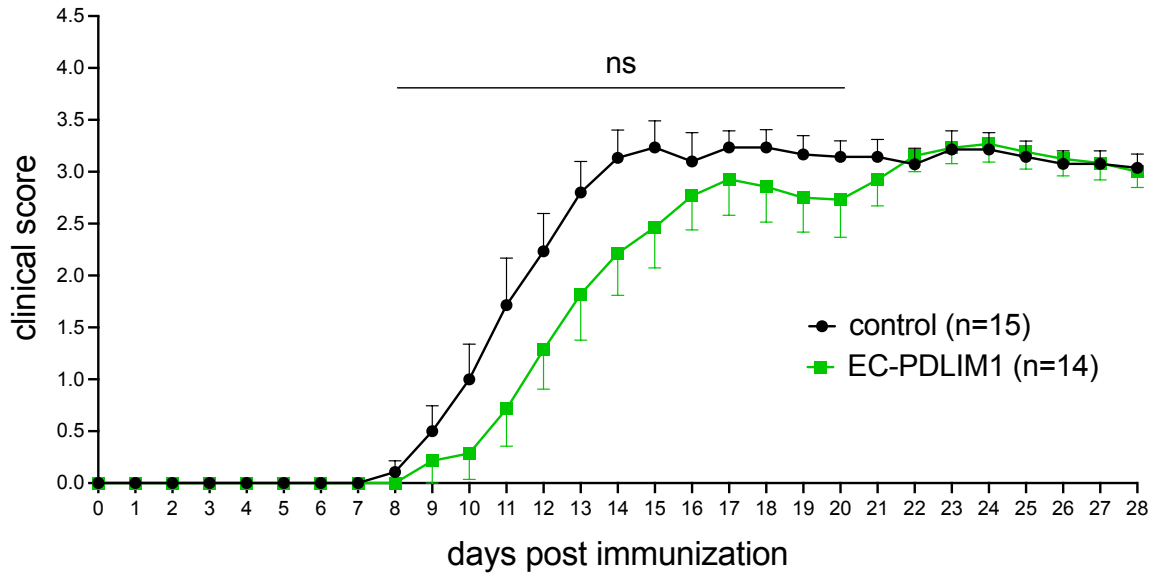


**Figure 1.4 PDLIM1 overexpression in a model of multiple sclerosis**. EAE was induced in 10–15-week-old male and female EC-PDLIM1 mice (green) and littermate controls (black). Mice were observed each day and scored based on levels of paralysis, with a score of 0 indicating no symptoms and a score of 4 indicating full hindlimb paralysis. There were no significant differences in clinical score at any day of the disease course as assessed by two-tailed Student's t-test.

**Discussion**

BBB disruption occurs in neuropathologies with vastly diverse etiologies. For instance, MS, stroke, TBI, and seizures are driven by inflammation, hypoxia, physical impact, and neuronal hyperactivity, and yet all lead to increased BBB permeability. Munji and Soung et al. found that, at acute timepoints after disease onset, transcriptomic changes in CNS endothelial cells varied among diseases[2]. However, by the subacute timepoint – the point at which BBB leakage is the most severe – the disease-related endothelial gene profiles were more similar across diseases, suggesting the existence of a BBB dysfunction gene cassette that is common across various neuropathologies[2]. This information is incredibly promising, as it increases the likelihood that a drug could be targeted to help prevent BBB leakage not in just one disease but in a wide range of neurological conditions. In trying to identify novel targets to modulate BBB function in disease, we found that PDLIM1 – a protein not previously studied in the context of the BBB – was upregulated in endothelial cells in all four disease models. We became most excited about PDLIM1 when we assessed its spatial expression in the CNS during disease. PDLIM1 was largely absent from healthy vasculature but, quite strikingly, was expressed throughout the vasculature specifically within regions of biotin leakage. This was exciting to us because, to our knowledge, there is no other endogenous protein whose expression so specifically distinguishes areas of BBB permeability without use of a tracer.

A protein upregulated during disease might be contributing to dysfunction or helping to protect against damage. PDLIM1 has been shown to perform a myriad of roles in different cell types and organ systems. It has been mostly studied in cancer, where it promotes metastasis in some cancers and prevents it in others. PDLIM1 is a cytoplasmic protein that associates with the actin cytoskeleton. It is thus in a perfect position to anchor signaling molecules to the cytoskeleton, preventing nuclear translocation and downstream signaling. For instance, PDLIM1 has been shown to prevent β-catenin and p65 nuclear translocation, thus inhibiting epithelial-mesenchymal transition and NF-κB signaling, respectively[6,12]. We hypothesized that PDLIM1 might drive BBB disruption by inhibiting Wnt signaling (which relies on β-catenin nuclear translocation) or might reduce inflammation by decreasing NF-κB signaling. However, we

were unable to show that PDLIM1 inhibited either of these processes in endothelial cells *in vitro*. It is still possible that PDLIM1 plays one or both of these roles *in vivo*. Intriguingly, we found that RECK, a co-factor for the CNS endothelial cell Wnt7a/7b receptor, FZD4[18], was downregulated by overexpression of PDLIM1 (Fig 1.3F). Perhaps more interestingly, it was downregulated not only in the GFP+ cell population but also the GFP- cell population from EC-PDLIM1 mice. We hypothesized that perhaps PDLIM1 was inhibiting Wnt signaling in endothelial cells and that, in response, more Wnt7a/7b was being produced in the brain as a compensatory mechanism, leading to the downregulation of RECK in a negative feedback loop. We tested this hypothesis by performing a qPCR for Wnt7a and 7b in whole brain homogenate. We did not find any differences in brain production of Wnt 7a/b in EC-PDLIM1 mice compared to littermate controls (data not shown). Thus, the reason for or effect of RECK downregulation by PDLIM1 overexpression remains unclear.

In analyzing how PDLIM1 overexpression alters the brain endothelial transcriptome, we found that PDLIM1 overexpression induced upregulation of a handful of cell adhesion molecules (Fig 1.3C, E). These genes do not fall into a specific category. *Frem2* and *Itga4* are BBB-enriched compared to peripheral endothelial cells, while *Nid1* and *Pcdh12* are periphery-enriched[2]. FREM2 and NID1 are extracellular matrix proteins, while FLRT2, ITGA4, and PCDH12 are membrane proteins. Their common denominator is a role in cell adhesion. The fact that PDLIM1 overexpression promotes cell adhesion in a general fashion suggests that it might be playing a protective role in disease. However, especially since most of these cell-adhesion molecules are expressed not only in the GFP+ but also the GFP- populations from EC-PDLIM1 mice, like the downregulation of RECK, it is possible these cell adhesion molecules were upregulated as a defense mechanism against PDLIM1-driven BBB disruption. Importantly, in the EAE model of MS, overexpression of PDLIM1 did not exacerbate disease severity and instead trended towards delaying and slowing disease progression. These data support the notion of PDLIM1 as a protective rather than harmful at the BBB (NYY).

Future directions include inducing disease models in Pdlim1$^{-/-}$ and littermate controls to assess how preventing PDLIM1 upregulation alters disease course and the transcriptome of brain or spinal cord

endothelial cells. This unbiased approach will allow us to further examine how PDLIM1 contributes to or prevents BBB dysfunction during disease.

**Acknowledgements**

Chapter I, in full, is currently being prepared for submission for publication and will include Kaja Bajc, Lucija Pintarić, Alexander Z. Zhang, Tony Z. Zhang, Joseph P. Miller, and Fabien Sohet as co-authors, and Professor Richard Daneman as the senior author. The dissertation author was the primary investigator and author of this material.

**References**

1 Profaci, C. P., Munji, R. N., Pulido, R. S. & Daneman, R. The blood-brain barrier in health and disease: Important unanswered questions. *J Exp Med* **217**, doi:10.1084/jem.20190062 (2020).

2 Munji, R. N., Soung, A. L., Weiner, G. A., Sohet, F., Semple, B. D., Trivedi, A., Gimlin, K., Kotoda, M., Korai, M., Aydin, S., Batugal, A., Cabangcala, A. C., Schupp, P. G., Oldham, M. C., Hashimoto, T., Noble-Haeusslein, L. J. & Daneman, R. Profiling the mouse brain endothelial transcriptome in health and disease models reveals a core blood-brain barrier dysfunction module. *Nat Neurosci*, doi:10.1038/s41593-019-0497-x (2019).

3 Bauer, K., Kratzer, M., Otte, M., de Quintana, K. L., Hagmann, J., Arnold, G. J., Eckerskorn, C., Lottspeich, F. & Siess, W. Human CLP36, a PDZ-domain and LIM-domain protein, binds to alpha-actinin-1 and associates with actin filaments and stress fibers in activated platelets and endothelial cells. *Blood* **96**, 4236-4245 (2000).

4 Tamura, N., Ohno, K., Katayama, T., Kanayama, N. & Sato, K. The PDZ-LIM protein CLP36 is required for actin stress fiber formation and focal adhesion assembly in BeWo cells. *Biochem Biophys Res Commun* **364**, 589-594, doi:10.1016/j.bbrc.2007.10.064 (2007).

5 Zhou, J. K., Fan, X., Cheng, J., Liu, W. & Peng, Y. PDLIM1: Structure, function and implication in cancer. *Cell Stress* **5**, 119-127, doi:10.15698/cst2021.08.254 (2021).

6 Chen, H. N., Yuan, K., Xie, N., Wang, K., Huang, Z., Chen, Y., Dou, Q., Wu, M., Nice, E. C., Zhou, Z. G. & Huang, C. PDLIM1 Stabilizes the E-Cadherin/beta-Catenin Complex to Prevent Epithelial-Mesenchymal Transition and Metastatic Potential of Colorectal Cancer Cells. *Cancer Res* **76**, 1122-1134, doi:10.1158/0008-5472.CAN-15-1962 (2016).

7 Huang, Z., Zhou, J. K., Wang, K., Chen, H., Qin, S., Liu, J., Luo, M., Chen, Y., Jiang, J., Zhou, L., Zhu, L., He, J., Li, J., Pu, W., Gong, Y., Li, J., Ye, Q., Dong, D., Hu, H., Zhou, Z., Dai, L., Huang, C., Wei, X. & Peng, Y. PDLIM1 Inhibits Tumor Metastasis Through Activating Hippo Signaling in Hepatocellular Carcinoma. *Hepatology* **71**, 1643-1659, doi:10.1002/hep.30930 (2020).

8 Liu, Z., Zhan, Y., Tu, Y., Chen, K., Liu, Z. & Wu, C. PDZ and LIM domain protein 1(PDLIM1)/CLP36 promotes breast cancer cell migration, invasion and metastasis through interaction with alpha-actinin. *Oncogene* **34**, 1300-1311, doi:10.1038/onc.2014.64 (2015).

9 Ahn, B. Y., Saldanha-Gama, R. F., Rahn, J. J., Hao, X., Zhang, J., Dang, N. H., Alshehri, M., Robbins, S. M. & Senger, D. L. Glioma invasion mediated by the p75 neurotrophin receptor (p75(NTR)/CD271) requires regulated interaction with PDLIM1. *Oncogene* **35**, 1411-1422, doi:10.1038/onc.2015.199 (2016).

10 Li, L. M., Luo, F. J. & Song, X. MicroRNA-370-3p inhibits cell proliferation and induces chronic myelogenous leukaemia cell apoptosis by suppressing PDLIM1/Wnt/beta-catenin signaling. *Neoplasma* **67**, 509-518, doi:10.4149/neo_2020_190612N506 (2020).

11 Milanesi, E., Manda, G., Dobre, M., Codrici, E., Neagoe, I. V., Popescu, B. O., Bajenaru, O. A., Spiru, L., Tudose, C., Prada, G. I., Davidescu, E. I., Pinol-Ripoll, G. & Cuadrado, A. Distinctive Under-Expression Profile of Inflammatory and Redox Genes in the Blood of Elderly Patients with Cardiovascular Disease. *J Inflamm Res* **14**, 429-442, doi:10.2147/JIR.S280328 (2021).

12 Ono, R., Kaisho, T. & Tanaka, T. PDLIM1 inhibits NF-kappaB-mediated inflammatory signaling by sequestering the p65 subunit of NF-kappaB in the cytoplasm. *Sci Rep* **5**, 18327, doi:10.1038/srep18327 (2015).

13 Gong, F. H., Cheng, W. L., Wang, H., Gao, M., Qin, J. J., Zhang, Y., Li, X., Zhu, X., Xia, H. & She, Z. G. Reduced atherosclerosis lesion size, inflammatory response in miR-150 knockout mice via macrophage effects. *J Lipid Res* **59**, 658-669, doi:10.1194/jlr.M082651 (2018).

14 Daneman, R., Agalliu, D., Zhou, L., Kuhnert, F., Kuo, C. J. & Barres, B. A. Wnt/beta-catenin signaling is required for CNS, but not non-CNS, angiogenesis. *Proc Natl Acad Sci U S A* **106**, 641-646, doi:10.1073/pnas.0805165106 (2009).

15 Liebner, S., Corada, M., Bangsow, T., Babbage, J., Taddei, A., Czupalla, C. J., Reis, M., Felici, A., Wolburg, H., Fruttiger, M., Taketo, M. M., von Melchner, H., Plate, K. H., Gerhardt, H. & Dejana, E. Wnt/beta-catenin signaling controls development of the blood-brain barrier. *J Cell Biol* **183**, 409-417, doi:10.1083/jcb.200806024 (2008).

16 Stenman, J. M., Rajagopal, J., Carroll, T. J., Ishibashi, M., McMahon, J. & McMahon, A. P. Canonical Wnt signaling regulates organ-specific assembly and differentiation of CNS vasculature. *Science* **322**, 1247-1250, doi:10.1126/science.1164594 (2008).

17 Chang, J., Mancuso, M. R., Maier, C., Liang, X., Yuki, K., Yang, L., Kwong, J. W., Wang, J., Rao, V., Vallon, M., Kosinski, C., Zhang, J. J., Mah, A. T., Xu, L., Li, L., Gholamin, S., Reyes, T. F., Li, R., Kuhnert, F., Han, X., Yuan, J., Chiou, S. H., Brettman, A. D., Daly, L., Corney, D. C., Cheshier, S. H., Shortliffe, L. D., Wu, X., Snyder, M., Chan, P., Giffard, R. G., Chang, H. Y., Andreasson, K. & Kuo, C. J. Gpr124 is essential for blood-brain barrier integrity in central nervous system disease. *Nat Med* **23**, 450-460, doi:10.1038/nm.4309 (2017).

18 Cho, C., Smallwood, P. M. & Nathans, J. Reck and Gpr124 Are Essential Receptor Cofactors for Wnt7a/Wnt7b-Specific Signaling in Mammalian CNS Angiogenesis and Blood-Brain Barrier Regulation. *Neuron* **95**, 1056-1073 e1055, doi:10.1016/j.neuron.2017.07.031 (2017).

19 Wang, Y., Rattner, A., Zhou, Y., Williams, J., Smallwood, P. M. & Nathans, J. Norrin/Frizzled4 signaling in retinal vascular development and blood brain barrier plasticity. *Cell* **151**, 1332-1344, doi:10.1016/j.cell.2012.10.042 (2012).

20 Ye, X., Wang, Y., Cahill, H., Yu, M., Badea, T. C., Smallwood, P. M., Peachey, N. S. & Nathans, J. Norrin, frizzled-4, and Lrp5 signaling in endothelial cells controls a genetic program for retinal vascularization. *Cell* **139**, 285-298, doi:10.1016/j.cell.2009.07.047 (2009).

21 Zhou, Y. & Nathans, J. Gpr124 controls CNS angiogenesis and blood-brain barrier integrity by promoting ligand-specific canonical wnt signaling. *Dev Cell* **31**, 248-256, doi:10.1016/j.devcel.2014.08.018 (2014).

## CHAPTER II

### Microglia are not necessary for blood-brain barrier properties in healthy brain vasculature


### Abstract

Microglia are resident immune cells of the central nervous system, yet their functions expand far beyond those related to pathology. From pruning neural synapses during development to preventing excessive neural activity throughout life, microglia are intimately involved in the brain's most basic processes. While studies have reported both helpful and harmful roles for microglia at the blood-brain barrier (BBB) in the context of pathology, much less work has been done to understand microglia-endothelial cell interactions in the healthy brain. Here, to probe the role of microglia at the healthy BBB, we used the colony-stimulating factor 1 receptor (CSF1R) inhibitor PLX5622 to deplete microglia. We then analyzed blood-brain barrier structure, permeability to tracers, and transcriptome. We found that microglia are not necessary for endothelial barrier function in the healthy brain. However, this does not preclude a meaningful microglial-endothelial cell interaction in contexts aside from barrier function.


### Introduction

Microglia were first clearly visualized in 1919 by Pío del Río-Hortega, and in 1924 became widely recognized as a distinct cell-type[1]. In the century since, research has shed light on the complex roles of microglia in countless brain processes throughout life. We now know that microglia are incredibly dynamic cells, constantly moving their ramified processes to survey their environment[2,3]. Studies have described the different "personalities" microglia can adopt in different situations, acting as patrollers, circuit sculptors, protectors, or villains depending on the context. Indeed, while many researchers have distinguished between polarized pro- and anti- inflammatory states by referring to them as M1 and M2 microglia, respectively, others have argued that this terminology oversimplifies the range of microglial phenotypes[4].

While perivascular, meningeal, and choroid plexus macrophages occupy different niches within the central nervous system (CNS), microglia are the only CNS parenchymal macrophages. They arise from

yolk sac progenitors, traveling to the brain at approximately embryonic day 9.5 (E9.5) in the developing mouse[5]. From the early days of their residency in the brain, microglia are intimately involved in refining neural circuits via synaptic pruning[6-8]. Their interaction with CNS vasculature also begins early. Juxtavascular microglia migrate along blood vessels as they colonize the developing brain[9], and microglia interact with endothelial tip cells to promote vascular anastomosis[10]. In the adult brain, approximately 20-30% of microglia make somatic contacts with vasculature[9,11]. Interestingly, this interaction is even higher in the first week of postnatal development in mice and at gestational weeks 18-24 in humans[9], although the functional reason for this peak is still undefined. In addition to somatic contacts with vasculature, microglia often contact vasculature with their dynamic processes, reaching between astrocyte endfeet to touch the endothelial basement membrane[12].

Despite the physical interaction between microglia and endothelial cells in the healthy CNS, research on this interaction has primarily focused on how microglia impact the blood-brain barrier (BBB) in disease states. Several groups have shown that microglia can actively help repair the BBB after injury. Fernández-López and colleagues found that, after neonatal stroke, microglial depletion increased hemorrhage in the injured region[13]. Lou and colleagues demonstrated that, upon two-photon laser injury of a single capillary, microglia immediately extend processes towards injury and help to reseal the BBB[14]. In zebrafish, Liu and colleagues captured videos of microglia adhering to two ends of an injured vessel, using mechanical forces to pull the endothelial cells back together[15]. However, there is also evidence that microglia might accelerate BBB dysfunction in some cases, likely in more extreme cases of neuroinflammation. For instance, microglia can be observed forming perivascular clusters in EAE, a mouse model of MS. At the peak of EAE, these clustered microglia produce increased levels of reactive oxygen species[16], known mediators of BBB disruption. It is likely that microglia can be both harmful and protective at the BBB in the context of disease, even playing dual roles within the time course of a single disease. For example, microglia were shown to be initially protective but eventually harmful to BBB integrity during systemic inflammation[17].

Despite a demonstrated – albeit dual – functional role for microglia at the BBB in pathological states, there is no clear understanding of whether microglia regulate the individual properties of the BBB (tight junctions, limited transcytosis, efflux, nutrient transport, limited leukocyte adhesion molecules). While Elmore et al. reported no BBB breakdown upon microglial depletion[18], they assessed the BBB by imaging the intact brain to detect parenchymal extravasation of Evans Blue dye, a method that would likely only reveal severe BBB disruption. Delaney et al. suggest that reduced CSF1R signaling can cause remodeling of BBB tight junctions *in vitro*, and they show evidence of vascular pathology in post-mortem samples from people with a CSF1R mutation[19]. However, any direct link between CSF1R signaling and BBB dysfunction has yet to be clearly demonstrated *in vivo*.

In this study, we probed the effect of microglial depletion on BBB structure, permeability, and transcriptome. We used a selective CSF1R inhibitor, PLX5622, to deplete microglia, reaching about 95% elimination. After one month of depletion, we assessed BBB structure via transmission electron microscopy (TEM). We used two different fluorescent tracers, sodium fluorescein and rhodamine 123, to probe barrier permeability. Finally, we acutely purified endothelial cells from control and microglia-deficient mice and performed RNA sequencing to determine the effects of microglial depletion on the endothelial transcriptome. We found that microglial depletion does not affect BBB structure or function and does not alter expression of genes associated with barrier properties.

## Methods

### *Animals*

Experiments were performed on 8-15-week-old male C57BL/6 mice purchased from Charles River Laboratories. PLX5622 was provided by Plexxikon, Inc. and incorporated into the AIN-76A rodent diet (D10001i) at 1200 mg/kg (D11100404i) by Research Diets, Inc. AIN-76A diet was used as a control. Both diets were irradiated prior to use. All experiments were performed one month after diet onset. All experiments were approved by the Institutional Animal Care and Use Committee at UCSD.

*Transmission electron microscopy (TEM)*

Mice were transcardially perfused with DPBS followed by 15 mL of 2% paraformaldehyde and 2.5% glutaraldehyde in 0.15M sodium cacodylate buffer. Brains were dissected and post-fixed in the same solution overnight at 4°C. Small cubes were cut from cortex and processed by the CMM Electron Microscopy Facility. Ultrathin sections were cut on a Leica microtome with a diamond knife and stained with uranyl acetate and lead. Images were captured on a JEOL 1400plus TEM at 80 kV with a Gatan 4kx4k camera. At least 20 individual vessel cross-sections were imaged per animal.

*Tight junction and transcytosis analysis*

The length of tight junctions across all TEM images was measured using the ImageJ line tool and converted to nanometers using the image scale bar. Sum length of all tight junctions was divided by the number of tight junctions to determine average tight junction length. Invaginating vesicles were counted across all images for each mouse. The total number of invaginating vesicles was divided by the number of vessel cross-sections analyzed.

*Sodium fluorescein*

Mice were injected (i.p.) with 25 mg/kg sodium fluorescein salt (Sigma F6377), 2 mg/mL in PBS. After 90 minutes, blood samples were taken from the right ventricle and transferred to an EDTA-coated tube on a rotator. Mice were perfused with DPBS. Brains were dissected, meninges were removed, and cortex and hippocampus were flash frozen. Plasma was collected from blood samples and flash frozen. Samples were stored at -80°C until further processing. Tissue was homogenized in PBS, plasma was diluted in PBS, and 2% TCA was added to each to extract sodium fluorescein overnight. Samples were spun, and supernatant was collected and diluted with borate buffer. A Tecan Infinite 200 plate reader was used to measure fluorescence (excitation 480, emission 538). Wells of 0.5% TCA, 50% borate buffer, and 25% PBS were used as a background control. Average of background signal was subtracted from that of each

experimental well. Brain fluorescence was divided by blood fluorescence within each sample to determine the amount of parenchymal extravasation.

*Rhodamine 123*

Mice were injected with 2 mg/mL rhodamine 123 (1:4 DMSO:sterile saline) at a dose of 25 mg/kg. Mice were perfused with DPBS. Brains were dissected, meninges were removed, and cortex and hippocampus together were flash frozen. Plasma was collected from blood samples and flash frozen. Samples were stored at -80°C until processing. Tissue was homogenized in PBS, plasma was diluted in PBS. Rhodamine123 was extracted by vortexing and incubating overnight with butanol. A Tecan Infinite 200 plate reader was used to measure fluorescence (excitation 505, emission 560). Wells of butanol were used as a background control. Average of background signal was subtracted from that of each experimental well. Brain fluorescence was divided by blood fluorescence within each sample to determine the amount of parenchymal extravasation.

*Endothelial enrichment*

Endothelial enrichment was performed as described in Chapter I. Cells were stained with AF647-conjugated anti-CD31 (Molecular Probes A14716), FITC-conjugated anti-CD13 (BD Biosciences 558744), FITC-conjugated anti-CD45 (eBioscience 11-0451-85), FITC-conjugated anti-CD11b (eBioscience), and DAPI. Cells positive for 647 and negative for FITC and DAPI were sorted into trizol at the UCSD Flow Cytometry Research Core Facility. RNA isolation was performed with the Qiagen RNeasy Micro kit (74004).

*RNA sequencing and bioinformatics*

RNA sequencing and bioinformatics were performed as described in Chapter I.

**Results**

*Microglial depletion does not affect tight junctions or transcytosis at the BBB*

To determine whether microglial depletion affects BBB structure, adult wildtype mice were fed control chow or chow containing 1200 mg/kg of the colony stimulating factor 1 receptor (CSF1R) inhibitor PLX5622 for one month. At this time point, mice fed PLX5622 chow exhibited 95% microglial depletion (Fig 2.1A-B). TEM was used to image cross-sections of blood vessels in cortical tissue from control and microglia-depleted mice. Twenty vessels per mouse were analyzed for BBB structural abnormalities. ImageJ was used to quantify tight junction length, and the number of invaginating vesicles in each vessel was counted (Fig 2.2A). Tight junctions from control mice were an average length of 385.0 ± 49.38 nm, and tight junctions from microglia-depleted mice were 480.9 ± 93.58 nm, a non-significant difference ($p=0.416$) (Fig 2.2B). Furthermore, control and microglia-depleted mice had 0.3 ± 0.15 and 0.3 ± 0.12 actively invaginating vesicles per vessel cross-section, respectively ($p>0.999$) (Fig 2.2B). Together, these data suggest that microglia do not regulate tight junction length or transcytosis at the healthy BBB.

*Microglial depletion does not alter BBB permeability*

To determine whether microglial depletion alters BBB permeability, adult wildtype mice were fed control or PLX5622 diet for one month. Mice were then injected with either sodium fluorescein or rhodamine 123 to detect BBB permeability. Sodium fluorescein is a small, hydrophilic molecule, and its detection in the brain parenchyma might signify disrupted tight junctions between neighboring endothelial cells. Rhodamine 123, in contrast, is a hydrophobic PGP substrate, and its increased presence in the brain parenchyma could be evidence of dysfunctional efflux transport at the BBB. Each tracer was injected i.p. and allowed to circulate for 1.5 hours. Prior to perfusion with DPBS, a sample of blood was taken from the right ventricle of the heart. After perfusion, the cortex and hippocampus were dissected and homogenized, and the tracer was extracted. Fluorescence of brain and blood samples was quantified using a plate reader, and permeability was measured as the ratio of brain:blood fluorescence ("permeability ratio"), with higher ratios being indicative of greater BBB permeability. Microglial depletion did not significantly alter the

permeability ratio of either sodium fluorescein or rhodamine 123. Control and PLX5622-treated mice exhibited permeability ratios of 0.084 ± 0.007 and 0.073 ± 0.005, respectively (p=0.183) in the sodium fluorescein assay (Fig 2.2C). In the rhodamine 123 assay, control and PLX5622-treated mice exhibited permeability ratios of 0.014 ± 0.001 and 0.011 ± 0.001, respectively (p=0.150) (Fig 2.2C). Together, these data suggest that microglia do not regulate BBB permeability to small hydrophilic or hydrophobic molecules.

*Microglial depletion does not alter expression of BBB genes*

Finally, to explore whether microglia depletion affects the expression of BBB-related genes, mice were fed control or PLX5622 chow for one month. Forebrain endothelial cells were acutely isolated with a series of enzymatic digestions and mechanical dissociations. Cells were stained for markers of endothelial cells, pericytes, microglia and dead cells. Fluorescently activated cell sorting (FACS) was used to negatively sort for dead cells, pericytes, and microglia and to positively sort for endothelial cells. Endothelial cell RNA was then isolated for bulk RNA sequencing. We compared mRNA expression levels of genes coding for tight junction proteins, efflux transporters, nutrient transporters, regulators of transcytosis, and leukocyte adhesion molecules. There were no significant differences in the expression of this module of BBB genes (Fig 2.3), suggesting that microglial are not necessary for the expression of BBB properties. We did, however, find that PLX5622 treatment increased endothelial expression of cholesterol synthesis enzymes and uptake receptor. This surprising finding will be discussed in Chapter III.

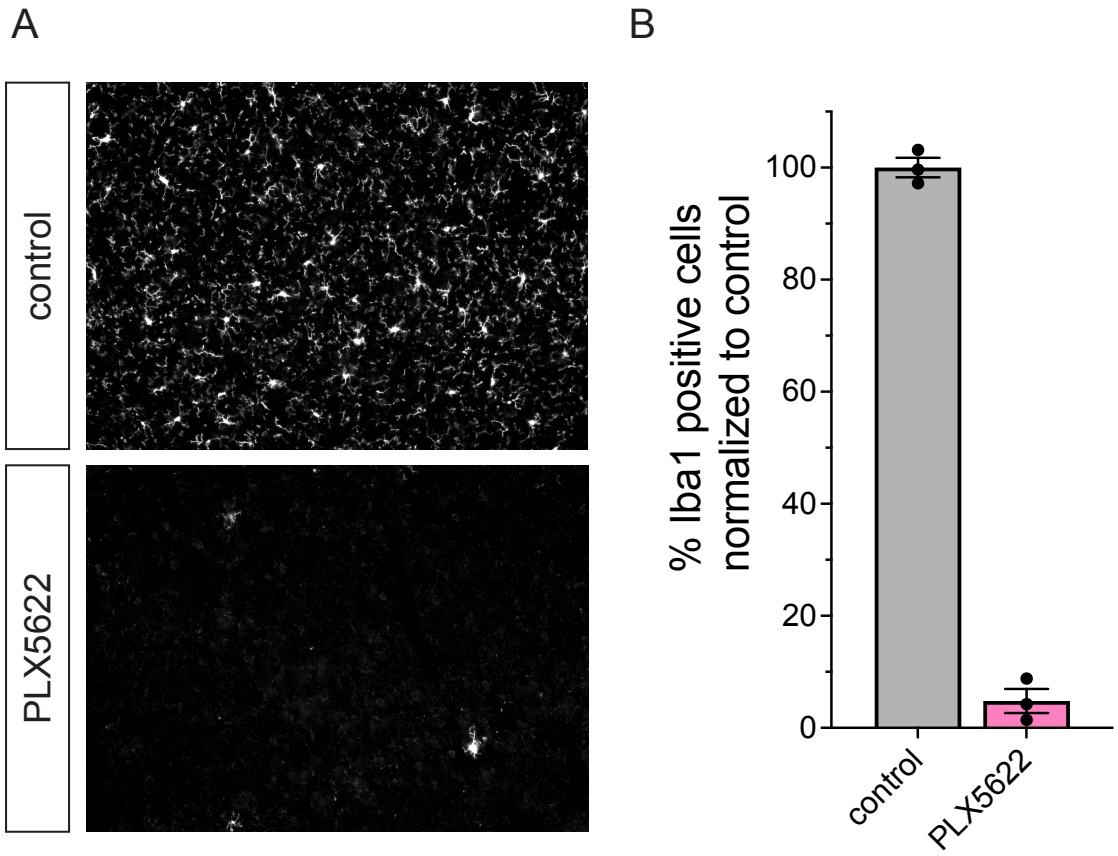


**Figure 2.1. One month of PLX5622 diet significantly depletes microglia.** Adult wildtype mice were fed control or PLX5622 (1200 mg/kg) diet for one month. **A)** Representative images of 10µm sections stained with IBA1 demonstrate that PLX5622 diet significantly depletes microglia. **B)** Microglial cell bodies in the cortex were counted in five 20x images per mouse. Each image came from a distinct 10µm section. Data are represented as a percentage of microglia normalized to the average control value. Each data point represents one mouse (n=3; $p<0.0001$)

**Figure 2.2. Microglial depletion does not affect BBB structure or function.** Adult wildtype mice were fed control or PLX5622 (1200 mg/kg) diet for one month to deplete microglia. **A)** Mice were perfusion-fixed with glutaraldehyde and pieces of cortex were prepared for TEM. Images show examples of tight junctions (left) and invaginating vesicles (right). **B)** Quantification of TEM images. Length of tight junctions were measured using ImageJ (left; n=3; p=0.416) and the number of invaginating vesicles were counted (right, n=3, p>0.999) across vessel cross-sections. Each data point represents one mouse, and error bars represent SEM. Tight junction length is an average of all tight junctions found across cross-sections per mouse. Invaginating vesicles is the average number of invaginating vesicles found per cross-section for each mouse. **C)** Mice were injected with sodium fluorescein or rhodamine 123. 90 minutes later, a blood sample was taken from the right ventricle and mice were perfused with DPBS. Brains were dissected and homogenized, and tracers were extracted from both plasma and brain homogenate. Fluorescence in brain and blood were measured, and permeability was quantified as a ratio of brain:blood fluorescence. There were no group differences in permeability to sodium fluorescein (left; n=9-12; p=0.183) or rhodamine 123 (right; n=12; p=0.150). Error bars represent SEM.

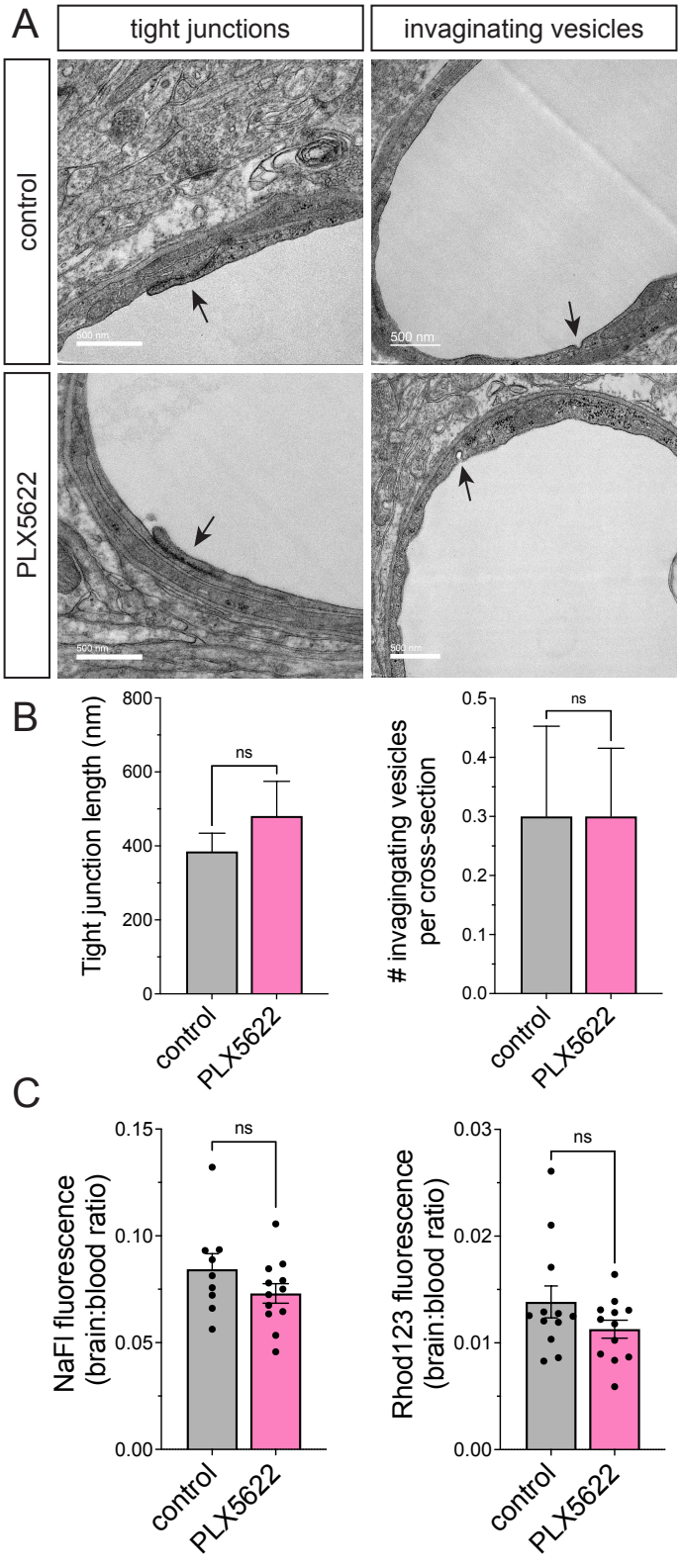
A
tight junctions
invaginating vesicles
control
PLX5622
500 nm
B
Tight junction length (nm)
800
600
400
200
0
ns
control
PLX5622
# invagingating vesicles per cross-section
0.5
0.4
0.3
0.2
0.1
0.0
ns
control
PLX5622
C
NaFl fluorescence (brain:blood ratio)
0.15
0.10
0.05
0.00
ns
control
PLX5622
Rhod123 fluorescence (brain:blood ratio)
0.03
0.02
0.01
0.00
ns
control
PLX5622

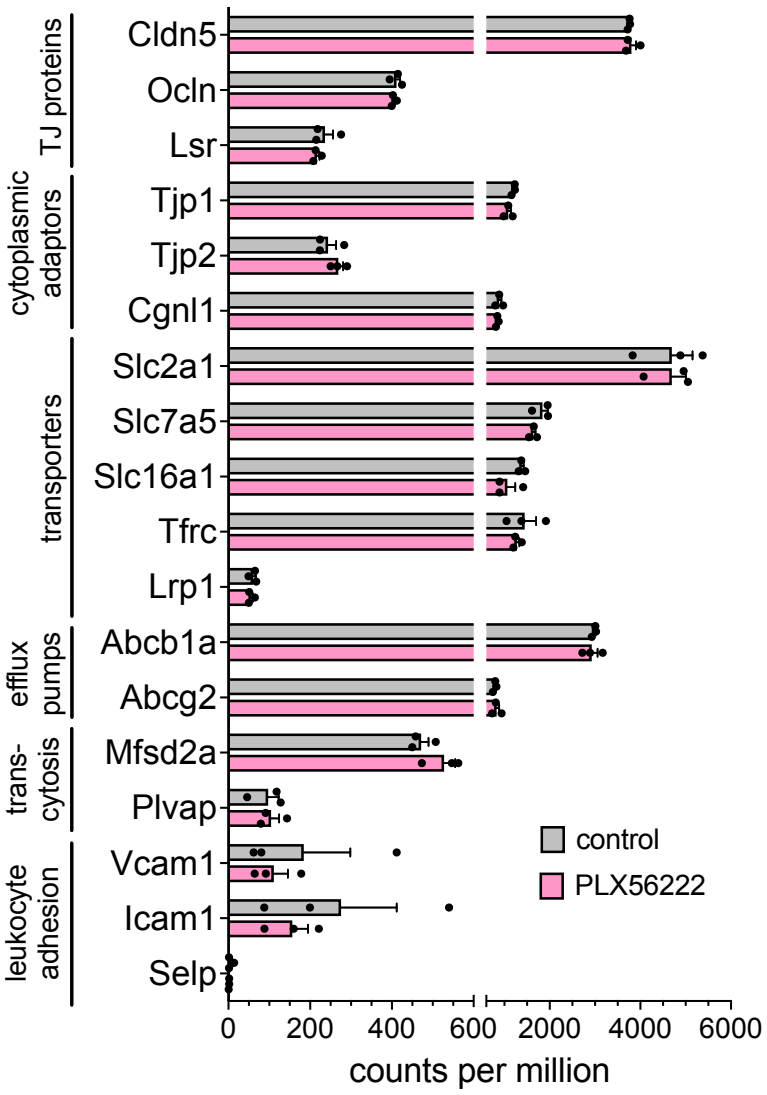


**Figure 2.3 Microglial depletion does not alter expression of genes associated with BBB properties.** Adult wildtype mice were put on control or PLX5622 (1200 mg/kg) diet for one month. Brains were dissected and dissociated in a series of enzymatic digestions and mechanical triturations. Endothelial cells were isolated by FACS and bulk RNA sequencing was performed on isolated mRNA. Expression is presented in counts per million (n=3 per group); error bars represent SEM. There were no significant differences among any genes associated with classic BBB properties (p-adj > 0.05 for all genes).

**Discussion**

The neurovascular unit includes endothelial cells, the pericytes and smooth muscle cells that lie across the endothelial basement membrane, and the astrocytes that ensheath the vasculature with their endfeet. The neurovascular unit can also include perivascular macrophages and perivascular fibroblasts, although these cell types are associated with larger vessels rather than capillaries. Diagrams of the neurovascular unit are sometimes void of microglia, and in other cases microglia are depicted floating off to the side in the parenchymal space. However, a subset of microglia intimately associates with blood vessels in the healthy brain; either their somas contact the vasculature, or they stick one of their dynamic processes in between astrocyte endfeet to touch the endothelial basement membrane. There is still much to understand about the functional relevance of these contacts.

While pericytes have recognized functional roles in generating and maintaining BBB properties, it was unknown whether microglia might influence barrier properties. Elmore et al. reported that microglial depletion does not disrupt the BBB[18], but their methodology – dye injection and imaging of the whole brain from above – was likely not sensitive enough to detect small changes in vascular permeability. Furthermore, the BBB is not simply "open" or "closed". There are a series of BBB properties that might be altered without increasing permeability to non-specific molecules. For instance, a change in specialized transport of particular ions or nutrients would not lead to increased extravasation of injected tracers but would still alter the extracellular environment of the CNS.

Thus, to answer the question of whether microglia play a functional role at the healthy BBB, we depleted microglia and assessed BBB structure, permeability, and expression of genes associated with BBB properties. We found no significant differences in tight junction length, rates of transcytosis, permeability to different types of molecules, or expression of genes associate with junctional proteins, efflux transporters, specialized nutrient transporters, or leukocyte adhesion molecules. The two tracers used to measure BBB permeability were chosen because of their different polarities. Sodium fluorescein is a small, hydrophilic molecule that would likely cross the BBB paracellularly or via vesicle transport. Rhodamine 123, in contrast, is a small, hydrophobic molecule that is able to diffuse across the endothelial cell membrane.

However, it is a substrate for the efflux transporter PGP and thus is pumped back into the bloodstream. These tracers therefore test two different types of permeability functions of endothelial cells, both of which seem to be intact in microglia-depleted mice.

Lastly, we found no differences in the expression of genes associated with BBB properties, helping to confirm our structural and functional data. It is important to note that while we found no functional role for microglia in maintaining the healthy BBB, this does not mean that microglia do not have other functional roles at the vasculature. For example, two recent studies suggest that microglial P2RY12 signaling is involved in neurovascular coupling[11,20]. More work is needed to fully explore microglia-vascular interactions in the healthy CNS.

**Acknowledgements**

Chapter II, in full, is currently being prepared for submission for publication and will include Tony Z. Zhang as a co-author and Professor Richard Daneman as the senior author. The dissertation author was the primary investigator and author of this material.

**References**

1 Tremblay, M. E., Lecours, C., Samson, L., Sanchez-Zafra, V. & Sierra, A. From the Cajal alumni Achucarro and Rio-Hortega to the rediscovery of never-resting microglia. *Front Neuroanat* **9**, 45, doi:10.3389/fnana.2015.00045 (2015).

2 Nimmerjahn, A., Kirchhoff, F. & Helmchen, F. Resting microglial cells are highly dynamic surveillants of brain parenchyma in vivo. *Science* **308**, 1314-1318, doi:10.1126/science.1110647 (2005).

3 Davalos, D., Grutzendler, J., Yang, G., Kim, J. V., Zuo, Y., Jung, S., Littman, D. R., Dustin, M. L. & Gan, W. B. ATP mediates rapid microglial response to local brain injury in vivo. *Nat Neurosci* **8**, 752-758, doi:10.1038/nn1472 (2005).

4 Ransohoff, R. M. A polarizing question: do M1 and M2 microglia exist? *Nat Neurosci* **19**, 987-991, doi:10.1038/nn.4338 (2016).

5 Ginhoux, F., Greter, M., Leboeuf, M., Nandi, S., See, P., Gokhan, S., Mehler, M. F., Conway, S. J., Ng, L. G., Stanley, E. R., Samokhvalov, I. M. & Merad, M. Fate mapping analysis reveals that adult microglia derive from primitive macrophages. *Science* **330**, 841-845, doi:10.1126/science.1194637 (2010).

6 Stevens, B., Allen, N. J., Vazquez, L. E., Howell, G. R., Christopherson, K. S., Nouri, N., Micheva, K. D., Mehalow, A. K., Huberman, A. D., Stafford, B., Sher, A., Litke, A. M., Lambris, J. D., Smith, S. J., John, S. W. & Barres, B. A. The classical complement cascade mediates CNS synapse elimination. *Cell* **131**, 1164-1178, doi:10.1016/j.cell.2007.10.036 (2007).

7 Schafer, D. P., Lehrman, E. K., Kautzman, A. G., Koyama, R., Mardinly, A. R., Yamasaki, R., Ransohoff, R. M., Greenberg, M. E., Barres, B. A. & Stevens, B. Microglia sculpt postnatal neural circuits in an activity and complement-dependent manner. *Neuron* **74**, 691-705, doi:10.1016/j.neuron.2012.03.026 (2012).

8 Paolicelli, R. C., Bolasco, G., Pagani, F., Maggi, L., Scianni, M., Panzanelli, P., Giustetto, M., Ferreira, T. A., Guiducci, E., Dumas, L., Ragozzino, D. & Gross, C. T. Synaptic pruning by microglia is necessary for normal brain development. *Science* **333**, 1456-1458, doi:10.1126/science.1202529 (2011).

9 Mondo, E., Becker, S. C., Kautzman, A. G., Schifferer, M., Baer, C. E., Chen, J., Huang, E. J., Simons, M. & Schafer, D. P. A Developmental Analysis of Juxtavascular Microglia Dynamics and Interactions with the Vasculature. *J Neurosci* **40**, 6503-6521, doi:10.1523/JNEUROSCI.3006-19.2020 (2020).

10 Fantin, A., Vieira, J. M., Gestri, G., Denti, L., Schwarz, Q., Prykhozhij, S., Peri, F., Wilson, S. W. & Ruhrberg, C. Tissue macrophages act as cellular chaperones for vascular anastomosis downstream of VEGF-mediated endothelial tip cell induction. *Blood* **116**, 829-840, doi:10.1182/blood-2009-12-257832 (2010).

11 Bisht, K., Okojie, K. A., Sharma, K., Lentferink, D. H., Sun, Y. Y., Chen, H. R., Uweru, J. O., Amancherla, S., Calcuttawala, Z., Campos-Salazar, A. B., Corliss, B., Jabbour, L., Benderoth, J., Friestad, B., Mills, W. A., 3rd, Isakson, B. E., Tremblay, M. E., Kuan, C. Y. & Eyo, U. B. Capillary-associated microglia regulate vascular structure and function through PANX1-P2RY12 coupling in mice. *Nat Commun* **12**, 5289, doi:10.1038/s41467-021-25590-8 (2021).

12 Lassmann, H., Zimprich, F., Vass, K. & Hickey, W. F. Microglial cells are a component of the perivascular glia limitans. *J Neurosci Res* **28**, 236-243, doi:10.1002/jnr.490280211 (1991).

13 Fernandez-Lopez, D., Faustino, J., Klibanov, A. L., Derugin, N., Blanchard, E., Simon, F., Leib, S. L. & Vexler, Z. S. Microglial Cells Prevent Hemorrhage in Neonatal Focal Arterial Stroke. *J Neurosci* **36**, 2881-2893, doi:10.1523/JNEUROSCI.0140-15.2016 (2016).

14 Lou, N., Takano, T., Pei, Y., Xavier, A. L., Goldman, S. A. & Nedergaard, M. Purinergic receptor P2RY12-dependent microglial closure of the injured blood-brain barrier. *Proc Natl Acad Sci U S A* **113**, 1074-1079, doi:10.1073/pnas.1520398113 (2016).

15 Liu, C., Wu, C., Yang, Q., Gao, J., Li, L., Yang, D. & Luo, L. Macrophages Mediate the Repair of Brain Vascular Rupture through Direct Physical Adhesion and Mechanical Traction. *Immunity* **44**, 1162-1176, doi:10.1016/j.immuni.2016.03.008 (2016).

16 Davalos, D., Ryu, J. K., Merlini, M., Baeten, K. M., Le Moan, N., Petersen, M. A., Deerinck, T. J., Smirnoff, D. S., Bedard, C., Hakozaki, H., Gonias Murray, S., Ling, J. B., Lassmann, H., Degen, J. L., Ellisman, M. H. & Akassoglou, K. Fibrinogen-induced perivascular microglial clustering is

required for the development of axonal damage in neuroinflammation. *Nat Commun* **3**, 1227, doi:10.1038/ncomms2230 (2012).

17 Haruwaka, K., Ikegami, A., Tachibana, Y., Ohno, N., Konishi, H., Hashimoto, A., Matsumoto, M., Kato, D., Ono, R., Kiyama, H., Moorhouse, A. J., Nabekura, J. & Wake, H. Dual microglia effects on blood brain barrier permeability induced by systemic inflammation. *Nat Commun* **10**, 5816, doi:10.1038/s41467-019-13812-z (2019).

18 Elmore, M. R., Najafi, A. R., Koike, M. A., Dagher, N. N., Spangenberg, E. E., Rice, R. A., Kitazawa, M., Matusow, B., Nguyen, H., West, B. L. & Green, K. N. Colony-stimulating factor 1 receptor signaling is necessary for microglia viability, unmasking a microglia progenitor cell in the adult brain. *Neuron* **82**, 380-397, doi:10.1016/j.neuron.2014.02.040 (2014).

19 Delaney, C., Farrell, M., Doherty, C. P., Brennan, K., O'Keeffe, E., Greene, C., Byrne, K., Kelly, E., Birmingham, N., Hickey, P., Cronin, S., Savvides, S. N., Doyle, S. L. & Campbell, M. Attenuated CSF-1R signalling drives cerebrovascular pathology. *EMBO Mol Med* **13**, e12889, doi:10.15252/emmm.202012889 (2021).

20 Császár, E., Lénárt, N., Cserép, C., Környei, Z., Fekete, R., Pósfai, B., Balázsfi, D., Hangya, B., Schwarcz, A. D., Szöllősi, D., Szigeti, K., Máthé, D., West, B. L., Sviatkó, K., Brás, A. R., Mariani, J.-C., Kliewer, A., Lenkei, Z., Hricisák, L., Benyó, Z., Baranyi, M., Sperlágh, B., Menyhárt, Á., Farkas, E. & Dénes, Á. Microglia control cerebral blood flow and neurovascular coupling via P2Y12R-mediated actions. bioRxiv, 2021.2002.2004.429741, doi:10.1101/2021.02.04.429741 (2021).

# CHAPTER III

## Dynamic, activity-dependent regulation of vascular cholesterol metabolism in the healthy brain


### Abstract

Current dogma considers brain and systemic cholesterol to be different pools, with brain cholesterol synthesized *de novo* primarily by astrocytes and oligodendrocytes. Brain endothelial cells – which sit at the border of these two separate pools – are not considered to be significant producers or transporters of cholesterol, and thus not much is known about the regulation or function of brain endothelial cholesterol metabolism. To our surprise, we found that treatment with PLX5622, a CSF1R inhibitor widely used to deplete microglia, causes brain endothelial cells to upregulate cholesterol synthesis enzymes and the cholesterol uptake receptor, low-density lipoprotein receptor (LDLR). This effect was restricted to CNS endothelial cells, occurred throughout the vascular tree, and was independent of microglial depletion. Here we show that brain endothelial cholesterol metabolism is bi-directionally regulated by neuronal activity: neuronal activity increases expression of endothelial cholesterol synthesis and uptake machinery, and neuronal silencing has the opposite effect. Furthermore, brain endothelial cholesterol inhibits arteriole dilation in response to capillary $K^+$ stimulation, suggesting that brain endothelial cholesterol synthesis and uptake act as a negative feedback mechanism for the processes of neurovascular coupling.


### Introduction

The endothelial cells that comprise the inner walls of CNS blood vessels lie at the interface between two rapidly changing environments. On the luminal side, endothelial cells are exposed to the blood and its milieu of proteins, lipids, small molecules, red blood cells, and leukocytes. On the abluminal side, endothelial cells interact with the CNS parenchyma and its intricate circuits of electrical and chemical communication. CNS endothelial cells are tasked with the role of protecting CNS cells from any bloodborne menaces, but they also play an essential role in making sure that neurons and other active brain cells have the energy and nutrients needed for proper function. Many of these crucial molecules must be transported

from the bloodstream through the blood vessel walls. Compared to peripheral endothelial cells, CNS endothelial cells possess unique properties that allow them to create a protective barrier as well as selectively transport specific molecules across it.

While CNS endothelial cells' barrier properties have been studied in depth, the field is just beginning to shed light on another important role for CNS endothelial cells in maintaining proper brain function. It was over a century ago that scientists found the first pieces of experimental evidence suggesting neural activity stimulates changes in blood flow dynamics[1-3]. The field has since come to appreciate that there is increased local blood flow following neuronal activity, thus ensuring that active neurons have sufficient oxygen and energy. This phenomenon is called "neurovascular coupling" (NVC). NVC is executed by constriction and dilation of smooth muscle cells (SMCs), causing constriction or dilation of underlying blood vessels. It was long thought that endothelial cells play only a passive role in this process, but recent work has uncovered that endothelial cells are indeed active NVC participants[4-6]. There is likely much more to understand about endothelial participation in and regulation of NVC.

Many factors released from several cell types contribute to NVC. These factors include ionic byproducts of neuronal activity itself, such as potassium ions ($K^+$). Neuronal activity increases the extracellular $K^+$ concentration, which activates abluminal $K_{IR}2.1$ channels on endothelial cells and SMCs[5]. Capillary $K^+$ activation causes endothelial cell hyperpolarization, and this current travels upstream – likely via endothelial gap junctions[7] – leading to upstream arteriole dilation due to endothelial-SMC signaling and SMC relaxation[5]. On the other hand, luminal $K_{IR}$ channels as well as calcium-sensitive $K^+$ ($K_{Ca}$) channels help arteries sense and respond to changes in shear stress and blood pressure not only in the brain but throughout the body[8,9].

A collection of studies has identified lipids as mediators of $K_{IR}$ activity. Depletion of phosphatidylinositol 4,5-biphosphate ($PIP_2$), a minor phospholipid component of cell membranes, has been shown to reduce endothelial $K_{IR}$ current, inhibiting capillary $K^+$ stimulation-mediated hyperemia[10] and rendering resistance arteries less sensitive to laminar flow[11]. Cholesterol has also been shown to mediate $K_{IR}$ current in various cell lines; an increase in cellular cholesterol dampens $K_{IR}$ current, while depleting

cholesterol or replacing it with an optical isomer increases current[12,13]. Furthermore, endothelial $K_{IR}$ dysfunction underlies deficits in flow-induced vasodilation in obese mice and humans[14].

As $K_{IR}$ channels play a crucial role in NVC, and as dysfunctional NVC can lead to cognitive deficits[15], $K_{IR}$ activity in brain vasculature is likely tightly regulated. We recently found that increasing neuronal activity upregulates brain endothelial expression of cholesterol synthesis enzymes, cholesterol synthesis regulators, and the cholesterol uptake receptor low-density lipoprotein receptor (LDLR). Conversely, silencing neuronal activity has the opposite effect, decreasing expression of these cholesterol-related genes in brain endothelial cells[16] (Fig 3.10A). The current dogma is that peripheral and brain cholesterol are largely separate pools, and the brain synthesizes its own cholesterol, with most synthesis occurring in astrocytes and oligodendrocytes[17-19]. Here we identify a new role for CNS endothelial cell cholesterol production and uptake. We show that brain endothelial cells dynamically regulate cholesterol synthesis and uptake *in vivo*, and that endothelial cholesterol can act as a negative feedback mechanism to suppress $K^+$-induced arteriole dilation.

**Methods**

*Animals*

Adult C57BL/6 mice were ordered from Charles River Laboratories or Jackson Labs. In diet experiments, mice were between 8-15 weeks of age except for long-term PLX5622 administration. For long-term administration, mice were put on diet at 2 months of age and tissue was collected 17.5 months of age. Special diets were manufactured by Research Diets, Inc. and included: AIN-76A control diet (D10001i), PLX5622 diet at 1200 mg/kg (D11100404i), high-fat diet with 60% kcal fat (D12492i), and high-fat diet with PLX5622 added at 1200 mg/kg (D15111301i). PLX5622 was provided by Plexxikon, Inc. or purchased from MedChem Express. All diets were irradiated prior to use. For acute PLX5622 timepoints <24 hours, onset of diet occurred at 6pm at the beginning of the mice's dark (waking) cycle. Male mice were used for sequencing experiments and most histology analysis, but the phenotype was confirmed in female mice. A mix of male and female mice were used for lipidomics, the capillary-

parenchymal arteriole preparations, and neuronal silencing experiments. All experiments were approved by the Institutional Animal Care and Use Committee at UCSD.

For astrocyte mRNA isolation, RiboTag mice (*Rpl22*$^{tm1.1Psam}$/SjJ)—which contain a ribosomal protein (Rpl22) with a floxed C-terminal exon followed by an identical exon tagged with hemagglutinin (HA) were mated to mice in which Cre-recombinase is driven by GFAP (B6.Cg-Tg(Gfap-cre)73.12Mvs/J). Both mouse lines were purchased from Jackson Labs (#029977; #012886).

*CamKIIa-tTA* mice[20] were crossed to *TRE-M4Di* mice[21] (hM4Di-Silencing) to generate a tool to silence glutamatergic neurons. Littermates not expressing the DREADDs were used as controls. IP injection of 1.0 mg/kg CNO strongly attenuated gamma LFP power and largely did not affect locomotor activity[16].

Tissue from adult *P2ry12-CreER*$^{T2}$*; Csf1rf*$^{f}$ mice was kindly provided by Dr. Tom Arnold. Mice were given eight days of tamoxifen treatment to deplete microglia prior to tissue collection on the ninth day. Tissue from P20 *Csf1r*$^{-/-}$ mice was kindly provided by Dr. Chris Bennett. Control samples for *Csf1r*$^{-/-}$ mice were wildtype and heterozygous littermates of knockouts.

*Endothelial enrichment*

Endothelial cells were enriched as described in Chapter I. Cells were stained with AF647-conjugated anti-CD31 (Molecular Probes A14716), FITC-conjugated anti-CD13 (BD Biosciences 558744), FITC-conjugated anti-CD45 (eBioscience 11-0451-85), FITC-conjugated anti-CD11b (eBioscience), BV421-conjugated anti-PDGFRα (BD Horizons 562774), and DAPI. Cells positive for 647 and negative for FITC, BV421, and DAPI were sorted into trizol at the UCSD Flow Cytometry Research Core Facility. For single-cell sequencing, cells were sorted into 0.04% BSA in PBS instead of trizol.

*Glial enrichment*

GFAP-Cre mice (control and PLX5622 groups) were euthanized with $CO_2$, a half forebrain from each mouse was dissected and homogenized in RNase-free water with 1% NP-40, 0.1M KCl, 50 mM Tris,

and 12 mM $MgCl_2$ supplemented with 0.1 mg/mL cycloheximide, protease inhibitors, 1 mg/mL heparin, RNAsin, and 1mM DTT. Homogenized tissue was spun down and supernatant was incubated with anti-HA (CST 3724) at 1:160 for four hours at 4°C. Magnetic IgG beads (Pierce 88847) were added and incubated overnight. Beads were washed 3 times with high salt buffer (RNase-free water with 0.3 M KCl, 1% NP-40, 50 mM Tris, 12 mM $MgCl_2$, 0.1 mg/mL cycloheximide, and 0.5 mM DTT) using a magnetic stand. RLT lysis buffer + 1% βME was added to beads and vortexed. Supernatant was collected and mRNA was purified by Qiagen RNAeasy Micro kit (74004).

*Bulk RNA sequencing and bioinformatics*

Bulk RNA sequencing and bioinformatics were performed as described in Chapter I. The $log_2$ (fold change) of each sample compared to the average of control samples was used to create heat map visualizations.

*Single-cell sequencing and bioinformatics*

Gene counts were obtained by aligning reads to the mm10 genome (refdata-gex-mm10-2020-A) using CellRanger software (v.6.0.1 – 10X Genomics). Using Seurat (v.4.0), quality control was performed using the following: 1) outliers with a high ratio of mitochondrial RNAs (>5%, <200 features) relative to endogenous RNAs and homotypic doublets (>5000 features) were removed in Seurat; 2) after scTransform normalization and integration, doublets and multiplets were removed using DoubletFinder; 3) cells were manually inspected using known cell-type specific marker genes, cells expressing more than one cell-type specific marker were removed.

In Seurat (v.4.0), gene counts were first normalized using scTransform, then Integration function was used to align data with default settings. Genes were projected into principal component (PC) space using the principal component analysis function RunPCA. The first 30 dimensions were used as inputs into Seurat's FindNeighbors and FindClusters functions. Then, RunUMAP function with default settings was

used to calculate 2-dimensional UMAP coordinates and search for distinct cell populations. Distinct cell types were determined using known cell-type specific markers. Differential gene expression of genes comparing PLX to control samples was performed with the FindMarkers function, specifically utilizing the Wilcoxon Rank Sum test.

*Immunohistochemistry*

Mice were transcardially perfused with DPBS followed by 4% paraformaldehyde in PBS. Tissue was cryopreserved in 30% sucrose, frozen in 2:1 OCT:30% sucrose and sectioned at 10 μm thickness. Sections for LDLR staining were further fixed in ice-cold methanol for 10 minutes. Sections for IBA1 staining were further fixed with 5 minutes of 4% PFA. All slides were blocked with 10% donkey serum, 0.2% triton-x-100 in PBS. Primary antibodies against LDLR (R&D Systems AF2255), IBA1 (Wako 019-19741; Novus Bio NB100-1028) and CD31 (BD Biosciences 553370) were used at 1:1000 (LDLR, CD31, Wako anti-IBA1) or 1:500 (Novus Bio anti-IBA1) with 10% blocking solution in PBS and incubated overnight at 4°C. Fluorescently conjugated secondary antibodies (Life Technologies) were used at 1:1000 and incubated for 1.5 hours at room temperature. Slides were coverslipped using DAPI-Fluoromount-G (SouthernBiothech 0100-20) and imaged with a Zeiss Axio Imager.D2.

*Analysis of LDLR+ vascular length*

To quantify LDLR+ vascular length, sections were stained for LDLR and CD31. LDLR signal was traced using the ImageJ line tool, with each segment saved as an ROI. ROIs were then opened on the CD31 channel, and any ROI not corresponding to CD31+ vasculature was deleted. The remaining ROIs were measured, and the sum of their lengths was used as the length of LDLR+ vasculature. The rest of the LDLR-/CD31+ vascular segments were then traced in the same way, and the ROIs measured. The sum total length of all segments was used as the vascular length. Percent vascular length was calculated as (LDLR+ vessel length)/(total vessel length)*100.

*Microglial repopulation*

For standard repopulation experiment, mice were kept on AIN-76A or PLX5622 diet for three weeks. After three weeks, the PLX5622 diet group was switched back to AIN-76A control diet for two weeks before tissue collection. For acute repopulation experiments, mice were kept on AIN-76A or PLX5622 diet for two weeks. After two weeks, at 6pm, mice in the repopulation group were switched back to AIN-76A control diet, and tissue was collected 24 or 48 hours later.

*Lipidomics*

Mice were anesthetized with a ketamine/xylazine mix. A blood sample was collected from the right ventricle and allowed to coagulate at room temperature for serum collection. Mice were transcardially perfused with DPBS. A lobe of liver and the brain were dissected. Cerebellum, olfactory bulbs, and meninges were removed. Tissue and serum were flash-frozen. Sterol isolation, saponification, and LC-MS analysis were performed by the UCSD LIPID MAPS Lipidomics core. Samples were run on a Sciex6500 Qtrap mass spectrometer. Phenomenex Kinetics C18 2.1x150mm 1.7um columns were used.

*Neuronal silencing*

*CamKIIα-tTA; TRE-hM4Di* (hM4Di-Silencing) mice were given an i.p. injection of PLX5622 (50 mg/kg) or vehicle at 6 PM at the start of their waking cycle. All mice were also injected i.p. with clozapine-N-oxide (1mg/kg) (Enzo Life Sciences BML-NS105-0005) at this time, and again at 10 PM and 2 AM. At 6 AM, mice were transcardially perfused for immunostaining and analysis of LDLR+ vascular length.

*Capillary-parenchymal arteriole preparation and stimulation*

Capillary-parenchymal arteriole preparation, potassium stimulation, and dilation analysis were performed as described in Longden and Dabertrand et al.[5]. Vessel preparations were treated with 5mM

methyl-beta cyclodextrin (MβCD) (Cayman Chemicals 21633) for 30 minutes to deplete membrane cholesterol.

*RTK inhibition*

Mice were given an i.p. injection of PZ-1 (30 mg/kg) (MedChem Express HY-U00437) or vehicle (10% DMSO, 90% corn oil). 12 hours after injection, mice were transcardially perfused for immunostaining and analysis of LDLR+ vascular length.

**Results**

*PLX5622 treatment causes upregulation of brain endothelial cholesterol genes*

To study the role of microglia at the blood-brain barrier, we treated adult wildtype mice with PLX5622 (1200 mg/kg chow), a CSF1R inhibitor used to deplete microglia, for one month and then acutely isolated brain endothelial cells for RNA sequencing. Microglial depletion did not alter brain endothelial expression of genes associated with BBB properties (Fig 2.3, 3.1A). Surprisingly, however, we found that PLX5622 treatment increased brain endothelial expression of a series of cholesterol synthesis enzymes including the rate-limiting enzyme *Hmgcr1*. PLX5622 also upregulated the cholesterol synthesis regulators *Insig1* and *Srebf2*, as well as the cholesterol uptake receptor *Ldlr*. Conversely, the main cholesterol efflux receptor, *Abca1*, was downregulated in PLX5622-treated mice (Fig 3.1A). To validate this phenotype, we quantified vascular length positive for LDLR in control and PLX5622-treated mice (Fig 3.1B-C). We found that the percentage of LDLR+ vascular length increased from 14.63% ± 1.66 to 73.4% ± 5.56 (Fig 3.1C). Furthermore, vascular LDLR returned to baseline after microglial repopulation (Fig 3.1C).

To understand whether the expression of cholesterol-associated genes was upregulated throughout the vascular tree, we also performed single-cell RNA sequencing on brain endothelial cells isolated from mice after one month on control or PLX5622 diet. As expected, cells clustered according to their identity as arterial, venous, or capillary endothelial cells (Fig 3.2A). After PLX5622 treatment, a vast majority of

genes coding for cholesterol synthesis enzymes, synthesis regulators, and uptake receptor were expressed both in more cells and at a higher level per cell in all three endothelial cell populations (Fig 3.2B-C). These data suggest that PLX5622 affects endothelial cholesterol metabolism throughout the vascular tree.

To determine whether this endothelial response to PLX5622 was specific to brain endothelial cells, we fed adult wildtype mice control or PLX5622 diet for one week and examined tissue from the thymus, muscle, kidney, spinal cord, and eye. We found that PLX5622 increased vascular LDLR in the brain, spinal cord and retina, but not in the muscle, kidney, or the non-CNS choroidal vasculature of the eye (Fig 3.3A-B), suggesting that the effect is specific to CNS vasculature. To further confirm this finding, we fed adult wildtype mice control or PLX5622 diet for one month, acutely isolated liver endothelial cells, and performed RNA sequencing. As expected, liver endothelial cells expressed low levels of BBB-enriched genes and high levels of genes enriched in peripheral endothelial cells (Fig 3.3.C). PLX5622 did not induce significant changes in the expression of cholesterol genes in liver endothelial cells (Fig 3.3D). Together, these data suggest that PLX5622 increases cholesterol synthesis and uptake specifically in CNS endothelial cells.

To understand whether this effect is stable throughout time or whether endothelial cells adapt to PLX5622 treatment, we kept adult wildtype mice on control or PLX5622 diet for more than 15 months. Mice were 8 weeks old at the time of diet onset and 17.5 months old at the time of tissue collection. Remarkably, the expression of cholesterol-related genes was largely unaffected by aging in control mice, and the PLX5622-induced increase in expression of these genes was almost identical between mice on PLX5622 diet 1 month and >15 months (Fig 3.4). These data suggest that the effect of PLX5622 on CNS endothelial cholesterol metabolism is extremely stable throughout time.

*The effect of PLX5622 on cholesterol metabolism is specific to endothelial cells*

To understand whether PLX5622 affects cholesterol metabolism in other cell types throughout the brain, we put adult wildtype mice on control or PLX5622 diet for one month and performed RNA sequencing on acutely purified mRNA from a mixed population of astrocytes, oligodendrocytes, and

neurons (Fig 3.5A). We found no significant differences in expression of cholesterol genes between mice on control and PLX5622 diet (Fig 3.5B). These data suggest that PLX5622 alters cholesterol metabolism specifically in brain endothelial cells.

Microglia express low levels of cholesterol synthesis genes, yet cholesterol is one of a few factors they need to survive, and they likely rely on astrocytes for cholesterol synthesis[22]. As microglia are cholesterol consumers, we thought it was possible that loss of microglia might alter overall brain levels of cholesterol, thus causing endothelial cells to respond by altering their own production. To test this, we isolated forebrain, liver, and serum samples from adult wildtype mice fed control or PLX5622 diet for one month and performed lipidomics analysis via mass spectrometry. There were no significant differences in cholesterol concentration in forebrain, liver, or serum samples from male or female mice (Fig 3.6A-C), although there was a trend towards decreased cholesterol in the serum of PLX5622-treated mice of both sexes (Fig 3.6C). These data suggest that microglial depletion does not alter overall cholesterol content in the brain. Instead, these results suggest that either microglia regulate brain endothelial cholesterol metabolism or that PLX5622 influences endothelial cholesterol independent of microglial depletion.

*Upregulation of endothelial cholesterol machinery is independent of microglial depletion*

Our first hypothesis was that microglia regulate vascular cholesterol synthesis and uptake, however follow-up experiments suggested that the effect might be independent of microglia. First, to understand the time course of the cholesterol phenotype, we analyzed brain tissue sections from mice on PLX5622 diet for 6, 12, 24, 48, and 72 hours. Surprisingly, vascular LDLR was significantly increased as early as 12 hours after diet onset (Fig 3.7A). At this timepoint, there was not yet a significant reduction in microglia (Fig 3.7B), suggesting that PLX5622 acts directly on endothelial cells. However, microglial morphology is clearly affected just 6 hours after diet onset, with microglia appearing less ramified and with increased IBA1 signal (Fig 3.7C), thus we reasoned that microglia – while not yet dead – might lose some of their homeostatic roles in the first few hours of PLX5622 treatment.

To further test whether the cholesterol phenotype was microglia-mediated, we first fully depleted microglia by treating adult wildtype mice with PLX5622 or control diet for two weeks, then switched the PLX5622 group back to control diet and subsequently quantified vascular LDLR at acute timepoints of microglial repopulation. At 24 hours post PLX5622 removal, there was a large variation in vascular LDLR, with some mice still expressing high vascular LDLR levels and others already showing a large decrease (Fig 3.7D). At 48 hours after PLX5622 removal, levels of vascular LDLR had returned to control levels (Fig 3.7D). At this time point of 48 hours, microglia density varies but is still approximately 20% of control microglial density (Fig 3.7E), suggesting the LDLR phenotype is not dependent on microglia. Indeed, at both 24- and 48-hour time points, there was no significant linear relationship between microglial density and vascular LDLR expression (Fig 3.7F). Together, the acute depletion and repopulation experiments suggest that the effect of PLX5622 on brain endothelial cholesterol metabolism is not mediated through microglia: vascular LDLR is upregulated before microglia are eliminated and is back to control levels before microglia levels reach even a quarter of their previous density.

To confirm that microglia do not regulate vascular cholesterol metabolism, we quantified vascular LDLR in genetic microglial depletion models. We first looked at adult *P2ry12-CreER$^{T2}$;Csf1r$^{f/f}$* mice, in which Csf1r is excised from microglia, leading to their death. The conditional knockouts had varying levels of microglial depletion but none had high levels of vascular LDLR (Fig 3.8A). While there was bright LDLR signal in some mice, it was localized to dying microglia rather than endothelial cells (Fig 3.8A). We also tested *Csf1r$^{-/-}$* mice, which do not have any microglia and die before adulthood. Microglia were completely absent from P19-21 *Csf1r$^{-/-}$* mice (Fig 3.8B) and while overall there was more extensive neuronal LDLR in both wildtype and knockout young mice compared to adults, there was no increase in vascular LDLR in the knockout compared to control (Fig 3.8C). These data further confirm that the observed effects of PLX5622 on endothelial cholesterol metabolism are independent of microglial depletion.

*Dietary cholesterol does not regulate brain endothelial cholesterol metabolism*

As brain endothelial cells lie at the interface between the brain and blood stream, we wanted to understand whether changes in peripheral cholesterol could regulate brain endothelial cholesterol metabolism. To answer this question, we put adult wildtype mice on control, high fat, PLX5622, or high fat + PLX5622 diet for one month. We then acutely isolated brain endothelial cells and performed RNA sequencing. Interestingly, high fat diet did not affect brain endothelial expression of cholesterol-related genes, and high fat diet did not interact with PLX5622 to alter the effect of PLX5622 (Fig 3.9). These data demonstrate that brain endothelial cholesterol metabolism is not regulated by dietary cholesterol.

*Neuronal activity regulates brain endothelial cholesterol metabolism*

We next set out to understand whether brain endothelial cholesterol metabolism is dynamically regulated by brain factors. We queried a published dataset of brain endothelial gene expression under conditions of normal, activated, and silenced neuronal activity[16]. Remarkably, we found that the cassette of cholesterol genes is bidirectionally modulated by neuronal activity: activating glutamatergic neurons upregulates brain endothelial expression of genes involved in cholesterol synthesis, synthesis regulation, and uptake, while silencing neural activity has the opposite effect (Fig 3.10A). As with PLX5622 administration, in response to neuronal activity modulation, the cholesterol efflux transporter *Abca1* changed in the opposite direction from the other cholesterol-related genes. These data suggest that neuronal activity upregulates brain endothelial cholesterol synthesis and uptake *in vivo*.

As microglia have been shown to regulate neuronal activity[23,24], we wanted to address whether PLX5622 might be affecting endothelial cholesterol metabolism indirectly by increasing neuronal activity. We thought this unlikely, as our data point to a microglia-independent mechanism (Figs 3.7-3.8). We looked at the effect of PLX5622 on the 53 endothelial genes most strongly bidirectionally regulated by neuronal activity[16]. Only a handful were significantly altered by PLX5622, and the strongest PLX5622-mediated change by far was S*qle*, the only cholesterol synthesis gene on the list (Fig 3.10B). Thus, it seems as if PLX5622 is directly affecting cholesterol metabolism rather than influencing endothelial cholesterol metabolism by increasing neuronal activity.

To understand how PLX5622 treatment and neuronal activity interact in the context of vascular cholesterol metabolism, we combined PLX5622 treatment (which increases cholesterol gene expression) and silencing neuronal activity (which decreases cholesterol gene expression). Specifically, *CamKIIα-tTA; TRE-hM4Di* (hM4Di-Silencing) mice and littermate controls were injected with PLX5622 (50 mg/kg) or vehicle at the beginning of the dark cycle (awake period). They were also injected with clozapine-N-oxide at the onset and every four hours throughout the 12-hour dark cycle. At the end of the dark period, mice were perfused, and their brains were analyzed for vascular LDLR. PLX5622 had a stronger effect on vascular LDLR than neuronal activity did: vehicle-control vs PLX-control and vehicle-silencing vs PLX-silencing were the most significantly different group comparisons (3.10C; $p<0.0001$). While silencing alone or with PLX did not have significant effect on vascular LDLR, there was a clear trend towards lower vascular LDLR in the silencing compared to control groups, with silencing activity decreasing vascular LDLR by ~10% compared to control (Fig 3.10C; $p=0.067$ and $p=0.097$). These data suggest that, while PLX5622 has a stronger effect on endothelial cholesterol than that of neuronal activity, the manipulations are additive in the context of vascular LDLR.

*PLX5622-induced increase in vascular cholesterol inhibits $K^+$-mediated hyperemia*

As neuronal activity regulates brain endothelial cholesterol synthesis, we hypothesized that endothelial cholesterol might be dynamically regulated as a part of neurovascular coupling. Longden, Dabertrand, and colleagues showed that neuronal activity-generated extracellular $K^+$ can activate capillary $K_{IR}2.1$, causing a hyperpolarizing current that travels upstream, leading to arteriole dilation and increased blood flow[5]. As cellular cholesterol has been shown to modulate $K_{IR}$ channel activity[12,13], we tested whether PLX5622-induced increases in cholesterol synthesis and uptake would affect $K_{IR}$ function. Specifically, mice were fed control or PLX5622 diet for at least a month. We then used the *ex vivo* capillary-parenchymal arteriole (CaPA) preparation[5,25] to measure arteriole dilation in response to capillary $K^+$-stimulation. This *ex vivo* preparation (which contains just vascular cell types) was particularly ideal in that it removed any confounding factors of microglial depletion or changes in baseline neuronal activity. Remarkably,

PLX5622 abolished arteriole dilation in response to capillary $K^+$ stimulation (Fig 3.11A-B). Direct arteriole stimulation with $K^+$ still generated a dilation response (Fig 3.11A-B), demonstrating that the arteriole itself was still capable of dilation, likely through SMC $K_{IR}$ channels. These results show that PLX5622 causes a physiological change in brain vasculature independent of changes in baseline neuronal activity or presence of microglia. They further suggest that this vascular phenotype might contribute to NVC deficits previously reported in mice fed PLX3397, a similar, less specific CSF1R inhibitor[26].

We hypothesized that PLX5622 abolishes retrograde hyperpolarization because higher levels of endothelial cholesterol act to silence endothelial $K_{IR}$ channels. We therefore tested whether depleting cholesterol from PLX5622 vessels would rescue arteriole dilation response. We used methyl-beta-cyclodextrin (MβCD) to deplete membrane cholesterol from PLX5622 vessels, and cholesterol depletion almost completely restored arteriole dilation in response to capillary $K^+$ stimulation (Fig 3.11B-C). These results suggest that increased endothelial cholesterol underlies PLX5622-induced deficits in retrograde hyperpolarization. Together, these data lead us to hypothesize that neuronal activity increases endothelial cell cholesterol synthesis and uptake, and this cholesterol acts to inhibit activity-induced vasodilation, acting as a negative feedback mechanism for hyperemia (Fig 3.13).

*PLX5622 inhibits other tyrosine receptor kinases*

We found that PLX5622 treatment upregulates the expression of vascular cholesterol synthesis enzymes and uptake receptor, and we showed that this phenotype was independent of microglia depletion. Further, CSF1R expression is largely restricted to microglia[27-29], and we found Csf1r expression in less than 0.01% of endothelial cells (Fig 3.12A), suggesting the drug is working through a different target – likely another receptor tyrosine kinase (RTK) – on endothelial cells or another cell type. What receptor is PLX5622 acting on? PLX5622 is reported to have an $IC_{50}$ of 0.016 μM, 0.39 μM, 0.86 μM, 1.0 μM, and 1.1 μM against CSF1R, FLT3, KIT, AURKC, and KDR, respectively, and an $IC_{50}$ of ">1μM" for a panel of over 200 other RTKs[24], but the exact $IC_{50}$ values are not reported. Spangenberg and colleagues reported

that mice fed PLX5622 chow at a dose of 1200mg/kg (the same used in the current study) had a PLX5622 concentration of 22 μM and 6.04 μM in their blood, and brain parenchyma, respectively[30]. Thus, it is not unreasonable that such a high concentration of PLX5622 might have a significant inhibitory effect on another RTK.

Because PLX5622 affects CNS but not peripheral endothelial cells (Fig 3.3), we compared brain and liver endothelial expression of cell surface receptor tyrosine kinases. Based on brain specificity, level of expression, and dynamic modulation in response to neuronal activity, we focused our attention on insulin growth factor 1 receptor (IGF1R), rearranged during transfection (RET), and kinase insert domain receptor (KDR). We tested a panel of inhibitors against these receptors and found that PZ-1, a potent inhibitor of RET and KDR, upregulates vascular LDLR (Fig 3.12B), suggesting that endothelial cholesterol metabolism is regulated by RET or KDR, also known as VEGFR2. Future directions include specifying which of these receptors regulates vascular LDLR and determining which cell types are involved in this signaling pathway.

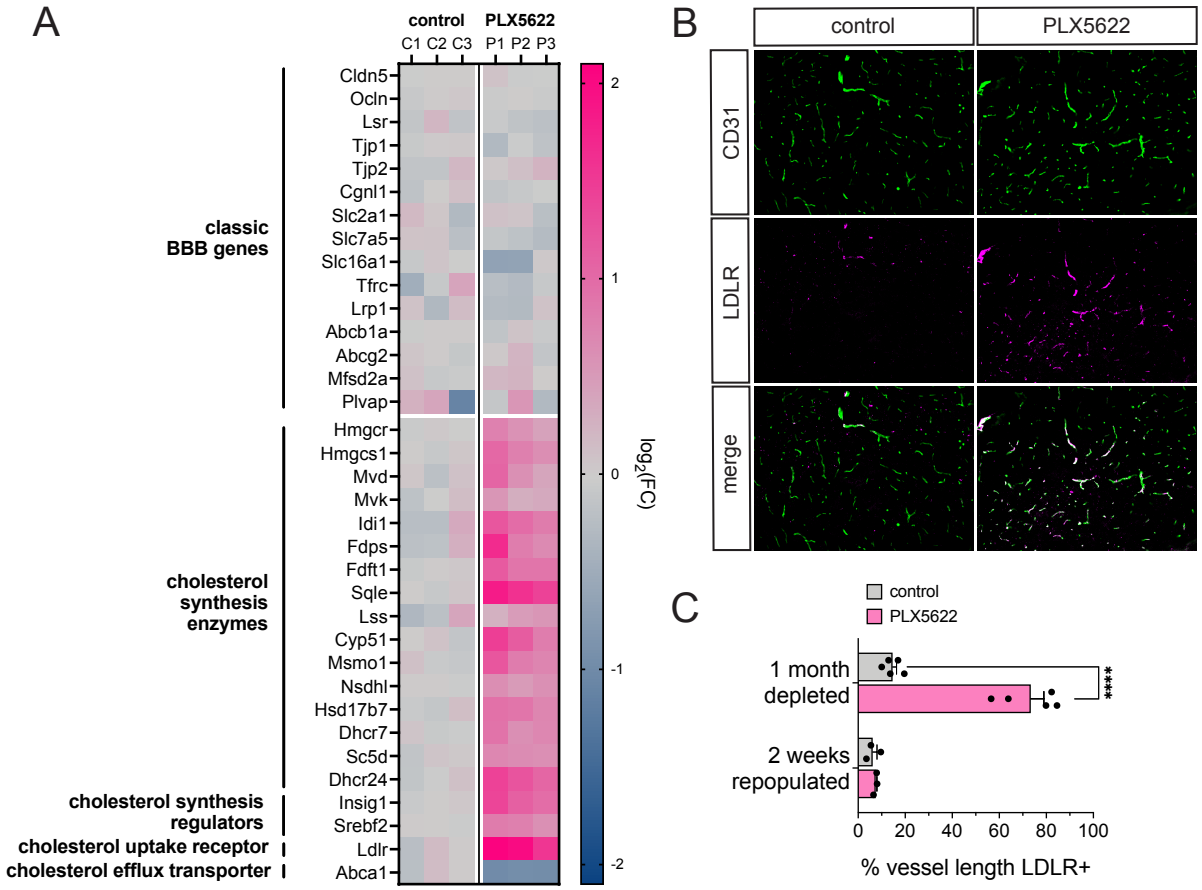


**Figure 3.1 PLX5622 treatment increases brain endothelial expression of cholesterol-related genes. A)** Adult wildtype mice were fed control or PLX5622 (1200 mg/kg) diet for one month. Brains were dissected and dissociated, and endothelial cells were isolated by FACS for RNA sequencing. Gene expression is presented as the $\log_2$(FC) from the average of control expression in counts per million, with pink representing an increase in expression and blue representing a decrease in expression. PLX5622 causes endothelial upregulation of genes coding for cholesterol synthesis enzymes and uptake receptor, and downregulation of the gene coding for the primary cholesterol efflux transporter. **B)** Representative images of cortex after one month control or PLX5622 diet. 10um images were stained with antibodies against CD31 (green, endothelial cells) and LDLR (magenta). PLX5622 diet causes a visible increase in vascular LDLR expression. **C)** Top: quantification of data shown in B). PLX5622 increases percent vascular length that is LDLR+ ($p<0.0001$; n=5). Bottom: Adult mice were fed control or PLX5622 diet for 3 weeks. PLX5622-fed mice were then switched to control diet for two weeks. Percent vascular length LDLR+ was not significantly different from control after two weeks microglial repopulation ($p=0.527$; n=3).

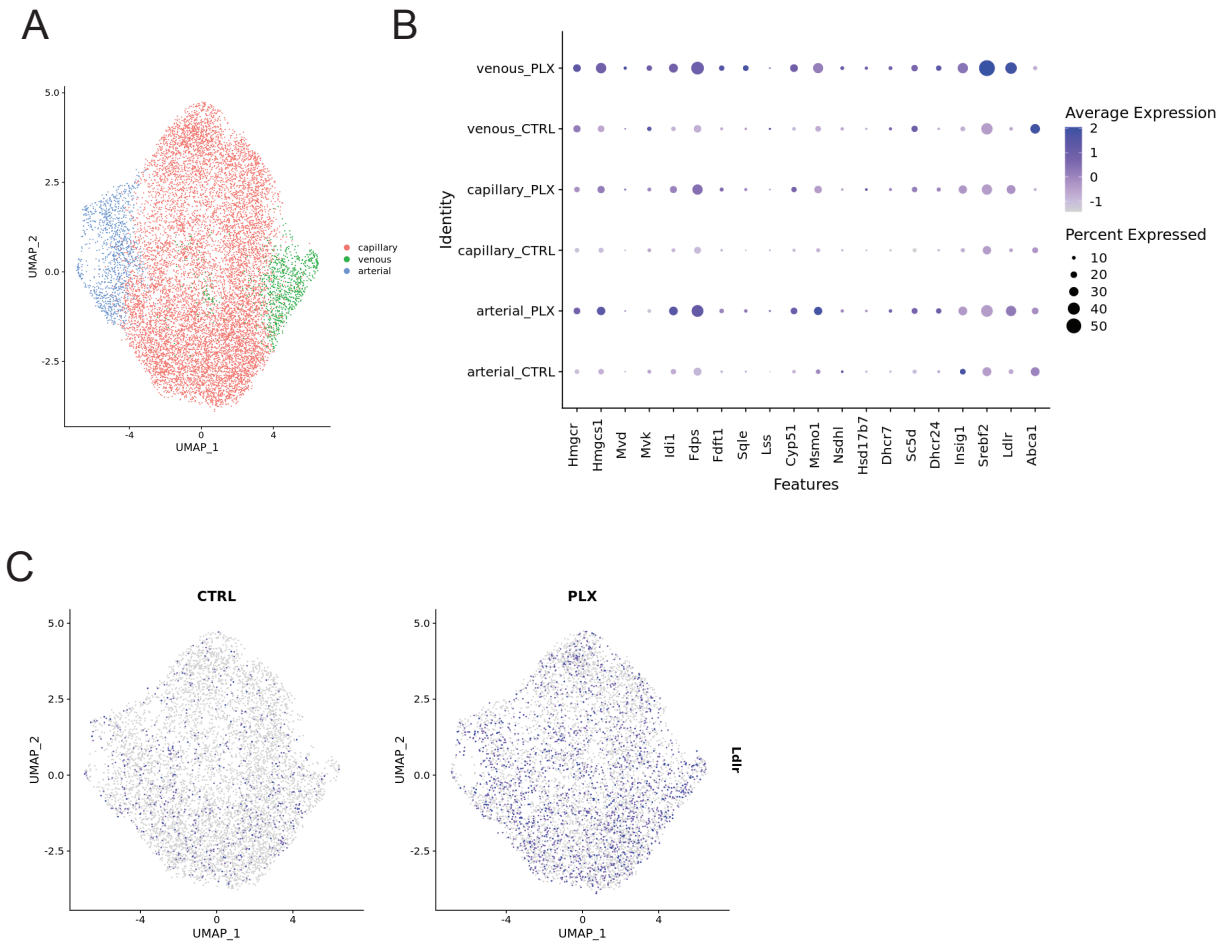


**Figure 3.2 PLX5622 increases the expression of cholesterol-related genes throughout the vascular tree.** Adult wildtype mice were fed control or PLX5622 diet for one month. Brains were dissected and dissociated, and endothelial cells were isolated by FACS for single-cell RNA sequencing. For each diet condition, cells were obtained from three brains across two samples **A)** Three main clusters as visualized by a UMAP plot were identified by expression profile as arterial (blue), capillary (red), or venous (green) endothelial cells. **B)** For each cholesterol-related gene, the size of the dot represents the percentage of endothelial cells expressing that gene, and the color of the dot represents average expression on a log scale, with darker purple signifying higher expression. In all three clusters, the expression of cholesterol synthesis enzymes, synthesis regulators, and uptake receptor were increased. The expression of the cholesterol efflux transporter was decreased. **C)** UMAP plots in which cells are colored based on their expression of LDLR, with darker purple signifying higher expression. PLX5622 treatment increased the percentage of endothelial cells expressing LDLR as well as the level of LDLR expression.

**Figure 3.3 PLX5622 increases expression of cholesterol-related genes in CNS, but not non-CNS, vasculature. A)** Adult wildtype mice were fed control or PLX5622 diet for one week. Thymus, muscle, and kidney tissue were dissected, sectioned, and analyzed for LDLR expression. PLX5622 did not increase vascular LDLR in these organs. **B)** Adult wildtype mice were fed control or PLX5622 for one month. Eyes were dissected, sectioned, and analyzed for LDLR expression. PLX5622 treatment increased vascular LDLR expression in the retina (yellow arrowheads) but not in the non-CNS choroidal vessels (white arrowheads). **C-D)** Adult wildtype mice were fed control or PLX5622 diet for one month. Livers were dissected and dissociated, and endothelial cells were isolated with FACS for RNA sequencing. Expression of pan-endothelial, as well as BBB- and periphery-enriched genes were assessed to confirm the identity of liver endothelial cells. As expected, liver endothelial cells highly expressed both pan-endothelial and periphery-enriched, but not BBB-enriched, genes. **D)** Expression of cholesterol related genes in liver endothelial cells, expressed as log2(FC) from the average expression in control mice. PLX5622 treatment did not increase expression of cholesterol-related genes in liver endothelial cells.

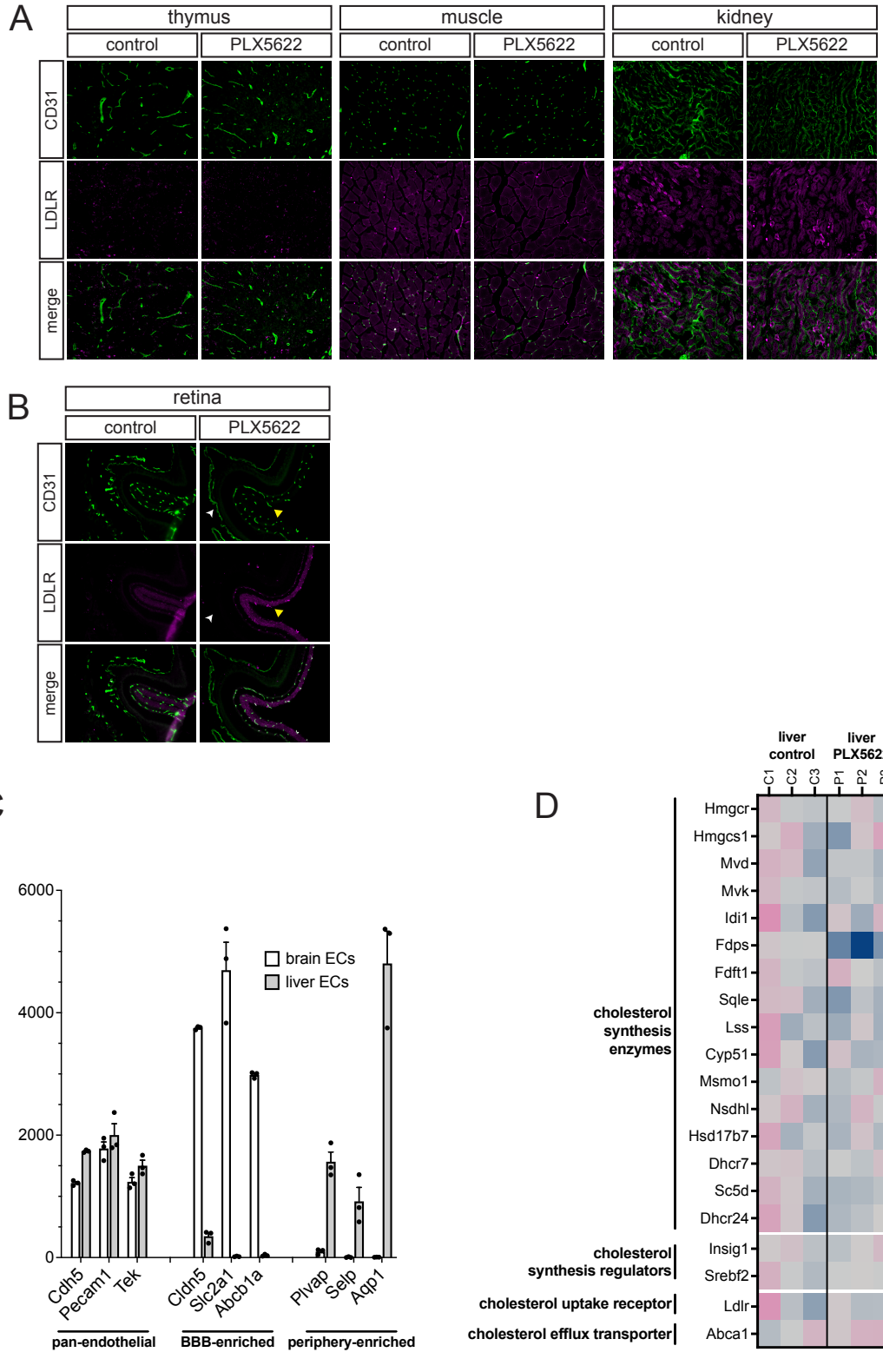
A
thymus
muscle
kidney
control
PLX5622
CD31
LDLR
merge
B
retina
C
counts per million
6000
4000
2000
0
brain ECs
liver ECs
Cdh5
Pecam1
Tek
Cldn5
Slc2a1
Abcb1a
Plvap
Selp
Aqp1
pan-endothelial
BBB-enriched
periphery-enriched
D
liver control
liver PLX5622
C1
C2
C3
P1
P2
P3
Hmgcr
Hmgcs1
Mvd
Mvk
Idi1
Fdps
Fdft1
Sqle
Lss
Cyp51
Msmo1
Nsdhl
Hsd17b7
Dhcr7
Sc5d
Dhcr24
cholesterol synthesis enzymes
Insig1
Srebf2
cholesterol synthesis regulators
Ldlr
cholesterol uptake receptor
Abca1
cholesterol efflux transporter
log2(FC)
2
1
0
-1
-2

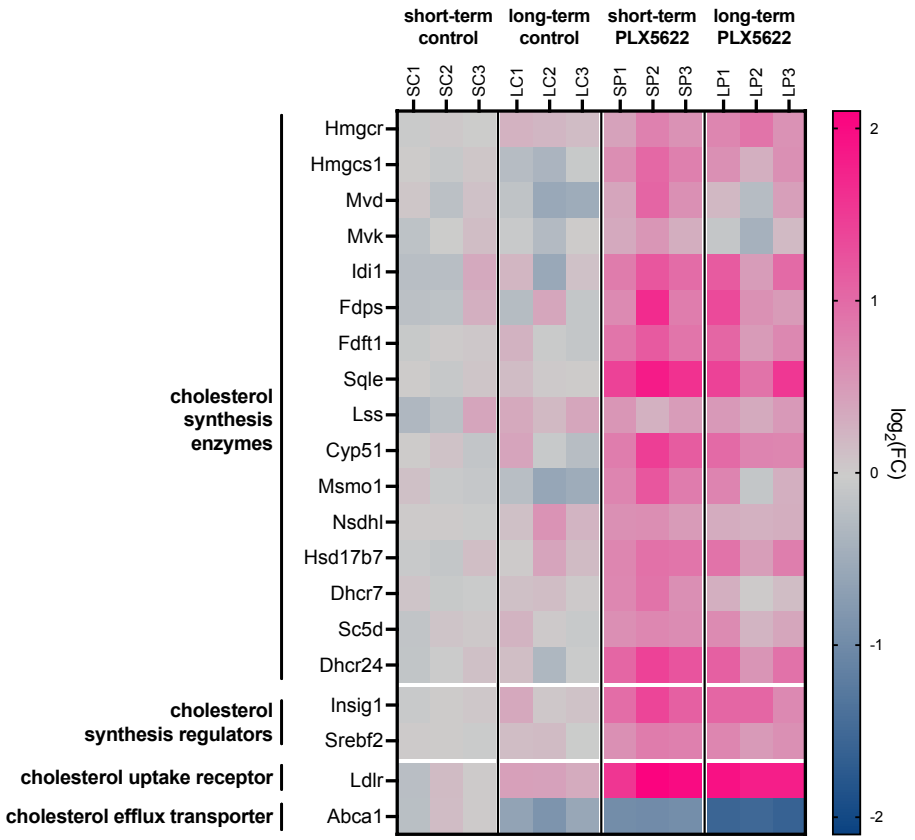


**Figure 3.4 Long-term PLX5622 treatment causes upregulation of endothelial cholesterol cassette** Adult wildtype mice were put on control or PLX5622 diet for one month or 15.5 months. Brains were dissected and dissociated, and endothelial cells were isolated by FACS for RNA sequencing. Gene expression is represented as $\log_2$(FC) compared to the average of the control, with pink representing increased expression and blue representing decreased expression. Aging did not affect the cholesterol cassette, and long- and short-term PLX5622 treatments had nearly identical effects, increasing expression genes involved in cholesterol synthesis and uptake and decreasing expression of the cholesterol efflux transporter.

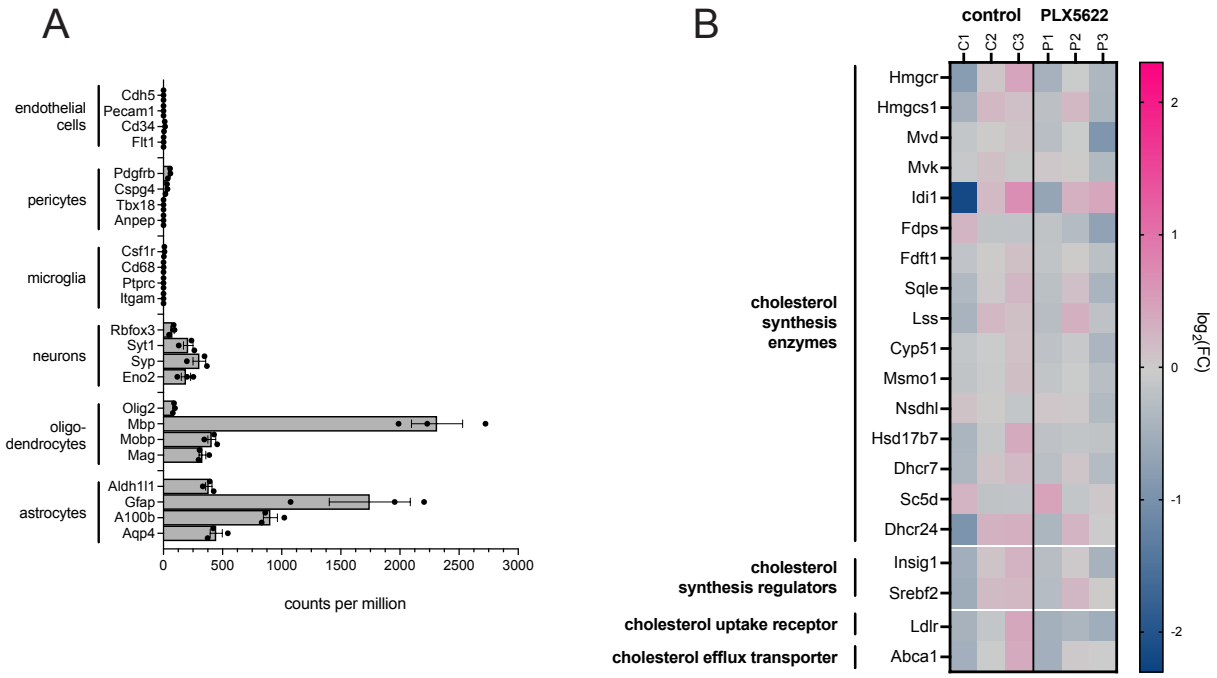


**Figure 3.5 PLX5622 treatment does not increase cholesterol-related gene expression in a mixed glial population.** Adult GFAP-ribotag mice were fed control or PLX5622 diet for one month. Brains were homogenized, and HA-tagged mRNA was isolated using magnetic beads. RNA sequencing was performed on isolated mRNA. **A)** Analyzing expression of different cell type markers showed that mRNA was from not only astrocytes but also oligodendrocytes, with some neuronal contamination as well. There was very little expression of endothelial, pericyte, or microglial markers. **B)** Assessment of cholesterol-related gene expression, with expression represented as $\log_2$(FC) from the average of controls. Pink signifies increased expression and blue signifies decreased expression. PLX5622 treatment did not affect cholesterol-related gene expression in the astrocyte-oligodendrocyte population.

**Figure 3.6 PLX5622 treatment does not cause global changes in lipid signatures in brain, liver, or serum.** Adult wildtype mice were fed control or PLX5622 diet for one month. Mass spectrometry was used to analyze lipid concentrations in brain, liver, and serum. Samples from male and female mice (n=3 per sex per condition) were submitted in separate batches and thus are analyzed separately. **A)** There were no significant differences in any analyzed lipid in male forebrain (left). In female forebrain, PLX5622 treatment increased concentration of DHL ($p=0.0467$) and lanosterol ($p=0.00569$), and decreased concentration of zymosterol ($p=0.0479$) (right). There were no significant changes in cholesterol concentration in male or female forebrain. **B)** PLX5622 treatment increased the concentration of campesterol ($p=0.0148$), cholestanol ($p=0.0211$), and DHL ($p=0.0208$) in male liver (left) but did not significantly alter lipid concentration in female liver (right). There were no significant changes in liver cholesterol in male or female mice after PLX5622 treatment. **C)** PLX5622 treatment had no effect on lipid concentrations in male serum (left). In female serum, PLX5622 treatment increased 7,25-dOHC concentration ($p=0.0113$) and decreased 7a-OH-ONE concentration ($p=0.0220$) (right). PLX5622 treatment did not alter cholesterol concentration in male or female serum samples.

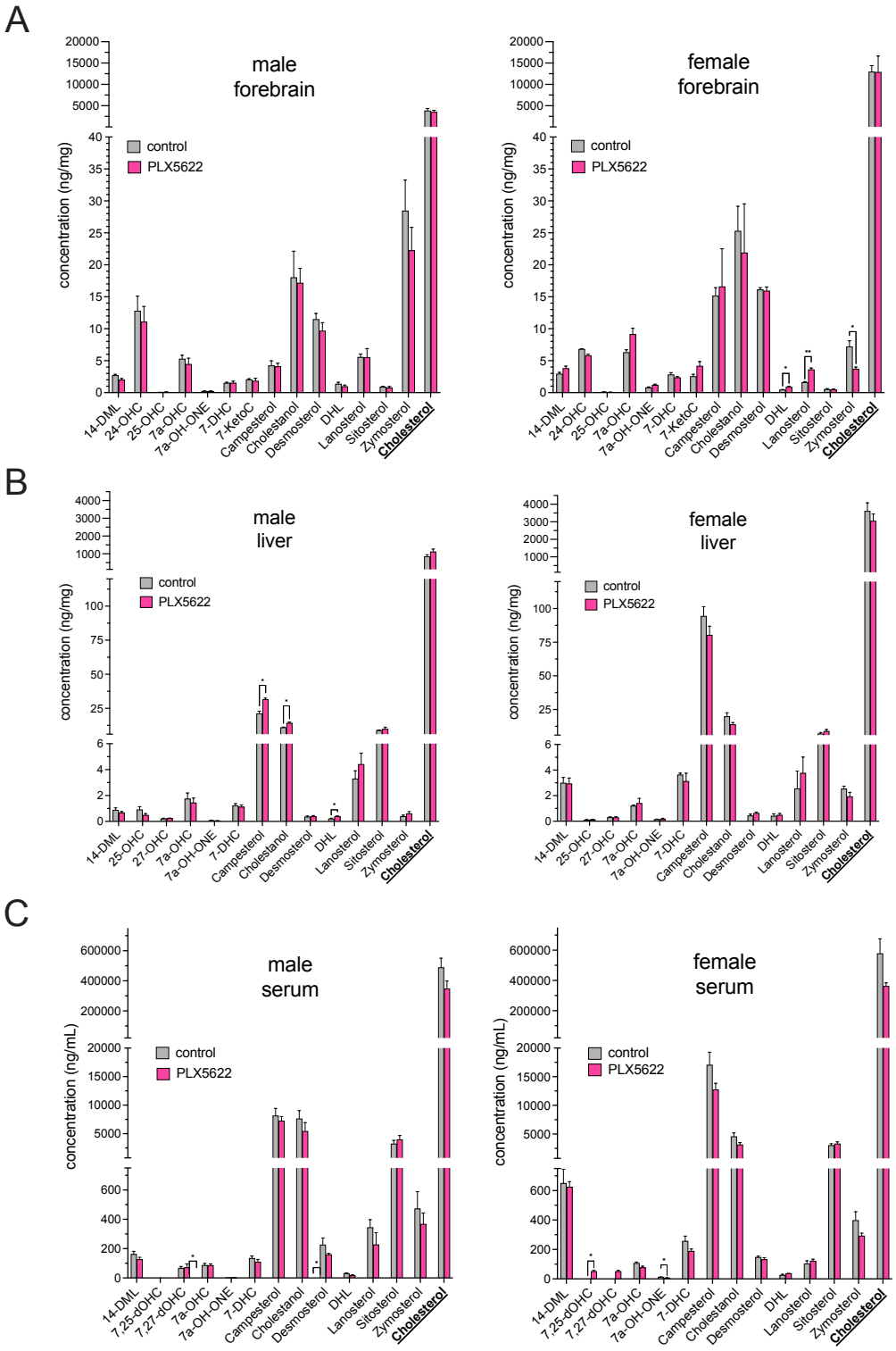
A
male
forebrain
female
forebrain
control
PLX5622
concentration (ng/mg)
14-DML
24-OHC
25-OHC
7a-OHC
7a-OH-ONE
7-DHC
7-KetoC
Campesterol
Cholestanol
Desmosterol
DHL
Lanosterol
Sitosterol
Zymosterol
Cholesterol
B
male
liver
female
liver
27-OHC
C
male
serum
female
serum
concentration (ng/mL)
7,25-dOHC
7,27-dOHC

**Figure 3.7 Upregulation of endothelial cholesterol machinery is independent of microglial depletion.** **A-C)** Adult wildtype mice were put on control or PLX5622 diet for 6, 12, 24, 48, or 72 hours. For 6- and 12-hour timepoints, diet onset coincided with the onset of the dark (waking) cycle. **A)** Percent vascular length positive for LDLR was significantly increased in the PLX5622 group by 12 hours after diet onset ($p=0.00009$; $n=5$) and plateaued at 24 hours. **B)** Microglia were quantified at acute depletion timepoints. Microglial density is presented as percent of average microglial density normalized to control samples at a given timepoint. Microglia were not significantly depleted until 24 hours post PLX5622 diet onset ($p=0.013$; $n=5$). **C)** Despite not being significantly depleted at the 6- and 12-hour PLX5622 timepoints, microglia had visibly more retracted processes. **D-F)** Adult wildtype mice were fed control or PLX5622 diet for two weeks to achieve full microglial depletion. At the onset of the dark (waking) cycle, the PLX5622 group was switched back to control diet. Brain samples were collected at 24 and 48 hours post diet switch. **D)** 24 hours after PLX5622 removal, percent LDLR+ vascular length was already decreased ($p=0.0032$) but still higher than in control mice ($p=0.0038$). By 48 hours after PLX5622 removal, percent LDLR+ vascular length was not significantly different from control levels ($p=0.999$). **E)** At 24 and 48 hours after PLX5622 removal, there was no significant microglial repopulation ($p=0.978$; $p=0.183$). Microglial density is presented as percentage of control density. **F)** A simple linear regression was performed to assess the relationship between percent LDLR+ vascular length and microglial density. There was not a significant linear relationship between these measurements at either 24 hours ($p=0.103$) or 48 hours ($p=0.780$) after PLX5622 removal.

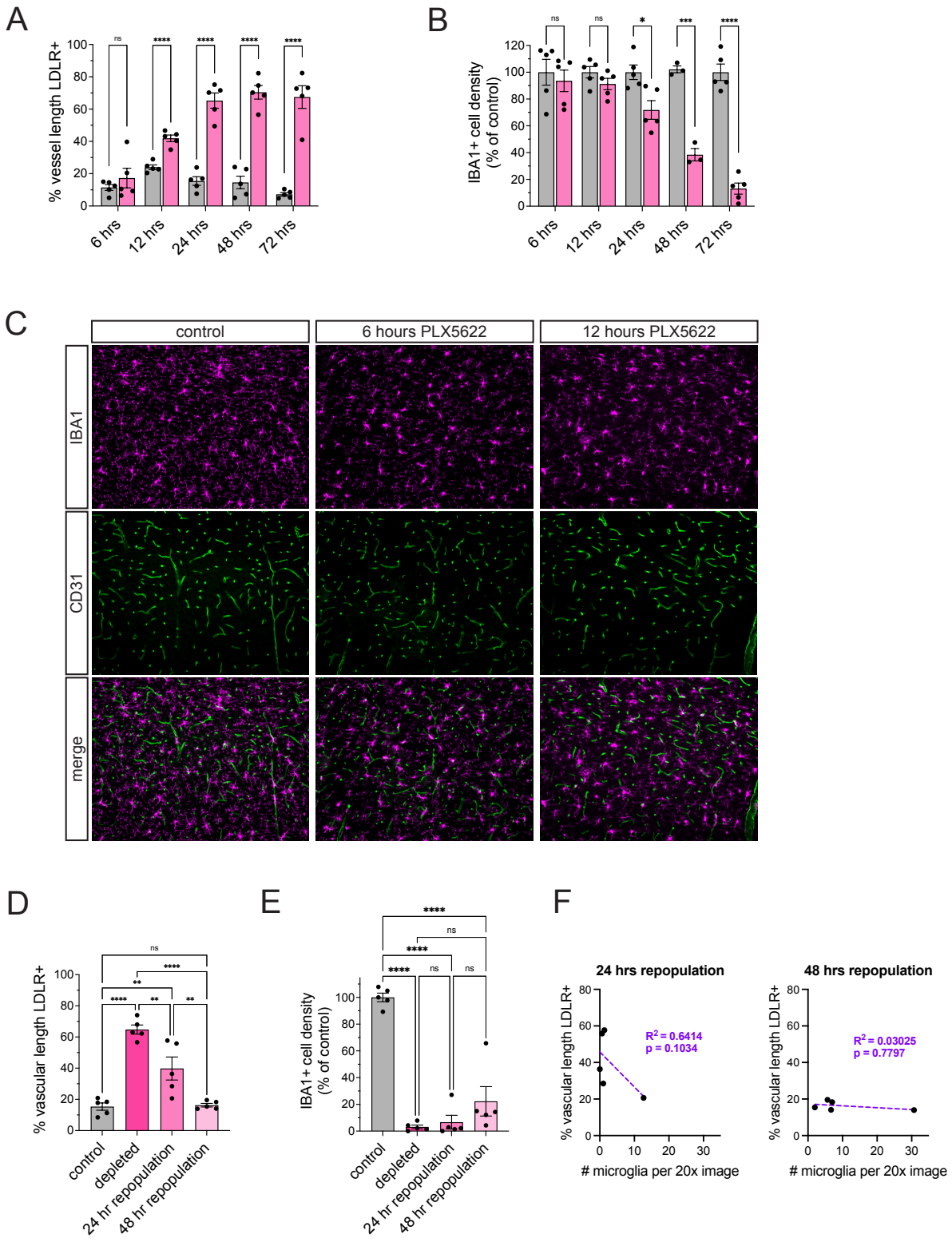
A
% vessel length LDLR+
ns
****
6 hrs
12 hrs
24 hrs
48 hrs
72 hrs
B
IBA1+ cell density
(% of control)
ns
*
***
C
control
6 hours PLX5622
12 hours PLX5622
IBA1
CD31
merge
D
% vascular length LDLR+
control
depleted
24 hr repopulation
48 hr repopulation
E
IBA1+ cell density
(% of control)
F
24 hrs repopulation
48 hrs repopulation
R2 = 0.6414
p = 0.1034
R2 = 0.03025
p = 0.7797
# microglia per 20x image

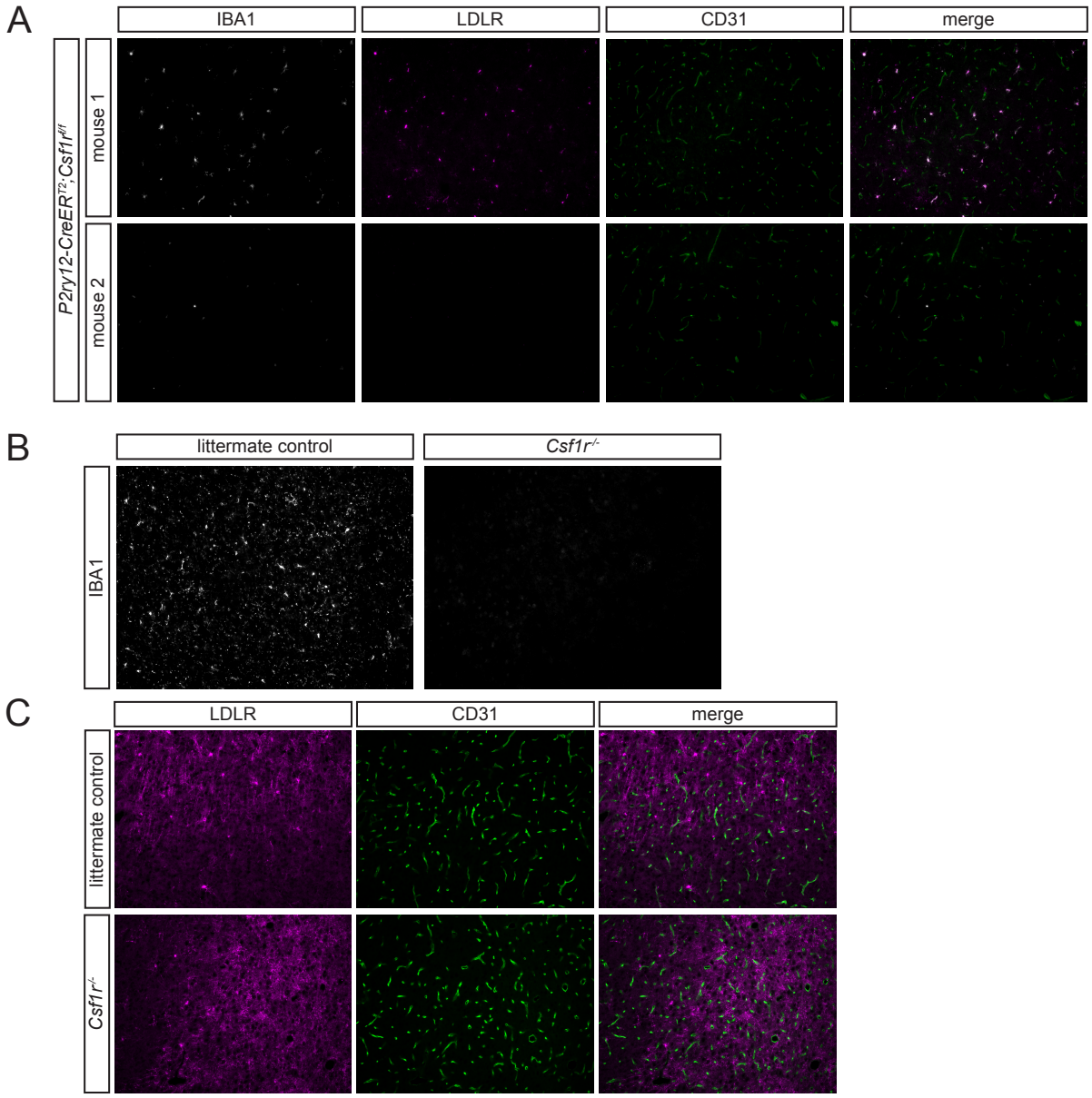


**Figure 3.8 Genetic depletion of microglia does not increase expression of cholesterol uptake receptor in endothelial cells. A)** Adult *P2ry12-CreER$^{T2}$; Csf1rf$^{f}$* mice were treated with tamoxifen for 8 days and tissue was collected on the 9$^{th}$ day. 10 µm brain sections were stained for microglia (anti-IBA1, gray), LDLR (magenta), and endothelial cells (anti-CD31, green). Efficiency of microglial depletion varied among knockout mice, but there was no increase in LDLR+ vasculature. **B-C)** *Csf1r-/-* mice and littermate controls were perfused at P20. **B)** 10 µm sections were stained for microglia (anti-IBA1). Knockout mice had no visible microglia. **C)** 10 µm brain sections were stained for LDLR (magenta) and endothelial cells (anti-CD31, green). There was no increase in vascular LDLR.

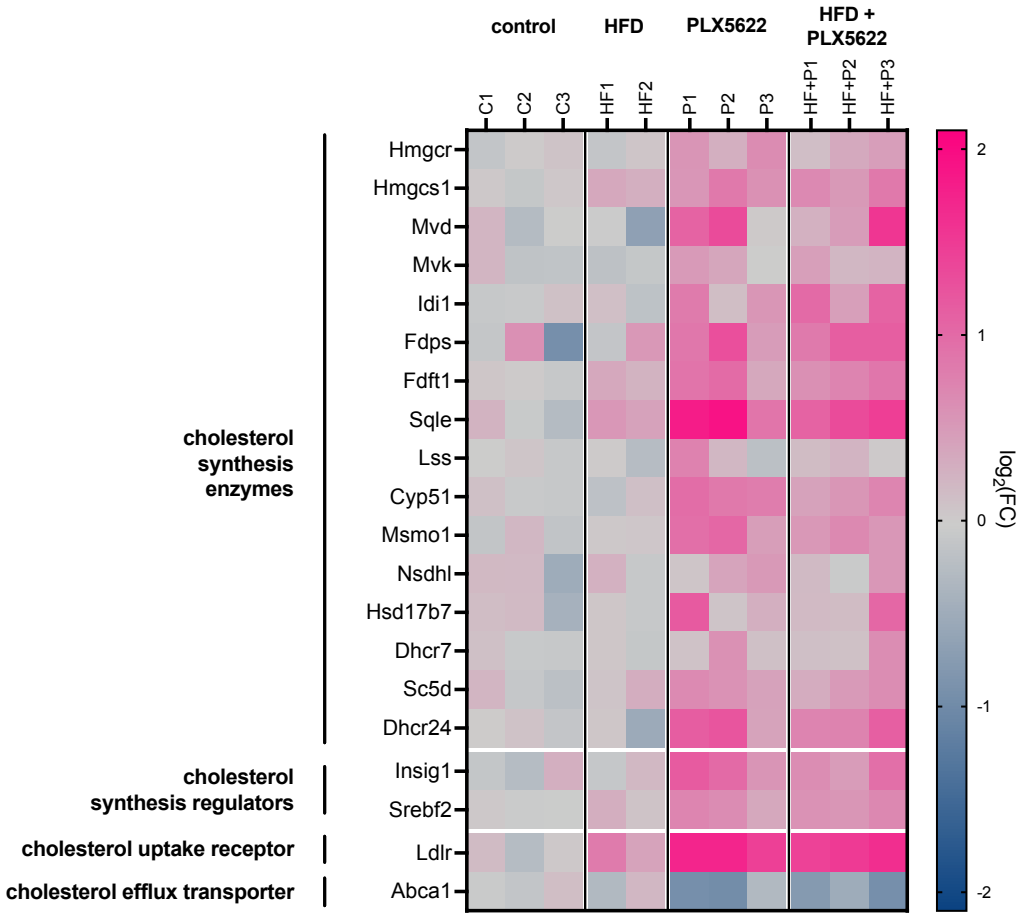


**Figure 3.9 High fat diet does not alter brain endothelial cholesterol metabolism.** Adult wildtype mice were fed control, high fat diet, PLX5622, or high fat diet + PLX5622 for one month. Brains were dissected and dissociated, and endothelial cells were isolate with FACS for RNA sequencing. Gene expression is presented as $log_2$(FC) from the average of control samples. High fat diet did not alter endothelial cholesterol-related gene expression and did not interact with PLX5622 to alter the PLX5622-mediated cholesterol phenotype.

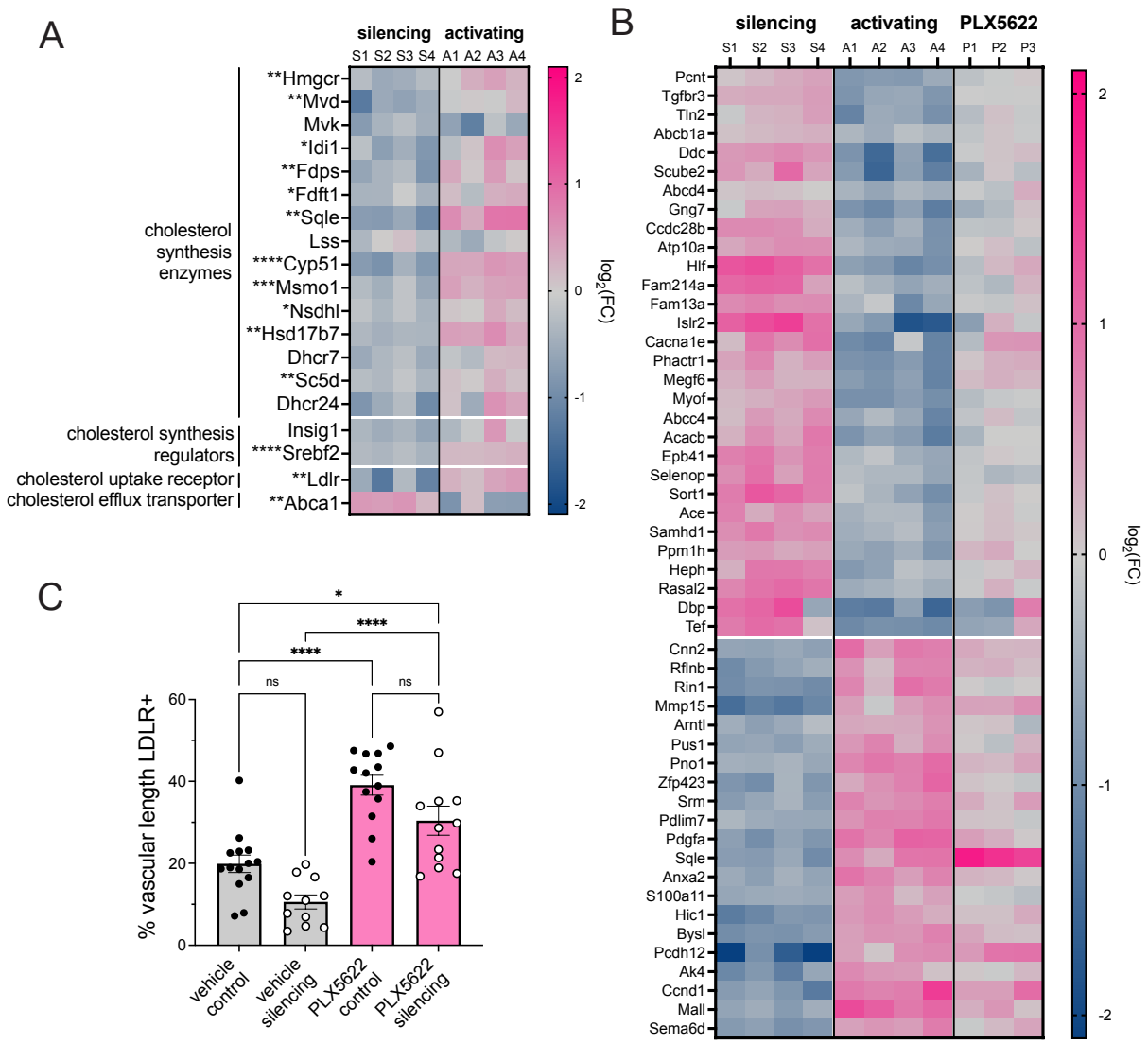


**Figure 3.10 Neuronal activity regulates brain endothelial cholesterol metabolism. A)** After chemogenetic activation or silencing of neuronal activity, brains were dissected and dissociated, and endothelial cells were isolated with FACS for RNA sequencing[16]. Gene expression is presented as $\log_2$(FC) from the average of each condition's respective controls. Neuronal activation increased expression of the cholesterol cassette, while silencing neuronal activity decreased expression of the cassette. Asterisks signify genes for which expression in the silencing vs activating conditions was significantly different, with each expression value normalized to the average of the expression in respective littermate control samples (*p<0.05; **p<0.01; ***p<0.001; ****p<0.0001). **B)** The genes most strongly bidirectionally regulated by neuronal activity are listed on the y-axis. Their expression level was assessed in PLX5622-fed mice. Expression is presented as $\log_2$(FC) from the average of each condition's respective controls. PLX5622 did not phenocopy neuronal activation. **C)** hM4Di-Silencing mice or littermate controls were injected with either vehicle or PLX5622 (50 mg/kg) at the onset of the dark (waking) cycle (time=0). All mice were injected with clozapine-n-oxide at times 0, 4, and 8 hours to maintain neuronal silencing, and tissue was harvested at 12 hours. PLX5622 has a stronger effect on vascular LDLR than neuronal activity. There was a trend towards decreased vascular LDLR (~10%) in the silencing conditions.

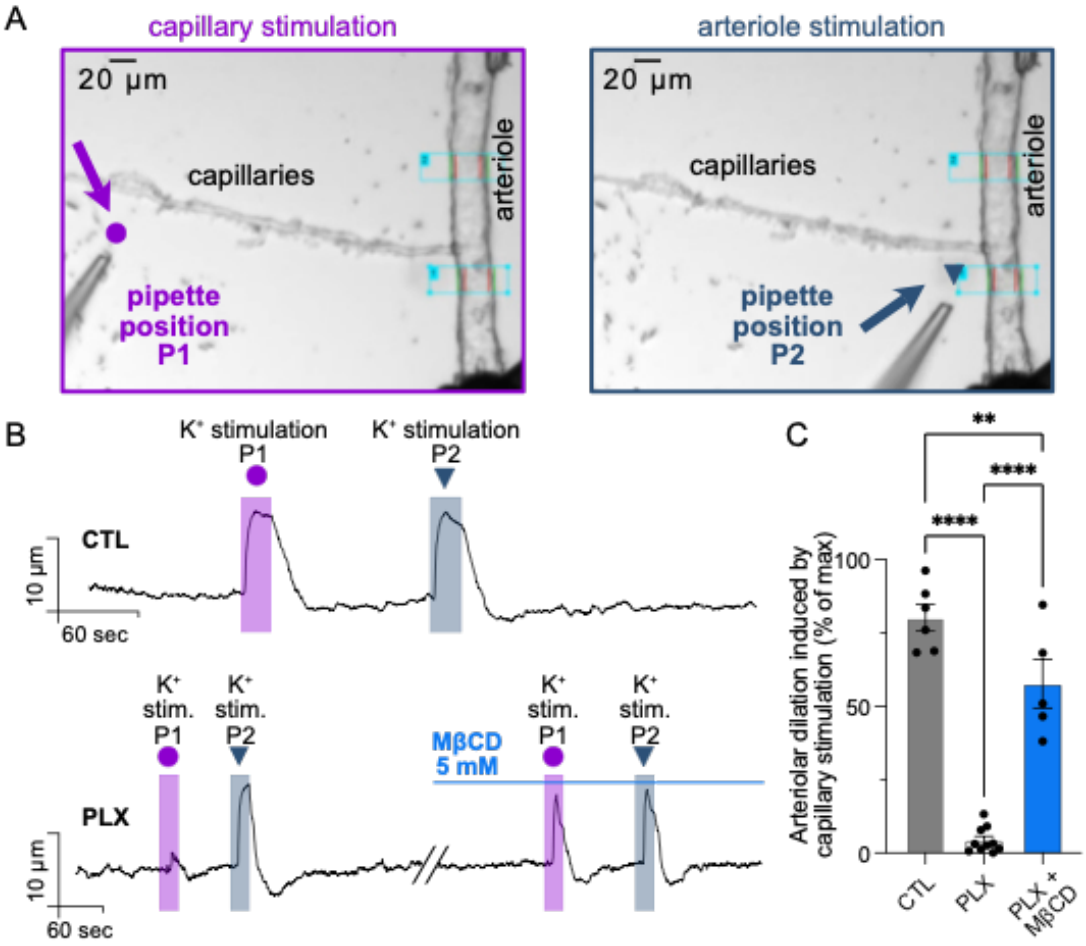


**Figure 3.11 Increased vascular cholesterol induced by PLX5622 treatment inhibits retrograde hyperpolarization in response to $K^+$.** Adult wildtype mice were fed control or PLX5622 diet for at least one month. Intact vascular segments were removed from the cortex and bathed in artificial CSF, and arterioles were cannulated. **A)** $K^+$ ions were ejected next to capillaries (left, yellow) or the arteriole (right, purple). **B)** Representative trace of arteriole dilation across time in response to capillary or arteriole $K^+$ stimulation. PLX5622 treatment inhibited arteriole dilation in response to capillary $K^+$ stimulation, while response to arteriole stimulation remained intact. Response to capillary stimulation was rescued in vessels from PLX5622-treated mice when membrane cholesterol was depleted with MβCD. **C)** Quantification of arteriole dilation in response to capillary $K^+$ stimulation. PLX5622 diet inhibited retrograde hyperpolarization, but treatment with MβCD partially rescued this effect.

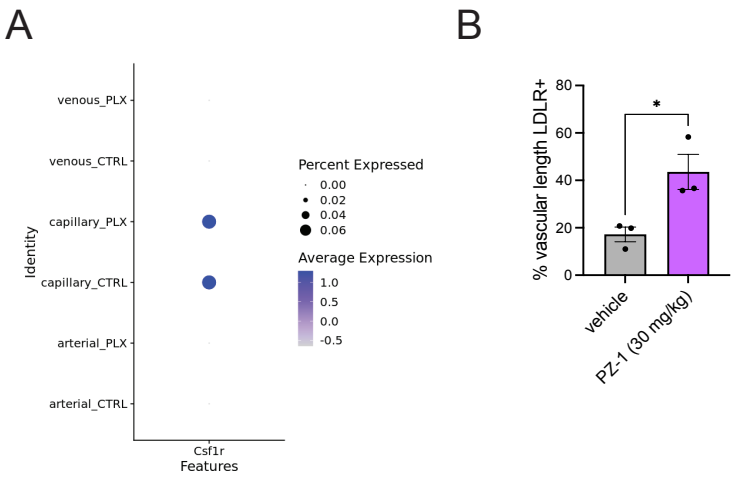


**Figure 3.12 PLX5622 acts on another receptor tyrosine kinase to increase endothelial cholesterol metabolism. A)** Adult wildtype mice were fed control or PLX5622 diet for one month. Brains were dissected and dissociated, and endothelial cells were isolated by FACS for single-cell RNA sequencing. For each diet condition, cells were obtained from three brains across two samples. Endothelial cells formed three main clusters which were identified as arterial, capillary, and venous endothelial cells. For *Csf1r*, the size of the dot represents the percentage of endothelial cells expressing *Csf1r*, and the color of the dot represents average expression on a log scale, with darker purple signifying higher expression. *Csf1r* is expressed by an extremely low percentage of endothelial cells. **B)** Adult wildtype mice were injected with vehicle (10% DMSO, 90% corn oil) or PZ-1, an inhibitor of RET and KDR, at a dose of 30 mg/kg. Brains were collected from perfusion-fixed mice 12 hours after injection. 10µm sections were stained for LDLR and CD31, and the percent vascular length positive for LDLR was calculated. PZ-1 significantly increased vascular LDLR expression ($p=0.030$; $n=3$).

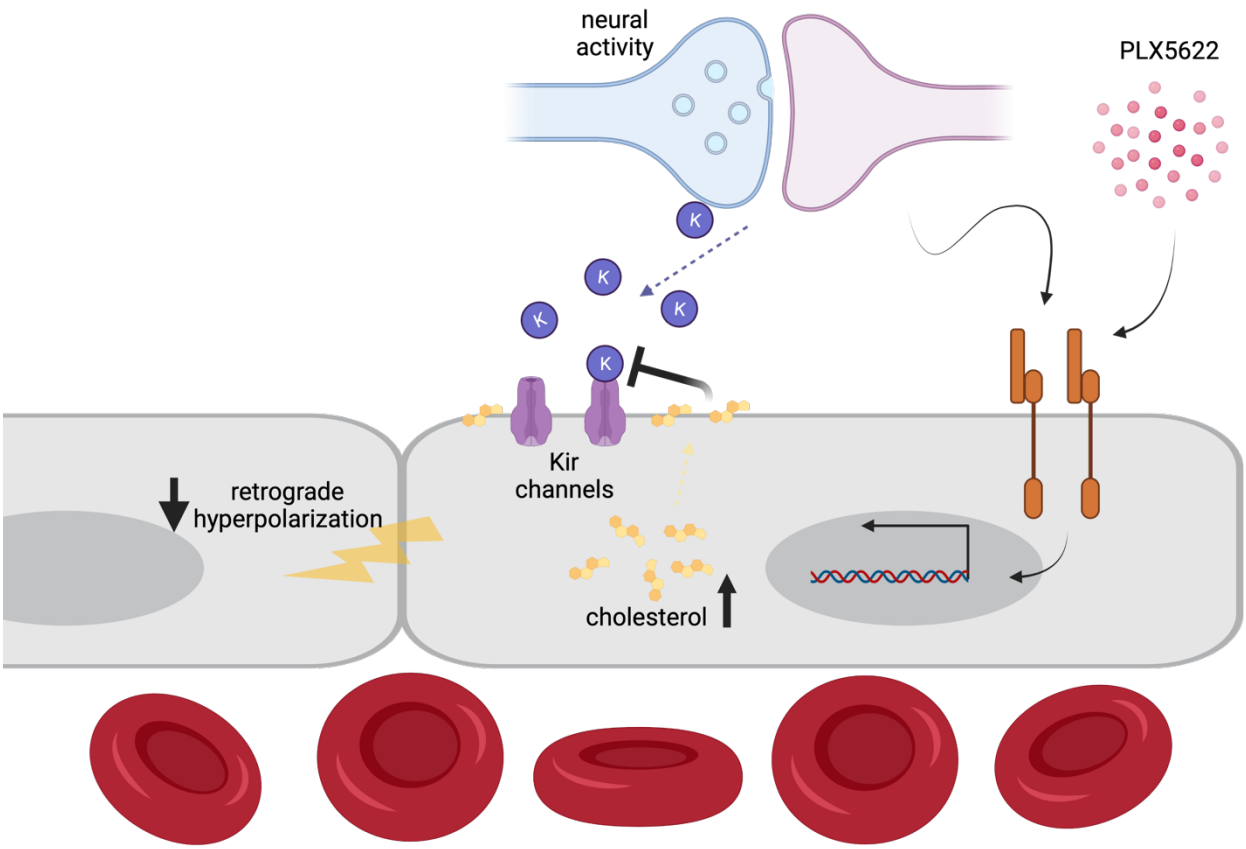


**Figure 3.13 Model: endothelial cholesterol as a negative feedback mechanism in neurovascular coupling** Neural activity increases extracellular potassium, which acts on capillary $K_{IR}$ channels to cause retrograde hyperpolarization and upstream arteriole dilation[5]. We think we have discovered a negative feedback mechanism in which neurovascular production of cholesterol is increased. As cholesterol is known to inhibit $K_{IR}$ channels, cholesterol thus reduces retrograde hyperpolarization and arteriole dilation. We think that PLX5622 is acting on this pathway, through inhibition of a receptor tyrosine kinase (RTK) related to CSF1R. *Created with BioRender*.

**Discussion**

Here we find that CNS endothelial cholesterol metabolism is dynamically regulated by neuronal activity, with neuronal activation leading to increases in endothelial cholesterol synthesis and uptake. We show that constitutive upregulation of endothelial cholesterol synthesis – as achieved by PLX5622 – inhibits retrograde hyperpolarization and arteriole dilation in response to capillary $K^+$ stimulation. This deficit in $K^+$-mediated arteriole dilation is rescued by depletion of membrane cholesterol. Together, these data suggest that increases in endothelial cholesterol act as a negative feedback mechanism in neurovascular coupling.

While several studies provide evidence that $K_{IR}$ channels are cholesterol-sensitive[12,13,31-33], and while we show that endothelial response to $K^+$ is inhibited by cholesterol, we cannot say whether cholesterol inhibits endothelial retrograde signaling solely by affecting $K_{IR}$ channels. Cholesterol can have a myriad of effects on cell signaling processes in the cell. For instance, membrane cholesterol has been shown to alter the function of PIEZO1, a mechanoreceptor important for sensation of blood pressure[34,35]. In the future it will be important to understand the range of functional effects of increased endothelial cholesterol content.

Functional hyperemia occurs in a matter of seconds after neuronal activity and is transient in nature. What we have captured in our transcriptional data is an endothelial response to sustained neuronal activity lasting over an hour[16], and we also see an increase in cholesterol-related gene expression three hours after kainic acid-induced seizures[36]. From these data, it seems evident that sustained neuronal activity leads to transcriptional changes in a cholesterol-related gene cassette. However, it remains unclear whether cellular cholesterol stores or cholesterol uptake are utilized on much shorter timescale to help vasodilation return to baseline following hyperemia. Alternatively, it may be that endothelial cholesterol metabolism provides negative feedback to NVC processes specifically in cases of sustained or pathological neuronal hyperactivity.

This study began as an inquiry into a role for microglia at the healthy BBB and thus with the use of PLX5622, a CSF1R inhibitor. PLX5622 is touted as very specific for CSF1R and has a ten-fold lower

affinity for related kinases compared to PLX3397, another CSF1R inhibitor used in the field to deplete microglia[37]. However, it is reported – albeit deep in supplementary information – that the standard high dose of 1200 mg/kg PLX5622 in rodent chow leads to a concentration of 22 μM and 6.04 μM in blood and brain parenchyma, respectively[30]. These concentrations are both far above PLX5622's reported $IC_{50}$ values for FLT3, KIT, AURKC, and KDR[30]. So while PLX5622 might be far more specific than PLX3397, the PLX5622 dose often used for microglial depletion is likely inhibiting other RTKs and altering biological function in cell types aside from microglia. While many microglial depletion studies have validated their findings using genetic models and alternative methods to link their phenotypes to microglia, others may have erroneously connected their results to microglial depletion. Thus, the data in the present study warrant re-visiting other studies using PLX3397 or PLX5622.

Interestingly, although we found our cholesterol phenotype to be independent of microglial depletion, a couple recent papers have suggested a link between microglial depletion and neurovascular coupling. Bisht et al. show that PLX3397 treatment increases baseline cerebral blood flow (CBF) and capillary diameter, and that PLX3397-treated mice have a lower percent increase in CBF in response to $CO_2$. These effects were phenocopied in *P2ry12*$^{-/-}$ and *Panx*$^{-/-}$ mice, and the authors thus suggest that microglial-vascular purinergic signaling is involved in neurovascular coupling[26]. Császár et al. similarly find that PLX5622 treatment, pharmacological P2RY12 inhibition, and P2RY12 knockout increase baseline CBF and decrease CBF response to a variety of manipulations, including whisker stimulation and hypercapnia[38]. While in both cases these studies replicate their CSF1R inhibition results with P2RY12 inhibition or knockout, these data do not conclusively show that microglia in particular directly regulate NVC. As we have shown, PLX5622 causes vascular changes independent of microglial depletion. And P2RY12, while highly expressed in microglia, is also expressed by activated platelets and leukocyte subtypes[39]. Of particular interest, some have also found P2RY12 to be expressed in SMCs and play a direct role in vasodilation and constriction[40]. Thus, while microglia may indeed be involved in NVC, use of the P2RY12 global knockout is not sufficient to claim a specific role for microglia in NVC. A conditional

P2RY12 knockout restricted to microglia would be more informative. It is also worth noting that, in both studies described above, CBF analyses were performed in anesthetized mice. As anesthesia can change CBF dynamics, it would be valuable to see these studies repeated in awake mice.

While we have focused on dynamic regulation of endothelial cholesterol metabolism in healthy adult mice, the regulation of endothelial cholesterol and its effects on vascular function are also pertinent to several neuropathologies and cardiovascular diseases. Atherosclerosis is characterized by the buildup of fats – including cholesterol – on the inner walls of blood vessels, causing obstruction of blood flow. As the general dogma is that blood and brain cholesterol are separate pools, there has not been much focus on how this cholesterol might be taken up into brain endothelial cells and alter abluminal endothelial signaling. In light of the current study, it is possible that endothelial LDLR facilitates uptake of plaque-associated cholesterol, and that this uptake contributes to NVC dysfunction and cognitive deficits. Membrane cholesterol also affects processing of amyloid precursor protein, increasing amyloid-beta (Aβ) production [41-44]. Vascular Aβ plaques, termed cerebral amyloid angiopathy (CAA), are present in up to 98% of Alzheimer's disease (AD) patients and can also occur in the absence of AD[45]. CAA can cause stroke, dementia, inflammation, cortical microbleeds, and hemorrhage[46,47]. Despite its serious clinical ramifications, it remains unclear why plaques develop in vascular walls. One possibility is aberrant production of Aβ by endothelial cells. Interestingly, long-term PLX5622 treatment inhibited the formation of parenchymal plaques in a mouse model of AD, but Spangenberg et al. observed clear vascular plaques in PLX5622-treated mice[30]. This could be a result of dysfunctional Aβ clearance, but it could also arise from endothelial Aβ production resulting from PLX5622-mediated increases in endothelial cholesterol. There is still much to uncover about dynamic cholesterol metabolism in the context of disease.

The current study identifies neuronal activity as a modulator of CNS endothelial cholesterol metabolism and suggests a role for endothelial cholesterol in negatively regulating NVC processes. These data add to our understanding of the active role of endothelial cells in NVC and raise new questions regarding the role of endothelial cholesterol metabolism in health and disease.

**Acknowledgements**

Chapter III, in full, is currently being prepared for submission for publication and will include Lena Spieth, Sean S. Harvey, Alexander Z. Zhang, Jackson T. Fontaine, Vanessa Coelho-Santos, Kelsey M. Nemec, Gabriel L. McKinsey, Thomas D. Arnold, Frederick C. Bennett, Andy Y. Shih, Gesine Saher, and Fabrice Dabertrand as co-authors, and Professor Richard Daneman as the senior author. The dissertation author was the primary investigator and author of this material.

**References**

1 Mosso, A. Sulla circolazione del sangue nel cervello dell'uomo. *Revue Philosophique de la France Et de l* (1882).

2 Roy, C. S. & Sherrington, C. S. On the Regulation of the Blood-supply of the Brain. *J Physiol* **11**, 85-158 117, doi:10.1113/jphysiol.1890.sp000321 (1890).

3 Iadecola, C. The Neurovascular Unit Coming of Age: A Journey through Neurovascular Coupling in Health and Disease. *Neuron* **96**, 17-42, doi:10.1016/j.neuron.2017.07.030 (2017).

4 Chen, B. R., Kozberg, M. G., Bouchard, M. B., Shaik, M. A. & Hillman, E. M. A critical role for the vascular endothelium in functional neurovascular coupling in the brain. *J Am Heart Assoc* **3**, e000787, doi:10.1161/JAHA.114.000787 (2014).

5 Longden, T. A., Dabertrand, F., Koide, M., Gonzales, A. L., Tykocki, N. R., Brayden, J. E., Hill-Eubanks, D. & Nelson, M. T. Capillary K(+)-sensing initiates retrograde hyperpolarization to increase local cerebral blood flow. *Nat Neurosci* **20**, 717-726, doi:10.1038/nn.4533 (2017).

6 Chow, B. W., Nunez, V., Kaplan, L., Granger, A. J., Bistrong, K., Zucker, H. L., Kumar, P., Sabatini, B. L. & Gu, C. Caveolae in CNS arterioles mediate neurovascular coupling. *Nature* **579**, 106-110, doi:10.1038/s41586-020-2026-1 (2020).

7 Beach, J. M., McGahren, E. D. & Duling, B. R. Capillaries and arterioles are electrically coupled in hamster cheek pouch. *Am J Physiol* **275**, H1489-1496, doi:10.1152/ajpheart.1998.275.4.H1489 (1998).

8 Ahn, S. J., Fancher, I. S., Bian, J. T., Zhang, C. X., Schwab, S., Gaffin, R., Phillips, S. A. & Levitan, I. Inwardly rectifying K(+) channels are major contributors to flow-induced vasodilatation in resistance arteries. *J Physiol* **595**, 2339-2364, doi:10.1113/JP273255 (2017).

9 Hannah, R. M., Dunn, K. M., Bonev, A. D. & Nelson, M. T. Endothelial SK(Ca) and IK(Ca) channels regulate brain parenchymal arteriolar diameter and cortical cerebral blood flow. *J Cereb Blood Flow Metab* **31**, 1175-1186, doi:10.1038/jcbfm.2010.214 (2011).

10 Harraz, O. F., Longden, T. A., Dabertrand, F., Hill-Eubanks, D. & Nelson, M. T. Endothelial GqPCR activity controls capillary electrical signaling and brain blood flow through PIP2 depletion. Proc Natl Acad Sci U S A 115, E3569-E3577, doi:10.1073/pnas.1800201115 (2018).

11 Sancho, M., Fabris, S., Hald, B. O., Brett, S. E., Sandow, S. L., Poepping, T. L. & Welsh, D. G. Membrane Lipid-KIR2.x Channel Interactions Enable Hemodynamic Sensing in Cerebral Arteries. *Arterioscler Thromb Vasc Biol* **39**, 1072-1087, doi:10.1161/ATVBAHA.119.312493 (2019).

12 Romanenko, V. G., Fang, Y., Byfield, F., Travis, A. J., Vandenberg, C. A., Rothblat, G. H. & Levitan, I. Cholesterol sensitivity and lipid raft targeting of Kir2.1 channels. *Biophys J* **87**, 3850-3861, doi:10.1529/biophysj.104.043273 (2004).

13 Romanenko, V. G., Rothblat, G. H. & Levitan, I. Modulation of endothelial inward-rectifier K+ current by optical isomers of cholesterol. *Biophys J* **83**, 3211-3222, doi:10.1016/S0006-3495(02)75323-X (2002).

14 Fancher, I. S., Le Master, E., Ahn, S. J., Adamos, C., Lee, J. C., Berdyshev, E., Dull, R. O., Phillips, S. A. & Levitan, I. Impairment of Flow-Sensitive Inwardly Rectifying K(+) Channels via Disruption of Glycocalyx Mediates Obesity-Induced Endothelial Dysfunction. *Arterioscler Thromb Vasc Biol* **40**, e240-e255, doi:10.1161/ATVBAHA.120.314935 (2020).

15 Tarantini, S., Hertelendy, P., Tucsek, Z., Valcarcel-Ares, M. N., Smith, N., Menyhart, A., Farkas, E., Hodges, E. L., Towner, R., Deak, F., Sonntag, W. E., Csiszar, A., Ungvari, Z. & Toth, P. Pharmacologically-induced neurovascular uncoupling is associated with cognitive impairment in mice. *J Cereb Blood Flow Metab* **35**, 1871-1881, doi:10.1038/jcbfm.2015.162 (2015).

16 Pulido, R. S., Munji, R. N., Chan, T. C., Quirk, C. R., Weiner, G. A., Weger, B. D., Rossi, M. J., Elmsaouri, S., Malfavon, M., Deng, A., Profaci, C. P., Blanchette, M., Qian, T., Foreman, K. L., Shusta, E. V., Gorman, M. R., Gachon, F., Leutgeb, S. & Daneman, R. Neuronal Activity Regulates Blood-Brain Barrier Efflux Transport through Endothelial Circadian Genes. *Neuron* **108**, 937-952 e937, doi:10.1016/j.neuron.2020.09.002 (2020).

17 Edmond, J., Korsak, R. A., Morrow, J. W., Torok-Both, G. & Catlin, D. H. Dietary cholesterol and the origin of cholesterol in the brain of developing rats. *J Nutr* **121**, 1323-1330, doi:10.1093/jn/121.9.1323 (1991).

18 Dietschy, J. M. Central nervous system: cholesterol turnover, brain development and neurodegeneration. *Biol Chem* **390**, 287-293, doi:10.1515/BC.2009.035 (2009).

19 Nieweg, K., Schaller, H. & Pfrieger, F. W. Marked differences in cholesterol synthesis between neurons and glial cells from postnatal rats. *J Neurochem* **109**, 125-134, doi:10.1111/j.1471-4159.2009.05917.x (2009).

20 Mayford, M., Bach, M. E., Huang, Y. Y., Wang, L., Hawkins, R. D. & Kandel, E. R. Control of memory formation through regulated expression of a CaMKII transgene. *Science* **274**, 1678-1683, doi:10.1126/science.274.5293.1678 (1996).

21 Alexander, G. M., Rogan, S. C., Abbas, A. I., Armbruster, B. N., Pei, Y., Allen, J. A., Nonneman, R. J., Hartmann, J., Moy, S. S., Nicolelis, M. A., McNamara, J. O. & Roth, B. L. Remote control of neuronal activity in transgenic mice expressing evolved G protein-coupled receptors. *Neuron* **63**, 27-39, doi:10.1016/j.neuron.2009.06.014 (2009).

22 Bohlen, C. J., Bennett, F. C., Tucker, A. F., Collins, H. Y., Mulinyawe, S. B. & Barres, B. A. Diverse Requirements for Microglial Survival, Specification, and Function Revealed by Defined-Medium Cultures. *Neuron* **94**, 759-773 e758, doi:10.1016/j.neuron.2017.04.043 (2017).

23 Badimon, A., Strasburger, H. J., Ayata, P., Chen, X., Nair, A., Ikegami, A., Hwang, P., Chan, A. T., Graves, S. M., Uweru, J. O., Ledderose, C., Kutlu, M. G., Wheeler, M. A., Kahan, A., Ishikawa, M., Wang, Y. C., Loh, Y. E., Jiang, J. X., Surmeier, D. J., Robson, S. C., Junger, W. G., Sebra, R., Calipari, E. S., Kenny, P. J., Eyo, U. B., Colonna, M., Quintana, F. J., Wake, H., Gradinaru, V. & Schaefer, A. Negative feedback control of neuronal activity by microglia. *Nature* **586**, 417-423, doi:10.1038/s41586-020-2777-8 (2020).

24 Merlini, M., Rafalski, V. A., Ma, K., Kim, K. Y., Bushong, E. A., Rios Coronado, P. E., Yan, Z., Mendiola, A. S., Sozmen, E. G., Ryu, J. K., Haberl, M. G., Madany, M., Sampson, D. N., Petersen, M. A., Bardehle, S., Tognatta, R., Dean, T., Jr., Acevedo, R. M., Cabriga, B., Thomas, R., Coughlin, S. R., Ellisman, M. H., Palop, J. J. & Akassoglou, K. Microglial Gi-dependent dynamics regulate brain network hyperexcitability. *Nat Neurosci* **24**, 19-23, doi:10.1038/s41593-020-00756-7 (2021).

25 Rosehart, A. C., Johnson, A. C. & Dabertrand, F. Ex Vivo Pressurized Hippocampal Capillary-Parenchymal Arteriole Preparation for Functional Study. *J Vis Exp*, doi:10.3791/60676 (2019).

26 Bisht, K., Okojie, K. A., Sharma, K., Lentferink, D. H., Sun, Y. Y., Chen, H. R., Uweru, J. O., Amancherla, S., Calcuttawala, Z., Campos-Salazar, A. B., Corliss, B., Jabbour, L., Benderoth, J., Friestad, B., Mills, W. A., 3rd, Isakson, B. E., Tremblay, M. E., Kuan, C. Y. & Eyo, U. B. Capillary-associated microglia regulate vascular structure and function through PANX1-P2RY12 coupling in mice. *Nat Commun* **12**, 5289, doi:10.1038/s41467-021-25590-8 (2021).

27 Zhang, Y., Chen, K., Sloan, S. A., Bennett, M. L., Scholze, A. R., O'Keeffe, S., Phatnani, H. P., Guarnieri, P., Caneda, C., Ruderisch, N., Deng, S., Liddelow, S. A., Zhang, C., Daneman, R., Maniatis, T., Barres, B. A. & Wu, J. Q. An RNA-sequencing transcriptome and splicing database of glia, neurons, and vascular cells of the cerebral cortex. *J Neurosci* **34**, 11929-11947, doi:10.1523/JNEUROSCI.1860-14.2014 (2014).

28 Vanlandewijck, M., He, L., Mae, M. A., Andrae, J., Ando, K., Del Gaudio, F., Nahar, K., Lebouvier, T., Lavina, B., Gouveia, L., Sun, Y., Raschperger, E., Rasanen, M., Zarb, Y., Mochizuki, N., Keller, A., Lendahl, U. & Betsholtz, C. A molecular atlas of cell types and zonation in the brain vasculature. *Nature* **554**, 475-480, doi:10.1038/nature25739 (2018).

29 He, L., Vanlandewijck, M., Mae, M. A., Andrae, J., Ando, K., Del Gaudio, F., Nahar, K., Lebouvier, T., Lavina, B., Gouveia, L., Sun, Y., Raschperger, E., Segerstolpe, A., Liu, J., Gustafsson, S., Rasanen, M., Zarb, Y., Mochizuki, N., Keller, A., Lendahl, U. & Betsholtz, C. Single-cell RNA sequencing of mouse brain and lung vascular and vessel-associated cell types. *Sci Data* **5**, 180160, doi:10.1038/sdata.2018.160 (2018).

30 Spangenberg, E., Severson, P. L., Hohsfield, L. A., Crapser, J., Zhang, J., Burton, E. A., Zhang, Y., Spevak, W., Lin, J., Phan, N. Y., Habets, G., Rymar, A., Tsang, G., Walters, J., Nespi, M., Singh, P., Broome, S., Ibrahim, P., Zhang, C., Bollag, G., West, B. L. & Green, K. N. Sustained microglial depletion with CSF1R inhibitor impairs parenchymal plaque development in an Alzheimer's disease model. *Nat Commun* **10**, 3758, doi:10.1038/s41467-019-11674-z (2019).

31 Epshtein, Y., Chopra, A. P., Rosenhouse-Dantsker, A., Kowalsky, G. B., Logothetis, D. E. & Levitan, I. Identification of a C-terminus domain critical for the sensitivity of Kir2.1 to cholesterol. *Proc Natl Acad Sci U S A* **106**, 8055-8060, doi:10.1073/pnas.0809847106 (2009).

32 Tikku, S., Epshtein, Y., Collins, H., Travis, A. J., Rothblat, G. H. & Levitan, I. Relationship between Kir2.1/Kir2.3 activity and their distributions between cholesterol-rich and cholesterol-poor membrane domains. *Am J Physiol Cell Physiol* **293**, C440-450, doi:10.1152/ajpcell.00492.2006 (2007).

33 Le, N. T. & Abe, J. I. Regulation of Kir2.1 Function Under Shear Stress and Cholesterol Loading. *J Am Heart Assoc* **7**, doi:10.1161/JAHA.118.008749 (2018).

34 Buyan, A., Cox, C. D., Barnoud, J., Li, J., Chan, H. S. M., Martinac, B., Marrink, S. J. & Corry, B. Piezo1 Forms Specific, Functionally Important Interactions with Phosphoinositides and Cholesterol. *Biophys J* **119**, 1683-1697, doi:10.1016/j.bpj.2020.07.043 (2020).

35 Ridone, P., Pandzic, E., Vassalli, M., Cox, C. D., Macmillan, A., Gottlieb, P. A. & Martinac, B. Disruption of membrane cholesterol organization impairs the activity of PIEZO1 channel clusters. *J Gen Physiol* **152**, doi:10.1085/jgp.201912515 (2020).

36 Munji, R. N., Soung, A. L., Weiner, G. A., Sohet, F., Semple, B. D., Trivedi, A., Gimlin, K., Kotoda, M., Korai, M., Aydin, S., Batugal, A., Cabangcala, A. C., Schupp, P. G., Oldham, M. C., Hashimoto, T., Noble-Haeusslein, L. J. & Daneman, R. Profiling the mouse brain endothelial transcriptome in health and disease models reveals a core blood-brain barrier dysfunction module. *Nat Neurosci*, doi:10.1038/s41593-019-0497-x (2019).

1 Mosso, A. Sulla circolazione del sangue nel cervello dell'uomo. Revue Philosophique de la France Et de l (1882).

2 Roy, C. S. & Sherrington, C. S. On the Regulation of the Blood-supply of the Brain. J Physiol 11, 85-158 117, doi:10.1113/jphysiol.1890.sp000321 (1890).

3 Iadecola, C. The Neurovascular Unit Coming of Age: A Journey through Neurovascular Coupling in Health and Disease. Neuron 96, 17-42, doi:10.1016/j.neuron.2017.07.030 (2017).

4 Chen, B. R., Kozberg, M. G., Bouchard, M. B., Shaik, M. A. & Hillman, E. M. A critical role for the vascular endothelium in functional neurovascular coupling in the brain. J Am Heart Assoc 3, e000787, doi:10.1161/JAHA.114.000787 (2014).

5 Longden, T. A., Dabertrand, F., Koide, M., Gonzales, A. L., Tykocki, N. R., Brayden, J. E., Hill-Eubanks, D. & Nelson, M. T. Capillary K(+)-sensing initiates retrograde hyperpolarization to increase local cerebral blood flow. Nat Neurosci 20, 717-726, doi:10.1038/nn.4533 (2017).

6 Chow, B. W., Nunez, V., Kaplan, L., Granger, A. J., Bistrong, K., Zucker, H. L., Kumar, P., Sabatini, B. L. & Gu, C. Caveolae in CNS arterioles mediate neurovascular coupling. Nature 579, 106-110, doi:10.1038/s41586-020-2026-1 (2020).

7 Beach, J. M., McGahren, E. D. & Duling, B. R. Capillaries and arterioles are electrically coupled in hamster cheek pouch. Am J Physiol 275, H1489-1496, doi:10.1152/ajpheart.1998.275.4.H1489 (1998).

8 Ahn, S. J., Fancher, I. S., Bian, J. T., Zhang, C. X., Schwab, S., Gaffin, R., Phillips, S. A. & Levitan, I. Inwardly rectifying K(+) channels are major contributors to flow-induced vasodilatation in resistance arteries. J Physiol 595, 2339-2364, doi:10.1113/JP273255 (2017).

9 Hannah, R. M., Dunn, K. M., Bonev, A. D. & Nelson, M. T. Endothelial SK(Ca) and IK(Ca) channels regulate brain parenchymal arteriolar diameter and cortical cerebral blood flow. J Cereb Blood Flow Metab 31, 1175-1186, doi:10.1038/jcbfm.2010.214 (2011).

10 Harraz, O. F., Longden, T. A., Hill-Eubanks, D. & Nelson, M. T. PIP2 depletion promotes TRPV4 channel activity in mouse brain capillary endothelial cells. Elife 7, doi:10.7554/eLife.38689 (2018).

11 Sancho, M., Fabris, S., Hald, B. O., Brett, S. E., Sandow, S. L., Poepping, T. L. & Welsh, D. G. Membrane Lipid-KIR2.x Channel Interactions Enable Hemodynamic Sensing in Cerebral Arteries. Arterioscler Thromb Vasc Biol 39, 1072-1087, doi:10.1161/ATVBAHA.119.312493 (2019).

12 Romanenko, V. G., Fang, Y., Byfield, F., Travis, A. J., Vandenberg, C. A., Rothblat, G. H. & Levitan, I. Cholesterol sensitivity and lipid raft targeting of Kir2.1 channels. Biophys J 87, 3850-3861, doi:10.1529/biophysj.104.043273 (2004).

13 Romanenko, V. G., Rothblat, G. H. & Levitan, I. Modulation of endothelial inward-rectifier K+ current by optical isomers of cholesterol. Biophys J 83, 3211-3222, doi:10.1016/S0006-3495(02)75323-X (2002).

14 Fancher, I. S., Le Master, E., Ahn, S. J., Adamos, C., Lee, J. C., Berdyshev, E., Dull, R. O., Phillips, S. A. & Levitan, I. Impairment of Flow-Sensitive Inwardly Rectifying K(+) Channels via Disruption of Glycocalyx Mediates Obesity-Induced Endothelial Dysfunction. Arterioscler Thromb Vasc Biol 40, e240-e255, doi:10.1161/ATVBAHA.120.314935 (2020).

15 Tarantini, S., Hertelendy, P., Tucsek, Z., Valcarcel-Ares, M. N., Smith, N., Menyhart, A., Farkas, E., Hodges, E. L., Towner, R., Deak, F., Sonntag, W. E., Csiszar, A., Ungvari, Z. & Toth, P. Pharmacologically-induced neurovascular uncoupling is associated with cognitive impairment in mice. J Cereb Blood Flow Metab 35, 1871-1881, doi:10.1038/jcbfm.2015.162 (2015).

16 Pulido, R. S., Munji, R. N., Chan, T. C., Quirk, C. R., Weiner, G. A., Weger, B. D., Rossi, M. J., Elmsaouri, S., Malfavon, M., Deng, A., Profaci, C. P., Blanchette, M., Qian, T., Foreman, K. L., Shusta, E. V., Gorman, M. R., Gachon, F., Leutgeb, S. & Daneman, R. Neuronal Activity Regulates Blood-Brain Barrier Efflux Transport through Endothelial Circadian Genes. Neuron 108, 937-952 e937, doi:10.1016/j.neuron.2020.09.002 (2020).

17 Edmond, J., Korsak, R. A., Morrow, J. W., Torok-Both, G. & Catlin, D. H. Dietary cholesterol and the origin of cholesterol in the brain of developing rats. J Nutr 121, 1323-1330, doi:10.1093/jn/121.9.1323 (1991).

18 Dietschy, J. M. Central nervous system: cholesterol turnover, brain development and neurodegeneration. Biol Chem 390, 287-293, doi:10.1515/BC.2009.035 (2009).

19 Nieweg, K., Schaller, H. & Pfrieger, F. W. Marked differences in cholesterol synthesis between neurons and glial cells from postnatal rats. J Neurochem 109, 125-134, doi:10.1111/j.1471-4159.2009.05917.x (2009).

20 Mayford, M., Bach, M. E., Huang, Y. Y., Wang, L., Hawkins, R. D. & Kandel, E. R. Control of memory formation through regulated expression of a CaMKII transgene. Science 274, 1678-1683, doi:10.1126/science.274.5293.1678 (1996).

21 Alexander, G. M., Rogan, S. C., Abbas, A. I., Armbruster, B. N., Pei, Y., Allen, J. A., Nonneman, R. J., Hartmann, J., Moy, S. S., Nicolelis, M. A., McNamara, J. O. & Roth, B. L. Remote control of neuronal activity in transgenic mice expressing evolved G protein-coupled receptors. Neuron 63, 27-39, doi:10.1016/j.neuron.2009.06.014 (2009).

22 Bohlen, C. J., Bennett, F. C., Tucker, A. F., Collins, H. Y., Mulinyawe, S. B. & Barres, B. A. Diverse Requirements for Microglial Survival, Specification, and Function Revealed by Defined-Medium Cultures. Neuron 94, 759-773 e758, doi:10.1016/j.neuron.2017.04.043 (2017).

23 Badimon, A., Strasburger, H. J., Ayata, P., Chen, X., Nair, A., Ikegami, A., Hwang, P., Chan, A. T., Graves, S. M., Uweru, J. O., Ledderose, C., Kutlu, M. G., Wheeler, M. A., Kahan, A., Ishikawa, M., Wang, Y. C., Loh, Y. E., Jiang, J. X., Surmeier, D. J., Robson, S. C., Junger, W. G., Sebra, R., Calipari, E. S., Kenny, P. J., Eyo, U. B., Colonna, M., Quintana, F. J., Wake, H., Gradinaru, V. & Schaefer, A. Negative feedback control of neuronal activity by microglia. Nature 586, 417-423, doi:10.1038/s41586-020-2777-8 (2020).

24 Merlini, M., Rafalski, V. A., Ma, K., Kim, K. Y., Bushong, E. A., Rios Coronado, P. E., Yan, Z., Mendiola, A. S., Sozmen, E. G., Ryu, J. K., Haberl, M. G., Madany, M., Sampson, D. N., Petersen, M. A., Bardehle, S., Tognatta, R., Dean, T., Jr., Acevedo, R. M., Cabriga, B., Thomas, R., Coughlin, S. R., Ellisman, M. H., Palop, J. J. & Akassoglou, K. Microglial Gi-dependent dynamics regulate brain network hyperexcitability. Nat Neurosci 24, 19-23, doi:10.1038/s41593-020-00756-7 (2021).

25 Rosehart, A. C., Johnson, A. C. & Dabertrand, F. Ex Vivo Pressurized Hippocampal Capillary-Parenchymal Arteriole Preparation for Functional Study. J Vis Exp, doi:10.3791/60676 (2019).

26 Bisht, K., Okojie, K. A., Sharma, K., Lentferink, D. H., Sun, Y. Y., Chen, H. R., Uweru, J. O., Amancherla, S., Calcuttawala, Z., Campos-Salazar, A. B., Corliss, B., Jabbour, L., Benderoth, J., Friestad, B., Mills, W. A., 3rd, Isakson, B. E., Tremblay, M. E., Kuan, C. Y. & Eyo, U. B. Capillary-associated microglia regulate vascular structure and function through PANX1-P2RY12 coupling in mice. Nat Commun 12, 5289, doi:10.1038/s41467-021-25590-8 (2021).

27 Zhang, Y., Chen, K., Sloan, S. A., Bennett, M. L., Scholze, A. R., O'Keeffe, S., Phatnani, H. P., Guarnieri, P., Caneda, C., Ruderisch, N., Deng, S., Liddelow, S. A., Zhang, C., Daneman, R., Maniatis, T., Barres, B. A. & Wu, J. Q. An RNA-sequencing transcriptome and splicing database of glia, neurons, and vascular cells of the cerebral cortex. J Neurosci 34, 11929-11947, doi:10.1523/JNEUROSCI.1860-14.2014 (2014).

28 Vanlandewijck, M., He, L., Mae, M. A., Andrae, J., Ando, K., Del Gaudio, F., Nahar, K., Lebouvier, T., Lavina, B., Gouveia, L., Sun, Y., Raschperger, E., Rasanen, M., Zarb, Y., Mochizuki, N., Keller, A., Lendahl, U. & Betsholtz, C. A molecular atlas of cell types and zonation in the brain vasculature. Nature 554, 475-480, doi:10.1038/nature25739 (2018).

29 He, L., Vanlandewijck, M., Mae, M. A., Andrae, J., Ando, K., Del Gaudio, F., Nahar, K., Lebouvier, T., Lavina, B., Gouveia, L., Sun, Y., Raschperger, E., Segerstolpe, A., Liu, J., Gustafsson, S., Rasanen, M., Zarb, Y., Mochizuki, N., Keller, A., Lendahl, U. & Betsholtz, C. Single-cell RNA sequencing of mouse brain and lung vascular and vessel-associated cell types. Sci Data 5, 180160, doi:10.1038/sdata.2018.160 (2018).

30 Spangenberg, E., Severson, P. L., Hohsfield, L. A., Crapser, J., Zhang, J., Burton, E. A., Zhang, Y., Spevak, W., Lin, J., Phan, N. Y., Habets, G., Rymar, A., Tsang, G., Walters, J., Nespi, M., Singh, P., Broome, S., Ibrahim, P., Zhang, C., Bollag, G., West, B. L. & Green, K. N. Sustained microglial depletion with CSF1R inhibitor impairs parenchymal plaque development in an Alzheimer's disease model. Nat Commun 10, 3758, doi:10.1038/s41467-019-11674-z (2019).

31 Epshtein, Y., Chopra, A. P., Rosenhouse-Dantsker, A., Kowalsky, G. B., Logothetis, D. E. & Levitan, I. Identification of a C-terminus domain critical for the sensitivity of Kir2.1 to cholesterol. Proc Natl Acad Sci U S A 106, 8055-8060, doi:10.1073/pnas.0809847106 (2009).

32 Tikku, S., Epshtein, Y., Collins, H., Travis, A. J., Rothblat, G. H. & Levitan, I. Relationship between Kir2.1/Kir2.3 activity and their distributions between cholesterol-rich and cholesterol-poor membrane domains. Am J Physiol Cell Physiol 293, C440-450, doi:10.1152/ajpcell.00492.2006 (2007).

33 Le, N. T. & Abe, J. I. Regulation of Kir2.1 Function Under Shear Stress and Cholesterol Loading. J Am Heart Assoc 7, doi:10.1161/JAHA.118.008749 (2018).

34 Buyan, A., Cox, C. D., Barnoud, J., Li, J., Chan, H. S. M., Martinac, B., Marrink, S. J. & Corry, B. Piezo1 Forms Specific, Functionally Important Interactions with Phosphoinositides and Cholesterol. Biophys J 119, 1683-1697, doi:10.1016/j.bpj.2020.07.043 (2020).

35 Ridone, P., Pandzic, E., Vassalli, M., Cox, C. D., Macmillan, A., Gottlieb, P. A. & Martinac, B. Disruption of membrane cholesterol organization impairs the activity of PIEZO1 channel clusters. J Gen Physiol 152, doi:10.1085/jgp.201912515 (2020).

36 Munji, R. N., Soung, A. L., Weiner, G. A., Sohet, F., Semple, B. D., Trivedi, A., Gimlin, K., Kotoda, M., Korai, M., Aydin, S., Batugal, A., Cabangcala, A. C., Schupp, P. G., Oldham, M. C., Hashimoto, T., Noble-Haeusslein, L. J. & Daneman, R. Profiling the mouse brain endothelial transcriptome in health and disease models reveals a core blood-brain barrier dysfunction module. Nat Neurosci, doi:10.1038/s41593-019-0497-x (2019).

37 Dagher, N. N., Najafi, A. R., Kayala, K. M., Elmore, M. R., White, T. E., Medeiros, R., West, B. L. & Green, K. N. Colony-stimulating factor 1 receptor inhibition prevents microglial plaque association and improves cognition in 3xTg-AD mice. J Neuroinflammation 12, 139, doi:10.1186/s12974-015-0366-9 (2015).

38 Császár, E., Lénárt, N., Cserép, C., Környei, Z., Fekete, R., Pósfai, B., Balázsfi, D., Hangya, B., Schwarcz, A. D., Szöllősi, D., Szigeti, K., Máthé, D., West, B. L., Sviatkó, K., Brás, A. R., Mariani, J.-C., Kliewer, A., Lenkei, Z., Hricisák, L., Benyó, Z., Baranyi, M., Sperlágh, B., Menyhárt, Á., Farkas, E. & Dénes, Á. Microglia control cerebral blood flow and neurovascular coupling via P2Y12R-mediated actions. bioRxiv, 2021.2002.2004.429741, doi:10.1101/2021.02.04.429741 (2021).

39 Gachet, C. P2Y(12) receptors in platelets and other hematopoietic and non-hematopoietic cells. Purinergic Signal 8, 609-619, doi:10.1007/s11302-012-9303-x (2012).

40 Wihlborg, A. K., Wang, L., Braun, O. O., Eyjolfsson, A., Gustafsson, R., Gudbjartsson, T. & Erlinge, D. ADP receptor P2Y12 is expressed in vascular smooth muscle cells and stimulates

contraction in human blood vessels. Arterioscler Thromb Vasc Biol 24, 1810-1815, doi:10.1161/01.ATV.0000142376.30582.ed (2004).

41 Simons, M., Keller, P., De Strooper, B., Beyreuther, K., Dotti, C. G. & Simons, K. Cholesterol depletion inhibits the generation of beta-amyloid in hippocampal neurons. Proc Natl Acad Sci U S A 95, 6460-6464, doi:10.1073/pnas.95.11.6460 (1998).

42 Bodovitz, S. & Klein, W. L. Cholesterol modulates alpha-secretase cleavage of amyloid precursor protein. J Biol Chem 271, 4436-4440, doi:10.1074/jbc.271.8.4436 (1996).

43 Wahrle, S., Das, P., Nyborg, A. C., McLendon, C., Shoji, M., Kawarabayashi, T., Younkin, L. H., Younkin, S. G. & Golde, T. E. Cholesterol-dependent gamma-secretase activity in buoyant cholesterol-rich membrane microdomains. Neurobiol Dis 9, 11-23, doi:10.1006/nbdi.2001.0470 (2002).

44 Puglielli, L., Konopka, G., Pack-Chung, E., Ingano, L. A., Berezovska, O., Hyman, B. T., Chang, T. Y., Tanzi, R. E. & Kovacs, D. M. Acyl-coenzyme A: cholesterol acyltransferase modulates the generation of the amyloid beta-peptide. Nat Cell Biol 3, 905-912, doi:10.1038/ncb1001-905 (2001).

45 Attems, J. & Jellinger, K. A. The overlap between vascular disease and Alzheimer's disease--lessons from pathology. BMC Med 12, 206, doi:10.1186/s12916-014-0206-2 (2014).

46 Charidimou, A., Boulouis, G., Gurol, M. E., Ayata, C., Bacskai, B. J., Frosch, M. P., Viswanathan, A. & Greenberg, S. M. Emerging concepts in sporadic cerebral amyloid angiopathy. Brain 140, 1829-1850, doi:10.1093/brain/awx047 (2017).

47 Banerjee, G., Carare, R., Cordonnier, C., Greenberg, S. M., Schneider, J. A., Smith, E. E., Buchem, M. V., Grond, J. V., Verbeek, M. M. & Werring, D. J. The increasing impact of cerebral amyloid angiopathy: essential new insights for clinical practice. J Neurol Neurosurg Psychiatry 88, 982-994, doi:10.1136/jnnp-2016-314697 (2017).